The Interaction of Path Integration Cues and Landmarks in Positioning Estimations During Human Spatial Navigation in Small- and Large-scale Environment

by

Lei Zhang

A thesis submitted in partial fulfillment of the requirements for the degree of

Doctor of Philosophy

Department of Psychology

University of Alberta

Abstract

People use landmarks and the path integration cues to return to the origin of the route (i.e., home). This homing behavior is believed to be better when people can access both cues than when they can only access either cue, because two separate homing estimations are combined to reduce homing variability. This belief reflects a popular theory that two cues directly interact in the homing estimations (*homing hypothesis*). In contrast, we believe that two cues interact in the positioning (heading/position) estimations that are then used to determine the home locations (*positioning hypothesis*). Two studies were conducted to differentiate between the two hypotheses by investigating the cue interaction of positioning estimations and homing estimations, when people walked in a small-scale environment, and when people drove in a large-scale environment.

The study in Chapter 2 demonstrated that when people walked a two-leg path, they combined the path integration cues and landmarks to determine their heading (and position) estimations, but not homing estimations, in all path configurations. Furthermore, people used the heading and position estimations after cue interaction to determine their homing estimations. The study in Chapter 3 further suggests that path integration cues and landmarks could compete for the positioning estimations when people drove in a virtual city.

In sum, our work has demonstrated that the path integration cues and landmarks interact in positioning estimations, regardless of locomotion modes and landmark types. People use the positioning estimations after interaction to guide their homing.

Preface

This thesis is an original work by Lei Zhang. The experiments in this thesis has received research ethics approval from the University of Alberta Research Ethics Board, Project Name "Human Spatial cognition", No. Pro00052545, November 20, 2014.

Acknowledgments

To my advisor, Weimin Mou, I would like to express my greatest gratitude and appreciation for constantly offering guidance in every step on the way during my graduate life. I was deeply encouraged by your continuous support and inspired by your curiosity and insight towards research. Your patience and dedication to the students have shaped my mind to be whom I want to be in life. Your wisdom and passion to the research have motivated me to do what I want in work. I felt I was so cherished to have you as my supervisor. Many many thanks!

To my advisory committee members, Anthony Singhal and Kyle Elliott Mathewson, I would like to express my great appreciation for all your intriguing discussion and valuable feedback on my work.

To all my labmates in the Virtual Reality and Spatial Cognition Lab, Ruojing Zhou, Lin Wang, Karen Du, and Xuehui Lei, I would like to say thank you to you girls for all your company, help and support throughout years. I felt extremely warm and enjoyable by having you girls not just in the lab, but also in my life in Edmonton.

To all the former research assistants who helped at different stages of my thesis, Sarah Tan, So Yon Kwon, Wenyue Lu, Labiqa Nazar, Bowen Wu, Alyssa Serquina, thank you very much for your time and effort in assisting my work.

To all my dear family, my husband Shengchao Zhuang, my mother-in-law Yuefeng Zhou and my parents Xiangdong Zhang and Suqin Li, I would like to express greatest appreciation for your generous help and unconditional love in my life, particularly during my pregnancy and my graduate life. Without you, I would not be able finish my study, manage my life properly, and grow up as who I am now. Thank you very much all the way through! I love you the best!

Table of Contents

List of Figures

List of Tables

Chapter 1

General Introduction

Every summer, big flocks of snow geese make a long flight back from the southern part of the United States and Central Mexico to the Northern Alaskan coastal tundra in the vicinity of the coast for breeding. After every foraging trip, desert ants, Cataglyphis fortis, are able to return directly to the inconspicuous hole of their nest after hundreds of meters of detours. For a daily commute, we, humans, can effortlessly go back home from work. Such successful homing behaviors (i.e., returning to the origin of a path) in different species require the knowledge of self-localization in an environment. The self-localization knowledge refers to how people use different spatial information to represent where they are (position estimations) and which direction they are facing (heading estimations). In the literature, humans and non-human animals share two navigational systems in wayfinding: the path integration system and the piloting system (Etienne & Jeffery, 2004; Gallistel, 1990; Zhao & Warren, 2015a). The quest to understanding the success of homing behaviors would allow us to explore how we combine information from the two navigational systems to form representations of headings, positions, and home locations by combining information. Such a quest would also motivate us to study how the representations in the path integration and piloting systems interact.

1.1 The path integration system and the piloting system

The path integration system uses cues generated by self-movement to obtain one's moving direction and speed, and then calculates one's heading and position. These cues include vestibular cues, proprioceptive cues, motor efference copies, and optical flow (Etienne & Jeffery, 2004; Gallistal, 1990; Klatzky, Loomis, Beall, Chance, & Golledge, 1998; Loomis, Klatzky, Golledge, & Philbeck, 1999; Tcheang, Bulthoff, & Burgess, 2011; Warren, Kay, Zosh, & Sahuc, 2001). All of these cues are referred to as *idiothetic cues* (Whishaw & Brooks, 1999). All of them, with the exception of optical flow, are also referred to as *inertial cues* (Tcheang et al.,

2011). When individuals need to return home after a long journey, they could use the path integration system to compute the vector from the current position to the origin (i.e., homing vector) with respect to the current heading and position, and then return home. Hence, path integration is a continuous updating process where navigators need to represent the homing vector, add it to the vector of a new movement, and, therefore, obtain a new homing vector (Etienne & Jeffery, 2004; Shettleworth & Sutton, 2005; Wiener, Berthoz, & Wolbers, 2011). In this process, the path integration system only maintains the homing vector, not the path configuration. In contrast, some studies indicate that the path integration system might represent the path configuration (Fujita, Klatzky, Loomis, & Golledge, 1993). Using the configural knowledge of the path, navigators can represent and retrieve headings and positions at any point along the route that has been travelled. Navigators can also calculate vectors between any two points on the route. Recent studies showed that humans might have the capacity to encode either the homing vector or the path configuration depending on their intentions (He & McNamara, 2017; Wiener et al., 2011).

The piloting system is another mechanism of determining heading, position, and homing estimations during navigation. When navigators come to a new environment, they learn the spatial relationships between visual items, as well as the relationships between visual items and themselves (Cheng & Spetch; 1998; Doeller & Burgess, 2008; Mou & Zhang, 2014; Taube, 2007; Yoder, Clark, & Taube, 2011). These relationships are specified with respect to the distance and bearing relative to some salient visual items (i.e., landmarks). These specifications are kept in navigators' memory. Whenever the navigators see the visual items in this environment, they can then use the specifications in memory to judge their headings and positions or to directly determine their goal locations, including their home. The role of such landmarks in navigation

has been explored for a long time in the literature. Many studies have indicated their importance, particularly when navigators need to travel a long distance and the path integration system is not reliable (e.g., Dyer, 1991; Etienne, Maurer, Boulens, Levy & Rowe, 2004).

The path integration system and the piloting system can work independently (Chen, McNamara, Kelly, & Wolbers, 2017; Doeller & Burgess, 2008; Etienne & Jeffery, 2004; Etienne et al., 2004; Klatzky et al., 1998; Nardini, Jones, Bedford, & Braddick, 2008; Sjolund, Kelly, & McNamara, in press; Wiener et al., 2011; Zhao & Warren, 2015a; 2015b). On the one hand, people can navigate effectively by relying only on their path integration system. In a study by Klatzky et al. (1998), blindfolded participants walked a two-leg path and then, at the end of the path, they were asked to turn to face the path origin. The results showed that the participants performed this task accurately. As the participants required vision to use the piloting system, the blindfolded participants' accuracy in turning to face the path origin could only be attributed to the path integration system. On the other hand, people can also navigate by relying strictly on the piloting system. Nardini et al. (2008) demonstrated that human adults and children could locate a target relative to other objects after disorientation. Because the path integration system was disrupted during disorientation, the successful localization of the target could only be attributed to the piloting system.

1.2 Cue interaction: cue combination vs cue competition

In general, studies have examined two types of interaction between the piloting system and the path integration system. The first one is cue combination and the other one is cue competition. In cue combination, two estimations from the path integration system and the piloting system are weight averaged. In a *Bayesian combination* or *optimal combination*, the weight of an individual cue is inversely proportional to the variance of the estimations based on

an individual cue (Cheng, Shettleworth, Huttenlocher, & Riser, 2007; Ernst & Banks, 2002). In a *quasi-Bayesian combination* or *sub-optimal combination*, although the weight of an individual cue may not be exactly inversely proportional to the variance of the estimations based on an individual cue, a larger weight is assigned to the cue producing a more precise estimation.

In contrast to cue combination, in cue competition individuals rely only on one cue and ignore the other. To examine which cue individuals follow, researchers have widely used the conflict condition where landmarks are shifted after individuals move away from home. This condition makes home location predictions by the two systems discrepant, thus this condition is able to diagnose which cue is more dominant. Using this paradigm, a number of studies have shown that individuals prefer to use landmarks for home estimations when the angular difference between the two predictions is small. This is because the estimations from landmarks could be more accurate than those from the path integration system, and individuals would use landmarks to reset the estimations in the path integration system (Etienne & Jefferey, 2004; Gallistal, 1990; Klatzky et al., 1998; Loomis, et al., 1999; Tcheang et al., 2011; Whishaw & Brooks; 1999). On the other hand, when the angular difference (i.e., 140°) between the two predictions is large, the path integration system may serve as a back-up to detect the shift of landmarks (Chen et al., 2017; Zhao & Warren, 2015a; 2015b). Other studies also suggest that such factors as subjective confidence and prior experience could also affect how the two cues interact (e.g., Knight et al., 2014; Chen et al.). For instance, Chen et al. showed that people tend to follow the cues that they feel more confident about. Furthermore, Knight et al. found that when rats view the landmarks with a large shift, those that have experience of the small shift of landmarks tend to combine the two cues for their head direction cells' firing, while those without such experience would completely follow the shifted landmarks in their firing activity.

1.3 Cue interaction in homing behaviors

Despite the theories on how the path integration cues and landmarks interact, there are two competing hypotheses regarding when the two cues interact – the homing hypothesis and the position hypothesis. The homing hypothesis speculates that the two cues interact directly in homing estimations, whereas the positioning hypothesis stipulates that the two cues interact in heading and position estimations that are then joined to determine homing locations. I will elaborate further on these two hypotheses in the following two sub-sections.

1.3.1 The homing hypothesis

Most studies suggest that the path integration system and the piloting system interact directly in estimating home locations. This hypothesis assumes that each of the systems produces an independent homing estimation (Chen et al., 2017; Cheng et al., 2007; Nardini et al., 2008; Zhao & Warren, 2015a). When both systems are then available during navigation, the home representations from the two systems combine or compete. As this hypothesis speculates that cue interaction occurs during homing estimations, we term this hypothesis the *homing hypothesis*.

Previous studies that used the homing paradigm found evidence to support the homing hypothesis (e.g., Nardini et al., 2008). In these studies, participants started from the origin (home) in the presence of landmarks and then walked a path. When they finished the path, they walked back to the origin under different experimental manipulations. (1) In the path integration system only (PI) condition, before walking back, the landmarks were turned off. The participants walked back to the origin (O) in darkness. This manipulation only allows people to rely on the path integration system. (2) In the landmark only condition (LM), before returning to the origin, the landmarks were first turned off. The participants were then rotated for disorientation. After disorientation, the landmarks were turned on. The participants walked back to the origin in the

presence of the landmarks. The purpose of the disorientation procedure was to disrupt people's self-motion sense, which only allowed the participants to rely on landmarks in the piloting system. (3) In the both cue condition (BO), the landmarks remained, and the participants walked back to the origin. (4) In the conflict condition (CO), the landmarks rotated. The participants walked back to the origin in the presence of the rotated landmarks. In all four conditions, the responded origins (O') were recorded. The direction from the end of the path (P) to this response origin (O') is termed the *response homing direction,* PO'. This direction can be compared to the *correct homing direction* (PO) to calculate the difference and obtain the *homing error*. Furthermore, the distance between the response origin (O') and the actual origin (O) can be measured as *distance error*. These two measurements can both reflect different aspects of the homing estimation accuracy and they have been used in previous studies. For simplicity, I use the homing error (β) as an example to illustrate how the homing errors are combined from the two systems.

Bayesian theory offers a quantitative method to test the cue combination in the homing hypothesis. In the combined home representation, people assign weight to each single system to determine the combined homing estimations. In the optimal combination, the assigned weight is inversely proportional to the variance of the homing estimations. This weight is called *optimal weight*. In practice, we used the averaged homing direction in the CO condition to calculate the weight assigned to each cue system. This weight is called *observed weight*. If the homing direction in the CO condition is closer to the landmark prediction, then it indicates that people assign a larger observed weight to the piloting system. To determine the optimal combination, the observed weight should be comparable to the optimal weight. Furthermore, in the optimal combination, the variability of the homing estimations is the smallest among any combined ones

using other assigned weights. In practice, the observed homing variability in the BO or CO condition should be reduced compared to that in both the single cue conditions and should also be comparable to the optimal prediction using the optimal weights to calculate the estimation variability. A less strict form of the combination, the quasi-optimal combination, does not require an exact inverse relation between weights and variance. However, it still claims that people assign a larger observed weight to the cue system that produces more accurate homing estimations. In this case, the variability of the combined homing estimations could be larger than the optimally combined one, but it should still be smaller than that in the single systems.

Other studies also suggest that two cues compete for homing estimations. Instead of combining the home representations, people predominately use one system to determine home locations, even when both cue systems are available. When the two systems compete with each other, the homing estimations in the BO or CO condition should be similar to those in the one dominant system (Etienne et al., 2004; Zhao & Warren, 2015a). This cue competition could be conceptualized as a special case of cue combination, as people assign a full weight to one dominant system. Furthermore, both combination and competition models assume that each system has an independent home representation. In general, the homing hypothesis speculates that (no matter) whether the home representations combine or compete, the path integration and piloting systems directly interact in the homing estimations.

Previous studies suggest that people optimally combine cues for homing estimations. Nardini et al. (2008) found that the variability of the homing estimations in the BO and CO condition was reduced compared to that in both the single cue conditions. The variability of the homing estimations in the BO condition was comparable to the optimal combination prediction. The observed weight assigned to each of the path integration and piloting systems was also

comparable to the optimal weight. Chen et al. (2017) also found similar results in most of their experiments. However, Zhao and Warren (2015a) had inconsistent findings. Results suggest that people could near optimally integrate the two cue systems to reduce the variability of the homing estimations in the BO and CO conditions, while people dominantly use one cue to determine the averaged homing direction in the CO condition. Specifically, when landmarks shifted less than 90°, most participants used the piloting system, but they switched to the path integration system when the shift was greater than 90°. The discrepant results from the measurements of the variability and the means of the homing estimations do not support the Bayesian combination, as it requires both the observed variability and the observed weight to be comparable to the optimal predictions.

One possible explanation is that when landmarks are shifted less than 90°, people use landmarks to correct the errors in the path integration system. After this correction, people can combine the homing estimations from the reset/corrected path integration system and the piloting system to guide their navigation. However, when landmarks are shifted greater than 90°, the path integration system detects that the landmarks are not reliable; therefore, people switch to using the path integration system. This interpretation suggests that the two cues could combine to improve precision, and the dominance of landmarks in moderate cue conflict situations contributes to improving accuracy. However, this interpretation seems problematic in explaining why people still used the two systems to improve precision when the path integration system detected landmarks were unreliable and the path integration system served as a back-up in large cue conflict conditions. In such large conflict conditions, people seemed to not trust the piloting system and switched to the path integration system instead. Therefore, it is odd that people still combined these two cues to reduce the variance.

In summary, the homing hypothesis speculates that both the path integration and piloting systems produce an independent homing estimation. When both systems are available during navigation, the home representations from the two systems could then interact. In the literature, studies primarily found that the two cues combine for homing estimations. However, there are no consistent findings on how the two cues interact. Although some studies suggest that the variability of the homing estimations in the BO and CO conditions could be predicted by the optimal combination, the observed weights are not consistent with the optimal ones in the combination model (Zhao & Warren, 2015a). The observed weight in Zhao and Warren's study even suggests that the cues compete in homing estimations. It is difficult to reconcile these discrepant results by the homing hypothesis.

1.3.2 The positioning hypothesis

The positioning hypothesis is a different approach to conceptualizing the interaction between the piloting system and the path integration system. According to this hypothesis, neither the piloting system nor the path integration system produces a direct homing estimation. Instead, these two systems produce separate positioning (position/heading) estimations. These positioning estimations from the two systems then interact for combination or competition. Using the combined or competed positioning estimations, individuals determine goal locations, including home locations. Different from the homing hypothesis, this new hypothesis argues that cue interaction occurs in positioning estimations rather than in homing estimations. Below we refer to this new approach as the *positioning hypothesis*.

The positioning hypothesis stipulates that the piloting system and the path integration system may use one cognitive map to determine goal locations, as the single positioning estimation after cue interaction is represented in one cognitive map (Gallistel, 1990; Gallistel &

Matzel, 2013; Muller & Wehner, 1998; Wehner, 2003; Zhang, Mou, & McNamara, 2011). In contrast, the homing hypothesis implies that the piloting and path integration systems may use two different cognitive maps to determine goal locations (Vickerstaff & Cheung, 2010), as the home locations are represented and interacted directly in the two cognitive maps.

To evaluate each hypothesis, we need to obtain the heading, position, and homing estimations separately. Past studies used the homing estimations (e.g., homing errors) to indicate people's heading (or position) errors (Klatzky et al., 1998; Zhao & Warren, 2015a). However, the homing errors cannot accurately reflect the heading or position errors. As illustrated in Figure 1.1A, a hypothetical participant walks the path (O-T-P), and then is asked to turn to point to O, while standing at P and facing H. The participant points to O' as O. The response direction is PO' .The pointing error is measured as the difference between PO and PO' and is termed β. While standing at P and facing H, the participant estimates the heading as H' and estimates the position as P'. There are three possible interpretations of β. First, the participant updates the position accurately (P' = P), but not the heading (H' ≠ H). Therefore, β might occur due to an inaccurate heading estimation only, and β equals the difference between H and H' (Figure 1.1B). Second, the participant updates the heading accurately (H' = H), but not the position (P' ≠ P). Therefore, β might occur due to an inaccurate position estimation only, and β equals the difference between OP' and OP (Figure 1.1C). Third, the participant neither updates the heading nor the position accurately (H' ≠ H, P' ≠ P). β can be observed whenever the bearing of P'O in terms of H' equals the bearing of PO' in terms of H (Figure 1.1D). Hence, in general, we cannot dissociate the heading estimations and the position estimations by only using the homing estimations.

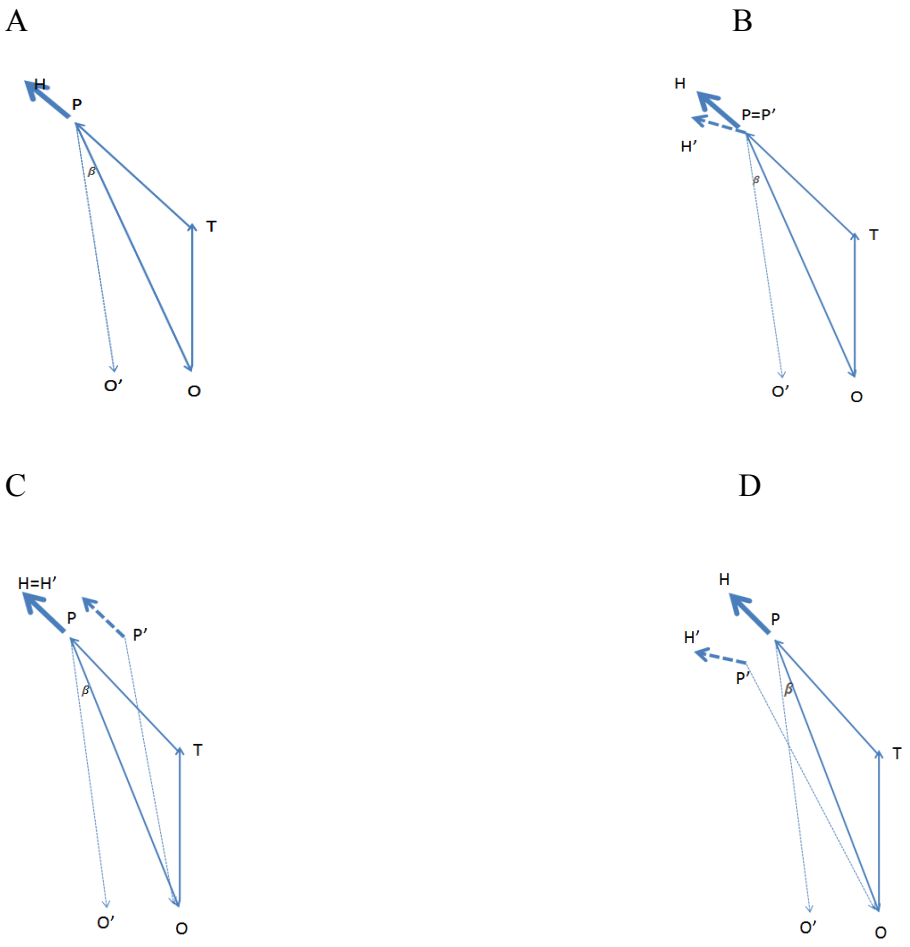

Figure 1.1 The source of the homing errors in Chapter 1.

(A)The homing error (β) could result from the heading error, position error, or both. A hypothetical participant walks a two-leg path, starting from O (origin), turning at T (turning), and ending at P (test position). The participant's test heading is referred to as "H". The participant points to O' as the origin of O. (B) The homing error occurs due to the heading error. (C) The homing error occurs due to the position error. (D) The homing error occurs due to both the heading and position errors.

In Chapter 2 studies, I used a new method that could dissociate heading and position errors from homing errors (Mou & Zhang, 2014; Zhang & Mou, 2017). In Figure 1.2, we assume that the participants use the represented locations of objects (O, X), position (P'), and heading

(H') of themselves to guide the responded locations of objects (O', X'), position (P), and heading (H) of themselves. Therefore, the spatial relations between the elements in the mental representations (O, X, P', H') are the same as the spatial relations between the corresponding elements (O', X', P, H) in the responses.

Hence, the bearing from O to P' relative to the bearing from O to X in memories should be the same as the bearing from O' to P relative to the bearing from O' to X' in responses. This is written as follows:

$$OP' - OX = O'P - O'X' \tag{1.1}$$

In the above equation, OP', OX, O'P, and O'X' are all bearings, defined as a signed angular distance from a reference direction. Since a bearing is a signed angle, the rules of math operations for real numbers can be applied to bearings.

By adding – (OP – OP) to the left side of Equation 1.1, we change Equation 1.1 to:

$$OP' - (OP - OP) - OX = O'P - O'X' \tag{1.2}$$

Moving (OP – OX) to the right of the equation, we obtain:

$$\begin{aligned} OP' - OP &= O'P - O'X' - (OP - OX) \\ &= (OX - OP) - (O'X' - O'P) \end{aligned} \tag{1.3}$$

Because OP = PO – 180 and O'P = PO' – 180, we obtain the proof:

$$OP' - OP = (OX - PO) - (O'X' - PO') \tag{1.4}$$

Following the same assumption, the bearing from O to P' relative to H' in memories should be the same as the bearing from O' to P relative to H in responses.

$$OP' - H' = O'P - H \tag{1.5}$$

From Equation 1.5 and several math operations, we obtain:

$$\begin{aligned} H' - H &= OP' - O'P \\ &= OP' - (OP - OP) - O'P \\ &= (OP' - OP) - (O'P - OP) \\ &= (OP' - OP) - ((PO' - 180) - (PO - 180)) \\ &= (OP' - OP) - (PO' - PO) \end{aligned} \tag{1.6}$$

We took the difference between the estimated heading (H') and the correct heading (H) in the testing as a heading error (HER). We used the direction of OP' as the position estimation and took the difference between the estimated position direction (OP') and the correct position direction (OP) in the testing as a position error (PER). From Equation 1.6, we obtain:

$$HER = PER - \beta \tag{1.7}$$

In summary, by measuring the bearing of PO and PO', β can be calculated. By measuring the bearing of OX, PO, O'X' and PO', using the Equation 1.4, PER can be calculated. Using the obtained PER and β, and Equation 1.7, HER can be calculated.

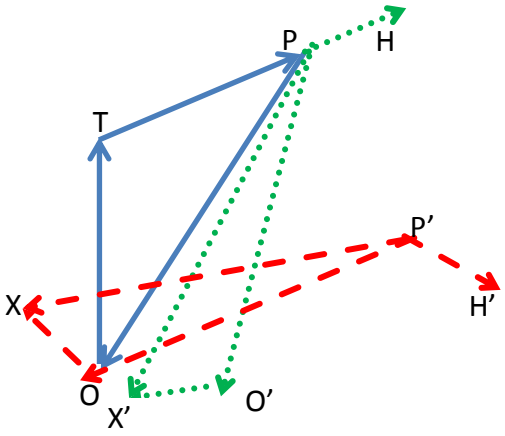

Figure 1.2 Illustration of the definition of HER, PER, and β in Chapter 1.

HER denotes a heading error, PER denotes a position error, and β denotes a homing error. A hypothetical person walks a path starting at O and ending at P, with the heading of H. The response locations of the origin O and another object X are O' and X', respectively. Assume that the person's estimations of P and H are P' and H', respectively. As defined, HER = H'- H; PER = OP' – OP; β = PO' – PO. In the above definitions, PO', PO, OP', and OP are all bearings, defined as a signed angular distance from a reference direction in a horizontal plane (e.g., the first walking leg, OT). β =PER – HER.

Two studies using this new method to measure the heading and position estimations have demonstrated that the path integration and piloting systems interact in heading estimations and position estimations. In Mou and Zhang (2014)'s study, participants learned five objects' locations in the presence of distal landmarks before walking the path where the landmarks and objects were removed. After the participants finished the path, the distal landmarks rotated. The participants had to replace the objects in the presence of the rotated landmarks. The participants' heading and position estimations were calculated from the response to objects' locations. The

results have shown that people use the rotated landmarks to determine their headings, while the path integration system to determine their positions. Furthermore, Zhang and Mou (2017) reported that a proximal visual landmark that had been displaced to the participants' testing position reset the participants' position estimations but not their heading estimations from the path integration system. Consistent with the positioning hypothesis, these two studies suggest that the heading and the position estimations from the two systems compete. After the competition, the single heading estimation and the position estimation are represented in one cognitive map (Gallistel, 1990; Muller & Wehner, 1988; Zhang et al., 2011).

In summary, the positioning hypothesis speculates that both the path integration and piloting systems produce an independent positioning (heading/position) estimation. When both systems are available during navigation, the positioning representations from the two systems interact. The target locations including home locations could be calculated by the positioning estimations after cue interaction. In the literature, two behavioural studies using a new method to measure heading and position estimations suggest that the positioning estimations from the two systems interact directly, providing evidence of a single map representation of positioning information and target locations (Mou & Zhang, 2014; Zhang & Mou, 2017).

1.4 Outlines of the thesis

The primary goal of my dissertation is to differentiate between the homing hypothesis and the positioning hypothesis. The critical difference between the homing hypothesis and the positioning hypothesis is when the path integration and piloting systems interact. The homing hypothesis predicts that the interaction occurs in homing estimations, whereas the positioning hypothesis suggests that the interaction occurs in positioning estimations.

One straightforward approach to achieve the goal to differentiate the two hypotheses is to examine the cue interaction in the positioning and homing estimations. If the two cues interact in positioning but not homing estimations, then the positioning hypothesis is supported. If the two cues interact in homing but not positioning estimations, then the homing hypothesis is supported. In the dissertation, I conducted two studies to investigate the cue interaction in positioning and homing estimations.

In Chapter 2, I used the homing paradigm and asked participants to walk two-leg paths by manipulating the path configurations. After walking each path, the participants' heading, position and homing estimations were measured in the conditions of PI, LM, BO and CO. In Experiment 1, distal landmarks were used to simplify the contrast between the positioning hypothesis and the homing hypothesis. As distal landmarks only affected the participants' heading estimations but not their position estimations, and people would only use the path integration cues to judge their positions in all four conditions, this study tested whether the two cues interacted in the heading or homing estimations. The results did not support the homing hypothesis, as the homing estimations were not combined in all path configurations. However, the results supported the positioning hypothesis. First, the heading estimations from the two cue systems were combined for all path configurations. Second, people used the path integration system to determine the positions in all conditions. Last, the heading and position estimations were joined to determine the home locations in all four cue conditions. Experiment 2 replicated the similar findings using the typical homing paradigm without measuring heading and position estimations. Experiment 3 and 4 were similar to Experiment 1 except proximal landmarks were used. We found similar findings that cue combination occurred during positioning estimations, but not during homing estimations.

In Chapter 3, I examined the cue interaction of positioning estimations in a large-scale environment. In an immersive virtual city, participants learned five buildings' locations in the presence of two proximal towers and four distal scenes. The proximal towers were considered as proximal landmarks, whereas distal scenes were considered as distal landmarks. Then the participants drove two streets without viewing these buildings, towers or scenes. When they finished driving, either one tower with displacement to the testing position or the scenes with rotation reappeared. The participants pointed to the five buildings' directions. Their heading and position estimations were calculated from their pointing responses. The results showed that when the displaced proximal tower reappeared, the participants used the tower to determine their positions; and when the rotated distal scenes reappeared, the participants used the scenes to determine their headings. These findings support the positioning hypothesis and suggest that when people drive in a large-scale environment, the path integration cues and landmarks compete for the positioning estimations.

In Chapter 4, I summarized the results of the studies. The relationship among heading, position and homing estimations are discussed. Finally, future studies are suggested to provide further evidence of the positioning hypothesis.

1.5 References

Chen, X., McNamara, T. P., Kelly, J.W., & Wolbers, T. (2017). Cue combination in human spatial navigation. *Cognitive Psychology, 95*, 105-144.

Cheng, K., Shettleworth, S.J., Huttenlocher, J., & Rieser, J.J. (2007). Bayesian integration of spatial information. *Psychological Bulletin*, *133*(4), 625-637.

Cheng, K., & Spetch, M. L. (1998). Mechanisms of landmark use in mammals and birds. In S. Healy (Ed.), *Spatial representation in animals* (pp. 1-17). Oxford: Oxford University Press.

Doeller, C. F., & Burgess, N. (2008). Distinct error-correcting and incidental learning of location relative to landmarks and boundaries. *Proceedings of the National Academy of Sciences of the United States of America, 105*(15), 5909-5914.

Dyer, F. C. (1991). Bees acquire route-based memories but not cognitive maps in a familiar landscape. *Animal Behaviour, 41*, 239-246.

Ernst, M. O., & Banks, M. S. (2002). Humans integrate visual and haptic information in a statistically optimal fashion. *Nature, 415*, 429–433.

Etienne, A. S., & Jeffery, K. J. (2004). Path integration in mammals. *Hippocampus, 14*(2), 180-192.

Etienne, A. S., Maurer, R., Boulens, V., Levy, A., & Rowe, T. (2004). Resetting the path integrator: a basic condition for route-based navigation. *Journal of Experimental Biology, 207*(9), 1491-1508.

Fujita, N., Klatzky, R. L., Loomis, J. M., & Golledge, R. G. (1993). The encoding-error model of pathway completion without vision. *Geographical Analysis*, *25*(4), 295-314.

Gallistel, C. R. (1990). *The organization of learning*. Cambridge, MA: MIT Press.

Gallistel, C. R., & Matzel, L. D. (2013). The neuroscience of learning: beyond the Hebbian synapse. *Annual Review of Psychology*, *64*, 169-200.

He, Q., & McNamara, T. P. (2017). Spatial Updating Strategy Affects the Reference Frame in Path Integration. *Psychonomic Bulletin & Review*, 1-7.

Klatzky, R. L., Loomis, J. M., Beall, A. C., Chance, S. S., & Golledge, R. G. (1998). Spatial updating of self-position and orientation during real, imagined, and virtual locomotion. *Psychological Science, 9*(4), 293-298.

Knight, R., Piette, C. E., Page, H., Walters, D., Marozzi, E., Nardini, M., ... & Jeffery, K. J. (2014). Weighted cue integration in the rodent head direction system. *Philosophical Transactions of the Royal Society of London B: Biological Sciences*, *369*(1635), 20120512.

Loomis, J. M., Klatzky, R. L., Golledge, R. G., & Philbeck, J. W. (1999). Human navigation by path integration. In R. G. Golledge (Ed.), *Wayfinding: Cognitive mapping and other spatial processes* (pp. 125-151). Baltimore: Johns Hopkins.

Mou, W., & Zhang, L. (2014). Dissociating position and heading estimation: rotated visual orientation cues perceived after walking reset headings but not positions. *Cognition*, *133,* 553-571.

Müller, M., & Wehner, R. (1988). Path integration in desert ants, Cataglyphis fortis. *Proceedings of the National Academy of Sciences*, *85*(14), 5287-5290.

Nardini, M., Jones, P., Bedford, R., & Braddick, O. (2008). Development of cue integration in human navigation. *Current Biology, 18*(9), 689-693.

Shettleworth, S. J., & Sutton, J. E. (2005). Multiple systems for spatial learning: dead reckoning and beacon homing in rats. *Journal of Experimental Psychology: Animal Behavior Processes, 31*, 125-141.

Sjolund, L. A., Kelly, J. W., & McNamara, T. P. (in press). Optimal combination of environmental cues and path integration during navigation. *Memory & Cognition.*

Taube, J. S. (2007). The head direction signal: origins and sensory-motor integration. *Annual Review of Neuroscience*, *30*, 181-207.

Tcheang, L., Bülthoff, H. H., & Burgess, N. (2011). Visual influence on path integration in darkness indicates a multimodal representation of large-scale space. *Proceedings of the National Academy of Sciences*, *108*(3), 1152-1157.

Vickerstaff, R. J., & Cheung, A. (2010). Which coordinate system for modelling path integration? *Journal of Theoretical Biology, 263*(2), 242-261.

Warren, W. H., Kay, B. A., Zosh, W. D., Duchon, A. P., & Sahuc, S. (2001). Optic flow is used to control human walking. *Nature Neuroscience*, *4*(2), 213-216.

Wehner, R. (2003). Desert ant navigation: how miniature brains solve complex tasks. *Journal of Comparative Physiology A*, *189*(8), 579-588.

Wiener, J. M., Berthoz, A., & Wolbers, T. (2011). Dissociable cognitive mechanisms underlying human path integration. *Experimental Brain Research, 208*(1), 61-71.

Whishaw, I. Q., & Brooks, B. L. (1999). Calibrating space: exploration is important for allothetic and idiothetic navigation. *Hippocampus, 9*(6), 659–667.

Yoder, R. M., Clark, B. J., & Taube, J. S. (2011). Origins of landmark encoding in the brain. *Trends in Neurosciences, 34*(11), 561-571.

Zhang, H., Mou, W., & McNamara, T. P. (2011). Spatial updating according to a fixed reference direction of a briefly viewed layout. *Cognition, 119*(3), 419-429.

Zhang, L., & Mou, W. (2017). Piloting systems reset path integration systems during position estimation. *Journal of Experimental Psychology: Learning, Memory, and Cognition, 43*(3), 472-491.

Zhao, M., & Warren, W. H. (2015a). How you get there from here: Interaction of visual landmarks and path integration in human navigation. *Psychological Science, 26*(6), 915-924.

Zhao, M., & Warren, W. H. (2015b). Environmental stability modulates the roles of path integration in human navigation. *Cognition, 142,* 96-109.

Chapter 2

Visual landmarks can increase variability of homing based on path integration

2.1 Abstract

Previous studies showed that visual landmarks and path integration (PI) cues, due to movement, jointly determine human homing behaviors. This study investigated whether the interaction of these two cues occurs in individuals' homing or in estimating positioning (position/heading) that then determines homing. In Experiment 1, the participants learned the locations of five objects (one located at the learning position) in the presence of distal landmarks before walking a two-leg path without viewing the landmarks and objects. At the end of the path, the participants replaced the objects in four cue conditions: 1) PI cue only (PI), 2) landmarks only (LM) where the participants were disoriented and the landmarks reappeared, 3) both the PI cue and the reappearing landmarks (BO), and 4) both the PI cue and conflicting landmarks rotated 45º (CO). The participants' heading, position, and homing estimations were calculated from the response locations of the objects. The ratio of the length of the second leg to that of the first leg (L2/L1) could be 0.5, 1, or 2. The results showed evidence of cue combination in heading estimations in all leg ratios, but evidence of cue combination in homing estimations only occurred in the leg ratio of 0.5. The following experiments, using the leg ratio of 2 only, demonstrated that there was no evidence of cue combination in homing estimation in a typical homing task where the participants walked paths and pointed to the origin without learning the objects (Experiment 2). However, there was evidence of cue combination in heading estimations rather than in homing estimations when proximal landmarks replaced distal landmarks (Experiments 3 and 4). A mathematical model stipulating that cue combination occurs in positioning rather than homing estimations is proposed to explain these findings.

2.2 Introduction

Human navigation relies on two systems. One is the path integration (PI) system, which calculates individuals' position relative to important goals (i.e., home) based on self-motion cues (Gallistel, 1990; Loomis, Klatzky, Golledge, Cicinelli, Pellegrino, & Fry, 1993; Tcheang, Bülthoff, & Burgess, 2011). The other is the piloting system, which calculates individuals' position relative to important goals based on the mental representation of spatial relations between the perceived landmarks and the goal (Collett & Collett, 2010). Homing, going back to the origin of a path (i.e., home), is one of the most importation navigation behaviors. To understand human spatial navigation, several studies have examined the interaction between the piloting system and the path integration system in human homing behavior (Chen, McNamara, Kelly, & Wolbers, 2017; Nardini, Jones, Bedford, & Braddick, 2008; Sjolund, Kelly, McNamara, in press; Zhao & Warren, 2015). Most studies investigated whether and how the cues in these two systems are combined to guide human homing behavior.

2.2.1 Cue combination versus cue competition

Cue combination has two different definitions, a broad one and a restricted one. Broadly speaking, cue combination refers to any linearly weighted average of the estimations based on each single cue as illustrated in the following equation:

$$E_{12} = W_1 \times E_1 + W_2 \times E_2 \quad (2.1)$$

where E_{12} is the combined estimation in the presence of both cues, E_1 and E_2 are the estimations based on each single cue. W_1 and W_2 are the weights, ranging from 0 to 1, and $W_1 + W_2 = 1$.

Assuming the estimations based on each single cue are independent, the variance of the combined estimation can be calculated from the variances of each single cue:

$$\sigma_{12}^2 = W_1^2 \times \sigma_1^2 + W_2^2 \times \sigma_2^2 \quad (2.2)$$

where σ_{12}^2 is the variance of the combined estimation in the presence of both cues; σ_1^2 and σ_2^2 are the variances of estimations based on each single cue.

A restricted definition of cue combination postulates that individuals combine two cues to reduce estimation variability based on each single cue. Individuals tend to weigh the cues with higher reliability (or smaller variability) heavier than the cues with lower reliability (or larger variability) in the combination. The combination that leads to the minimum variance of the combined estimation among all possible weights is called *Bayesian combination* or *optimal combination*. More specifically, in the Bayesian or optimal combination, the weight assigned to each cue is inversely proportional to the estimation variance based on the cue (Cheng, Shettleworth, Huttenlocher, & Rieser, 2007; Ernst & Banks, 2002). The minimum variance is termed *the optimal variance* and the weight leading to the optimal variance, *the optimal weight*. The following two equations illustrate how to calculate the optimal weight and variance from the variance of the estimation based on each single cue. The optimal weight for cue one and two ($W_{1_{optimal}}$ and $W_{2_{optimal}}$) are calculated:

$$W_{1_{optimal}} = \frac{\sigma_2^2}{\sigma_1^2 + \sigma_2^2} \quad (2.3)$$

$$W_{2_{optimal}} = \frac{\sigma_1^2}{\sigma_1^2 + \sigma_2^2} \quad (2.4)$$

Therefore, the variance of the combined estimate ($\sigma_{12_{optimal}}^2$) is:

$$\sigma^2_{12_{optimal}} = \frac{\sigma_1^2 \times \sigma_2^2}{\sigma_1^2 + \sigma_2^2} \quad (2.5)$$

The quasi-Bayesian combination does not require the exact inverse relation between the weight and variance, but still expects that a larger weight is assigned to the cue that produces a smaller estimation variance so that the variance of the combined estimation is reduced (a sub-optimal way).

In contrast to the Bayesian or quasi-Bayesian combination, cue competition stipulates that the homing estimation might primarily be determined by one system (e.g., the piloting system) regardless of the relative variance of the estimations based on either cue (Zhao & Warren, 2015). Note that cue competition falls under the broad definition of cue combination that refers to any linearly weighted average of the estimations based on each single cue.

Several studies investigated whether and how people combine landmarks and path integration cues to determine the home location (Chen et al., 2017; Nardini et al., 2008; Sjolund et al., in press; Zhao & Warren, 2015). In a typical paradigm, the participants started from the origin (home) in the presence of landmarks and then walked a path. When they finished the path, they walked back to the origin in different cue conditions. (1) In the path integration system only (PI) condition, the landmarks were removed before the participants walked back to the origin. This manipulation allows people to rely only on the path integration system in the inbound path. (2) In the landmark only condition (LM), the participants were rotated for disorientation before walking back to the origin. After disorientation, the landmarks were presented again. The participants walked back to the origin in the presence of the landmarks. The disorientation procedure was undertaken to disrupt people's self-motion sense and allow them to only rely on landmarks in the inbound path. (3) In the both cues condition (BO), the participants, without

being disoriented, walked back to the origin in the presence of the landmarks. (4) In the conflict condition (CO), the participants, without being disoriented, walked back to the origin in the presence of the landmarks that had been rotated. In this condition, the two cues indicated conflicting homes.

To study cue combination, researchers examined the observed homing variance in the four cue conditions (e.g., Chen et al., 2017; Nardini et al., 2008; Sjolund et al., in press; Zhao & Warren, 2015). A quasi-Bayesian combination is determined if the observed variances in the two cue conditions (BO and CO) are smaller than those in both the single cue conditions (PI and LM). Moreover, Bayesian combination is qualified if the observed variance in the BO/CO condition does not differ from the optimal variance (see Equation 2.5). The observed weight in the CO condition is also used to test the Bayesian combination. When the estimates from the two single cues differ, the relative proximity of the observed mean in the CO condition to the predictions by single cues reflects the weight assigned to each cue. In particular, the cue with a smaller proximity has a larger weight. The cue weight measured from the proximity is typically referred to as *the observed weight* in contrast to the optimal weight (Chen et al., 2017). In the Bayesian combination, the observed weight should be comparable to the optimal weight. In addition, the observed weight in the CO condition is also used to test cue competition. In cue competition, the observed weight is 0 or 1 for each cue regardless of the relative reliability (or variance).

The relations between the observed weight and observed variance in the CO condition are also used to test the broadly-defined cue combination (Nardini et al., 2008). In a linear combination (Equation 2.1), given the observed variance of single cue conditions, the variance of the combination can be calculated for any possible weight (see 2.2). Therefore, the variance of the combined estimation by assigning the observed weight is calculated. The linear combination

is qualified if the observed variance in the CO condition is not different from the predicted variance for the observed weight in the CO condition.

The majority of the past studies found that human adults could optimally or sub-optimally combine the homing estimations from the piloting and path integration systems (Chen et al., 2017; Nardini et al., 2008; Sjolund et al., in press; Zhao & Warren, 2015). Variability of the homing estimations in the BO or CO condition was reduced and could be predicted by the Bayesian or quasi-Bayesian combination. Furthermore, the observed weight assigned to each system was also comparable to the optimal weight. However, there are also results that undermine the cue combination. Zhao and Warren (2015) also found that the participants combined the two cues to reduce variability of the homing estimations in the BO or CO condition. However, the participants in the study dominantly used one cue to determine the homing direction in the CO condition, consistent with the cue competition theory. The discrepant results from the measurements of variability and the mean of the homing estimations cannot be explained by a broadly-defined combination. In a linear combination, cue competition (using a weight of 1 or 0) cannot reduce variance in the combined estimation. More recently, Petrini, Caradonna, Foster, Burgess, and Nardini (2016) demonstrated evidence that adults could not combine visual and self-motion cues in a task of path reproduction, opposite to the original findings in homing estimations in Nardini et al.'s (2008) study.

2.2.2 The homing hypothesis and the positioning hypothesis

Despite the substantial examination of whether and how the piloting and path integration systems are combined (cue combination or cue competition) to guide human homing behavior, there are few studies investigating when cue combination occurs. We posit that there are two possible stages at which the estimations from the path integration and the piloting systems are

combined. One possibility is that cue combination occurs in homing estimation. Both the path integration and piloting systems produce an independent estimation of home. These two home estimations are then combined to a final homing estimation. We refer to this possibility as *the homing hypothesis*. The second possibility is that cue combination occurs in determining the participants' position and heading. The piloting and the path integration systems do not produce two separate homing estimations. Instead, these two systems produce separate positioning (position/heading) estimations. These positioning estimations from the two systems are then combined. Using the combined positioning estimation, individuals determine the home location. We refer to this possibility as *the positioning hypothesis*. Figure 2.1 highlights the difference between these two possibilities.

The distinction between these two hypotheses is theoretically important. The positioning hypothesis implies that the piloting and path integration systems may use the same cognitive map rather than two different maps. The piloting and path integration systems determine individuals' positions and headings in a common cognitive map (Gallistel, 1990; Gallistel & Matzel, 2013; Müller & Wehner, 1988; Zhang, Mou, & McNamara, 2011). In contrast, the homing hypothesis implies that the piloting and path integration systems may use two different maps (Vickerstaff & Cheung, 2011). While the piloting system uses an allocentric map consisting of interobject spatial relations, the path integration system might use an egocentric map consisting of self-object spatial relations (Benhamou, Sauvé, & Bovet, 1990; Fujita, Loomis, Klatzky, & Golledge, 1990; Wang & Spelke, 2002).

A. The homing hypothesis[1]

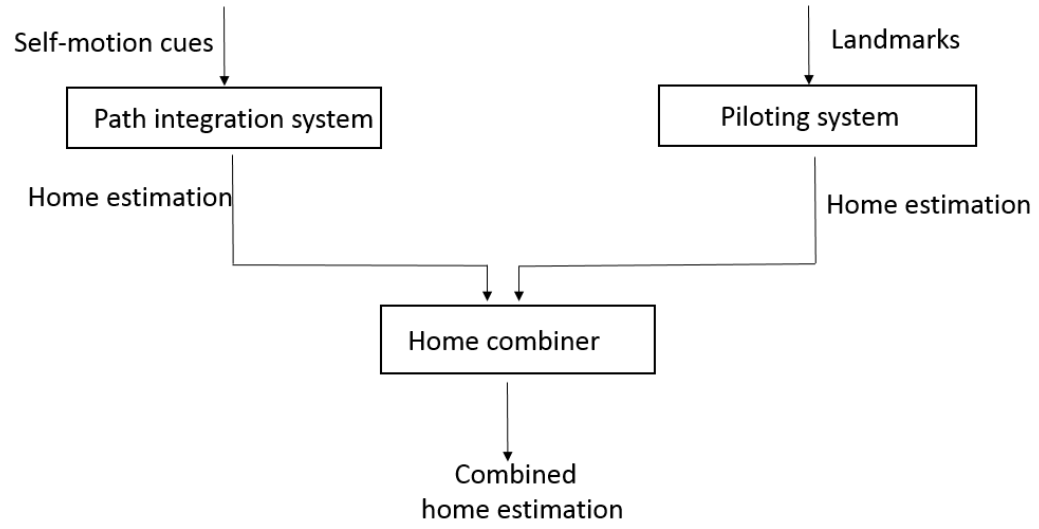

B. The positioning hypothesis

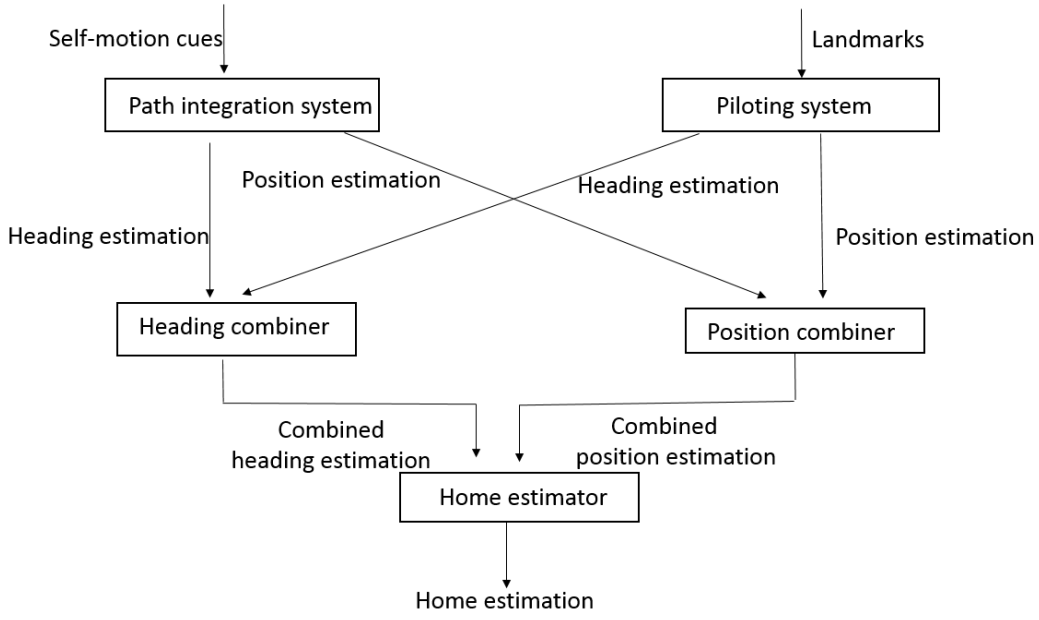

Figure 2.1 Schematic diagrams of the two hypotheses in Chapter 2.

A. The homing hypothesis. B. The positioning hypothesis.

[1] In the homing hypothesis, each system may also use position and heading representations to calculate the homing estimation within the system.

The majority of studies examining cue combination of the path integration and piloting systems showed that the homing response (homing location or direction) for human adults in the BO and CO conditions can be predicted by Bayesian or quasi-Bayesian combination of homing response in the single cue conditions (Chen et al., 2017; Nardini et al., 2008; Sjolund et al., in press; but see Zhao & Warren, 2015). Therefore, these findings are consistent with the homing hypothesis.

In contrast, the literature also shows evidence of cue interaction in the positioning estimations prior to homing estimations, consistent with the positioning hypothesis. In a path integration model for ants, Müller and Wehner (1988) proposed that ants used skylights to determine their headings before calcuating the homing vector, indicating that for ants, the piloting cues (skylights) affect the heading estimations in the path integration system. Etienne, Maurer, Boulens, Levy and Rowe (2004) showed that hamsters, after briefly seeing rotated environmental cues, went to the nest that was consistent with the rotated environmental cues, although these cues were not perceivable during homing. This finding indicates that the piloting system (rotated environmental cues) reset the positioning estimations in the path integration system prior to homing.

Neuroscience literature also shows that either path integration cues or landmarks can activate rodents' place cells or head direction cells (Muller, 1996; Taube, 2007). Studies also suggest that cue combination occurs in the monkeys' heading judgement. Fetsch and his colleagues found that monkeys could combine the visual and vestibular cues to improve the precision of their heading judgement (i.e., the direction of translational self-motion) in the Bayesian manner. Correspondingly, the population of multimodal neurons of the monkeys in the dorsal medial superior temporal area (MSTd) showed increased firing sensitivity when the visual

and vestibular cues showed congruent heading information. Furthermore, the correlation between the neuronal and behavioral responses was revealed in a trial-by-trial base (Fetsch, DeAngelis, & Angelaki, 2010; Fetsch, DeAngelis, & Angelaki, 2013; Fetsch, Pouget, DeAngelis, & Angelaki, 2012).

Two human studies measuring the heading and position estimations have also demonstrated that the path integration and piloting systems could interact in the positioning estimations prior to homing. In the study of Mou and Zhang (2014), the participants learned five objects' locations in the presence of distal landmarks. The participants then walked the path after the landmarks and objects had been removed. After the participants walked the path, the distal landmarks rotated and reappeared. The participants then replaced the objects at the end of the path. The participants' heading and position estimations were calculated from the response locations of the objects. The results showed that the participants' heading estimations were determined by the rotated landmarks, while their position estimations were determined by the path integration system. Furthermore, Zhang and Mou (2017) reported that a proximal visual landmark that had been displaced to the participants' testing position reset their position estimations but not their heading estimations from the path integration system. These results suggest that cue interaction occurs in human heading or position estimations prior to homing estimations, consistent with the positioning hypothesis.

However, there is no study examining cue combination of the path integration and piloting systems in human positioning and homing estimations simultaneously. Thus, no empirical evidence so far can dissociate the positioning hypothesis from the homing hypothesis.

2.2.3 Current study

The primary purpose of the current study was to distinguish between the homing hypothesis and the positioning hypothesis by simultaneously examining cue combination in positioning and homing estimations.

To simultaneously measure homing and positioning estimations, the current study adopted the method used in the previous studies to simultaneously calculate homing errors, position errors, and heading errors (Mou & Zhang, 2014; Zhang & Mou, 2017). The participants learned the locations of five objects (Figure 2.2 just showed one object X for illustration) in the presence of landmarks at the path origin (marked as O in Figure 2.2) in an immersive virtual reality environment. One of the objects was placed at the origin (i.e., O). The participants then walked a two-leg path (O-T-P, in Figure 2.2) after the objects and the landmarks were removed. After walking the path, the participants (standing at P, in Figure 2.2) replaced the five objects to their original locations. A homing estimation (the bearing of PO' in Figure 2.2) was obtained from the participants' response location of the object at O. As shown in Figure 2.2 and in the Appendix, the participants' position estimation (the bearing of OP') and heading estimation (the direction of H') were calculated from a pair between the participants' response locations to O and any one of the four other objects (e.g., X in Figure 2.2) (Mou & Zhang, 2014; Zhang & Mou, 2017). Four position estimations (OP') and heading estimations (H') were calculated in each trial, as there were four other objects. Their circular mean was used as measures of the estimated position and estimated heading for this trial.

To test cue combination, this study used four cue conditions as in the previous studies (Chen et al., 2017; Nardini et al., 2008; Sjolund et al., in press; Zhao & Warren, 2015) when the participants replaced objects at the end of the path. In the path integration condition (PI), the

participants just replaced the objects. In the landmark condition (LM), the participants were disoriented before the landmarks reappeared at the original locations. In the both cues condition (BO), the participants were not disoriented and the landmarks appeared at the original locations. In the conflict condition (CO), the participants were not disoriented and the landmarks reappeared at the locations rotated 45°. The participants conducted four trials (by walking four paths) in each of the four cue conditions. As we had four trials in each condition, we obtained the means and variabilities of the position and heading estimations in addition to the homing estimation across the trials for each cue condition.

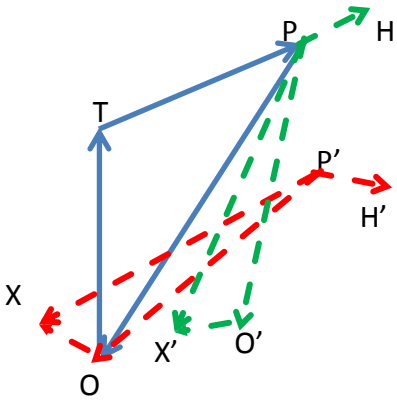

Figure 2.2 Illustration of HER, PER and β in Chapter 2.

A hypothetical person walks a path starting at O, turning at T and ending at P. H is the heading at P. The response locations of the origin O and another object X are O' and X', respectively. Assume that the person's estimations of P and H are P' and H', respectively. HER denotes the heading errors, PER denotes the position errors, and β denotes the homing errors. As defined, HER = H'- H; PER = OP' – OP; homing error (β) = PO' – PO. In the above definitions, PO', PO, OP', and OP are all bearings, defined as a signed angular distance from a reference direction in a horizontal plane (e.g., the first walking leg OT). In addition to β = PO' – PO, PER can be

calculated according to OP' – OP = (OX – PO) – (O'X'– PO') and HER can be calculated according to HER = PER – β.

The critical difference between the homing hypothesis and the positioning hypothesis occurs at the stage when the two cues combine. The homing hypothesis predicts that the combination occurs in homing estimations but not in positioning estimations, whereas the positioning hypothesis stipulates that the combination occurs in positioning estimations but not in homing estimations. To simplify the contrast between these two hypotheses, we primarily examined cue combination for heading and homing estimations. Cue combination for position estimations was examined only in the last experiment.

For both heading and homing estimations, we examined whether estimations in the BO and CO conditions could be explained by the Bayesian and quasi-Bayesian cue combination of estimations of PI and LM conditions. We also examined whether estimations in the CO condition could be explained by a broadly-defined combination (i.e., linear combination).

More specifically, first, in both BO and CO conditions, we tested whether people used two cues in the quasi-Bayesian combination manner. We compared the estimation variability in the BO/CO condition with the variabilities in the PI and LM conditions. If the observed variability in the BO/CO condition is larger than that in either of the single cue conditions, or is comparable to those in both LM and PI conditions, indicating a non-reduced or even increased variability in the BO/CO condition, then we reject the quasi-Bayesian combination. Otherwise,

we do not have clear evidence to reject the quasi-Bayesian combination[2]. Second, in both BO and CO conditions, we tested whether people used the two cues in the Bayesian combination manner. We compared the observed variability in the BO/CO condition to the optimal variability (from the combination by the optimal weights) (see Equation 2.5). If the former is larger than the latter, then we reject the Bayesian combination. Otherwise, we do not have clear evidence to reject the Bayesian combination. Third, in the CO condition, we compared the observed weight with the optimal weight (Equation 2.3 and 2.4). If the former differs from the latter, then we reject the Bayesian combination. Otherwise, we do not have clear evidence to reject the Bayesian combination. Last, in the CO condition, we also tested whether the relation between the observed variability and the observed weight can be explained by a broadly-defined cue combination, which can be any linear combination. If the observed variance differs from the predicted variance for the observed weight, then we reject the broadly-defined combination. Otherwise, we do not have clear evidence to reject the broadly-defined combination. Following these rules, we summarized the testing results against each combination models in previous studies using the homing paradigm as shown in Table 2.1A and Table 2.1B.

Before introducing the key manipulation that was used to dissociate the positioning hypothesis from the homing hypothesis in the current study, we first describe a mathematical model elaborating on the positioning hypothesis to predict heading estimations error (HER), position estimations error (PER), and homing estimations error (β) in each cue condition. To simplify the modeling, we assume that distal landmarks are only used to provide heading but not position information.

[2] When the variability of one cue (the better one) is much smaller than that of the other cue, although the variability of the quasi-Bayesian combination should be numerically smaller than those of both single cue conditions, it may not be significantly smaller than that of the better cue due to the statistic power.

As illustrated in Figure 2.2, HER is measured as the angular difference between the estimated heading (H') and the correct heading (H). PER is measured as the angular difference between the direction of the estimated testing position relative to the origin (OP') and the direction of the correct testing position relative to the origin (OP). The homing error (β) is measured as the angular difference between the estimated homing direction (PO') and the correct homing direction (PO). The model stipulates that β, PER, and HER should follow the equation:

$$\beta = \text{PER} - \text{HER} \tag{2.6}$$

Table 2.1 Summary of the homing combination results in the literature in Chapter 2

(A) Summary of the testing results of the standard deviation (SD) for the homing estimations in the both cue (BO) condition against the quasi-Bayesian combination model and the Bayesian-combination model in the literature.

Homing Estimations (BO condition)			
	Quasi-Bayesian combination		Bayesian-combination
	SD in the PI condition	SD in the LM condition	optimal SD
	>, =, or <	>, =, or <	>, =, or <
Chen et al., 2017, Exp 1A, rich environment	<	=	=
Chen et al., 2017, Exp 1A, poor environment	=	=	>
Chen et al., 2017, Exp 1B, no body rotation	=	<	>
Chen et al., 2017, Exp 1B, body rotation	<	<	=
Chen et al., 2017, Exp 2, stable LM	<	=	=
Chen et al., 2017, Exp 2, unstable LM	=	=	>
Chen et al., 2017, Exp 3, vision positive	<	<	=
Chen et al., 2017, Exp 3, self-motion positive	<	<	>
Chen et al., 2017, Exp 4	<	<	=
Nardini et al.'s, 2008, adult group	<	<	=
Sjolund et al., 2017,	<	<	=
Zhao & Warren, 2015, proximal landmark group	<	=	=
Zhao & Warren, 2015, distal landmark group	<	<	=
Zhao & Warren, 2015, distal PI group	<	<	=

(B). Summary of the testing results of the standard deviation (SD) for the homing estimations in the conflict (CO) condition against the quasi-Bayesian combination model, Bayesian combination model, and the linear combination model in the literature.

Homing Estimations (CO condition)					
	Quasi-Bayesian combination		Bayesian-combination		Linear combination
	SD in the PI condition	SD in the LM condition	optimal SD	optimal weight	predicted SD for the observed weight
	>, =, or <	>, =, or <	>, =, or <	>, =, or <	>, =, or <
Chen et al., 2017, Exp 1A, rich environment	<	=	=	>	NA
Chen et al., 2017, Exp 1A, poor environment	<	<	=	=	NA
Chen et al., 2017, Exp 1B, no body rotation	<	<	=	=	NA
Chen et al., 2017, Exp 1B, body rotation	<	=	=	=	NA
Chen et al., 2017, Exp 2, stable LM	<	=	=	=	NA
Chen et al., 2017, Exp 2, unstable LM	=	=	>	=	NA
Chen et al., 2017, Exp 3, vision positive	<	<	=	=	NA
Chen et al., 2017, Exp 3, self-motion positive	<	<	>	=	NA
Chen et al., 2017, Exp 4	<	<	=	=	NA
Nardini et al.`s, 2008, adult group	NA	NA	>	=	=
Sjolund et al., 2017, small conflict	<	=	NA	<	NA
Sjolund et al., 2017, large conflict	NA	NA	>	<	=
Zhao & Warren, 2015, proximal landmark group (LM shift $\leqslant 90°$)	NA	NA	=	>	=

Zhao & Warren, 2015, proximal landmark group (LM shift ⩾115°)	NA	NA	>	**<**	=
Zhao & Warren, 2015, distal landmark group	NA	NA	=	**>**	=
Zhao & Warren, 2015, distal PI group	NA	NA	=	**<**	=

Note: ">" indicates that the SD (or weight) in the BO/CO condition was significantly larger than the model prediction. "=" indicates that the SD (or weight) in the BO/CO condition was comparable to the model prediction. "<" indicates that the SD (or weight) in the BO/CO condition was significantly smaller than the model prediction. The symbol in red and bold indicates that the result is against the model.

It is important to note that in the path integration system, PER depends on the error in estimating the turning direction at T (Figure 2.2). As HER measures the error in estimating the turning direction (i.e., TP), PER depends on HER. Furthermore, the dependency of PER on HER increases with the leg ratio of the second leg to the first leg of the path. We use three special examples to illustrate this idea. As illustrated in Figure 2.3, when the leg ratio (L2/L1) is 1 (Figure 2.3A), PER is half of HER (0.5 × HER); when the leg ratio is infinitely large (Figure 2.3B), PER is the same as HER (1× HER); when the leg ratio is 0 (Figure 2.3C), PER is 0 and then independent of HER (0 × HER). Generalizing from these examples, we assume that PER and HER in the path integration system (PER_{PI} and HER_{PI}) follow a linear relation:

$$PER_{PI} = a \times HER_{PI} + ue \quad (2.7)$$

ue is short for unexplained error, the error that cannot be explained by HER_{PI}[3]. *a* is the slope that is assumed to increase with the leg ratio (e.g., should be 0, 0.5, and 1 when the ratio is 0, 1, and infinitely large, respectively). Using Equation 2.6 and 2.7, we calculate the homing error in the path integration system (β_{PI}) (See Table 2.2).

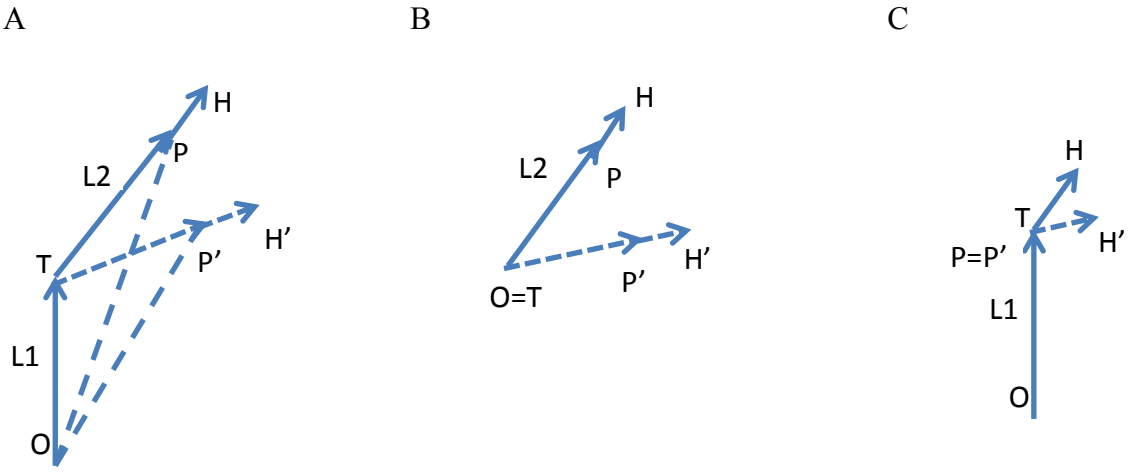

Figure 2.3 The relationship between PER and HER in the path integration system in Chapter 2. Illustrations of the relationship between PER (i.e., OP' – OP) and HER (i.e., H' – H) in the path integration system. An individual walks from O to T (i.e., L1) and turns at T and walks from T to P (i.e., L2), facing H. This individual estimates the turning angle with an error, which equals to HER. (A) When the leg ratio (L2/L1) is 1, PER should be half of HER. (B) When the leg ratio is infinitely large (just like the first leg is very short), the PER should be the same as HER. (C) When the leg ratio is 0, the PER should be 0 and independent of HER.

In the LM condition, as the participants were disoriented in place at the end of the path, the heading estimation in the path integration system was disrupted, while the position estimation was intact (Mou & Zhang, 2014). Furthermore, distal landmarks alone could provide heading

[3] Unexplained error could be due to distance estimation error and other random errors in estimating positions.

information, but not position information (Mou & Zhang; Taube, 2007; Zhao & Warren, 2015). Therefore, the participants' heading estimation was determined by the distal landmarks, whereas their position estimation was determined by the path integration (Mou & Zhang, 2014). Following 2.6, the homing error in the LM condition (β_{LM}) could be calculated by subtracting the heading estimation in the piloting system (HER_{LM}) from the position estimation in the path integration system (PER_{PI}).

Table 2.2 Summary of the predictions of HER, PER and β and their variances in Chapter 2. Summary of the predictions of the heading error (HER), position error (PER), homing error (β), variance of heading error (σ^2_{HER}), variance of position error (σ^2_{PER}), and variance of homing error (σ^2_{β}) in the conditions of landmark (LM), path integration (PI), and both cues (BO) based on a mathematical model elaborating on the positioning hypothesis. *ue* is the unexplained error and *a* is the slope of the regression line between HER_{PI} and PER_{PI}. $W_{HER_{LM}}$ is the heading weight assigned to the piloting system and $W_{HER_{PI}}$ is the heading weight assigned to the path integration system ($W_{HER_{LM}} + W_{HER_{PI}} = 1$). The model assumes that only distal landmarks are used.

	PI	LM	BO
HER	HER_{PI}	HER_{LM}	$W_{HER_{LM}} \times HER_{LM} + W_{HER_{PI}} \times HER_{PI}$
PER	$a \times HER_{PI} + ue$	$a \times HER_{PI} + ue$	$a \times HER_{PI} + ue$
β	$(a-1) \times HER_{PI} + ue$	$a \times HER_{PI} + ue - HER_{LM}$	$(a - W_{HER_{PI}}) \times HER_{PI} - W_{HER_{LM}} \times HER_{LM} + ue$
σ^2_{HER}	$\sigma^2_{HER_{PI}}$	$\sigma^2_{HER_{LM}}$	$W^2_{HER_{PI}} \times \sigma^2_{HER_{PI}} + W^2_{HER_{LM}} \times \sigma^2_{HER_{LM}}$
σ^2_{PER}	$a^2 \times \sigma^2_{HER_{PI}} + \sigma^2_{ue}$	$a^2 \times \sigma^2_{HER_{PI}} + \sigma^2_{ue}$	$a^2 \times \sigma^2_{HER_{PI}} + \sigma^2_{ue}$
σ^2_{β}	$(a-1)^2 \times \sigma^2_{HER_{PI}} + \sigma^2_{ue}$	$a^2 \times \sigma^2_{HER_{PI}} + \sigma^2_{HER_{LM}} + \sigma^2_{ue}$	$(a - W_{HER_{PI}})^2 \times \sigma^2_{HER_{PI}} + W^2_{HER_{LM}} \times \sigma^2_{HER_{LM}} + \sigma^2_{ue}$

In the both cues condition, according to this model, the heading estimation (HER_{BO}) was from a weighted average of the heading estimations produced by the two systems (HER_{PI} and HER_{LM}). As mentioned above, the participants' position estimation was determined by the path integration system. Following Equation 2.1, the homing error in the BO condition (β_{BO}) could be calculated by subtracting the combined heading estimation (HER_{BO}) from the position estimation in the path integration system (PER_{PI}).

The conflict condition should be the same as the both cues condition, except that there is a systematic difference between the prediction of HER_{LM} and the prediction HER_{PI}. For instance, if we define the predicted HER_{PI} as 0°, then the predicted HER_{LM} is the opposite of the signed rotation angle of the landmark (i.e., -45° if the landmark is rotated 45°). The weights assigned to different cues would change the observed means of HER and β, but not the variance of them in the CO condition.

We summarized all individual HER, PER, and β in all conditions in Table 2.2. Using these individual estimation errors, we can calculate the corresponding estimation variance (Table 2.2).

According to Table 2.2, if we have variance of HER_{PI}, *a,* and *ue* from the PI condition, and variance of HER_{LM}, we can calculate variance of the estimations for HER, PER, and β in all four conditions. Based on these equations in Table 2.2, Figure 2.4 plots a simulation of standard deviation (SD) for HER, PER, and β in the BO condition as a function of landmark weight in estimating headings (i.e., $W_{\mathrm{HER}_{LM}}$). This simulation assumes that the variance of HER_{LM} is much smaller than the variance of HER_{PI} (i.e., $\sigma^2_{\mathrm{HER_{LM}}}/\sigma^2_{\mathrm{HER_{PI}}} = 0.25$), as distal landmarks may produce a much more precise heading estimation than the path integration system (Taube, 2007; Zhao & Warren, 2015). This simulation also assumes that variance of *ue* is minimum (i.e., $\sigma^2_{ue} = 0$)[4]. Three different assumed values of *a* (i.e., 0.66, 0.5, and 0.33*)* are used.

[4] The conclusion from the simulation does not depend on the assumption that $\sigma^2_{ue} = 0$. According to Table 2.2, σ^2_{ue} is constant in σ^2_{β} for PI, LM, and BO conditions regardless of the weights of LM. The value of σ^2_{ue} should not affect the weight for largest reduction of σ^2_{β} in Figure 2.4.

A

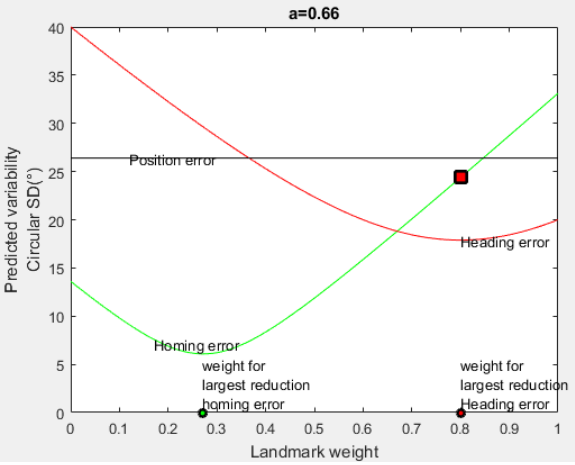

B

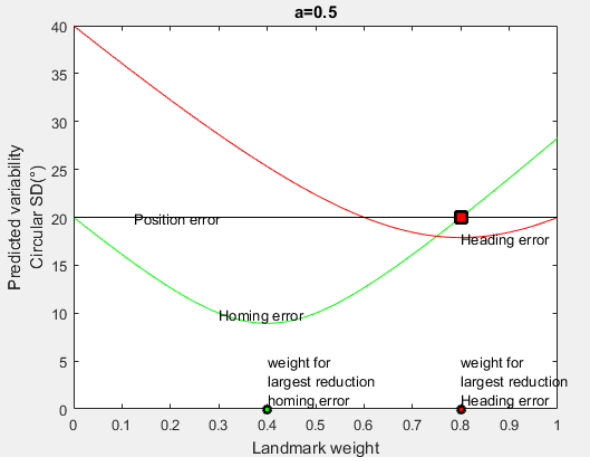

C

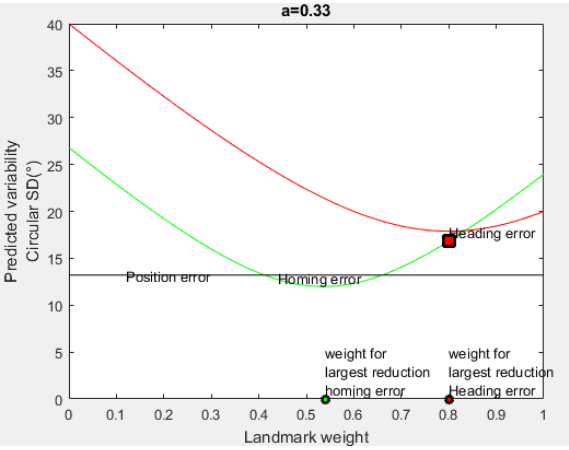

Figure 2.4. Simulations of SDs of HER, PER and β in Chapter 2.

Simulations of the standard deviation (SD) of heading errors (HER), position errors (PER) and homing errors (β), respectively, as a function of the landmark weight in heading estimations ($i.e.W_{\mathrm{HER}_{LM}}$) based on the equations in Table 2.2. In the simulation, the slope a is set to be 0.66 (A), 0.5 (B) or 0.33 (C). $\sigma^2_{\mathrm{HER_{LM}}}/\sigma^2_{\mathrm{HER_{PI}}}$= 0.25 and $\sigma^2_{ue} = 0$. The red curve plots the SD of HER as a function of a landmark weight in heading estimations. The black line plots the SD of PER as a function of a landmark weight in heading estimations. As the position estimation does not vary according to the landmark weight in heading estimations, the SD of PER is flat. The green curve plots the SD of β as a function of the landmark weight in heading estimations. The red square on

the green curve denotes the predicted SD of β corresponding to the landmark weight that produces the largest reduction of HER variability. The green and red dots on the x axis are the landmark weights in heading estimations that lead to the smallest SDs of β and HER, respectively. Note that the distance between the green and the red dots increased with the value of the slope *a*.

In general, the findings of this simulation indicate that variability of HER_{BO} is reduced by assigning a larger landmark weight in heading estimation because $\sigma^2_{\mathrm{HER_{LM}}}$ is smaller than $\sigma^2_{\mathrm{HER_{PI}}}$, consistent with the Bayesian or quasi-Bayesian cue combination model. The largest reduction occurs when the landmark weight is 0.8 regardless of the slope *a*. Importantly, the landmark weight in heading estimations that produces the largest reduction in variance of homing errors (β_{BO}) depends on the slope *a*. Note that, with an increase of *a*, the distance between the landmark weight that produces the largest reduction of β_{BO} variability (i.e., smallest SD of β_{BO}) and the landmark weight that produces the largest reduction of the HER_{BO} variability (i.e., smallest SD of HER_{BO}) increases. Therefore, with a larger *a*, it is less likely to obtain the reduction of β_{BO} variability and reduction of HER_{BO} variability given the same landmark weight. Therefore, the quasi-Bayesian or Bayesian combination cannot be evident for both heading estimation and homing estimation, dissociating the positioning hypothesis from the homing hypothesis. Indeed, with a larger *a*, the variability of $\beta_{BO,}$ given the landmark weight that produces the smallest HER_{BO} variability (indicated by the red square in Figure 2.4A), is even larger than the variability of β_{PI} (i.e., SD of β_{BO} when the landmark weight is 0). In other words, combining heading estimations from the path integration system and the piloting system to reduce heading variability could increase homing variability. Therefore, using a large slope of *a*,

we might confirm the Bayesian or quasi-Bayesian combination in heading estimations but disconfirm the Bayesian or quasi-Bayesian combination in homing estimations, dissociating the positioning hypothesis from the homing hypothesis. As discussed above (see Figure 2.3), the slope *a* increases with the leg ratio (L2/L1). Therefore, we could distinguish between the homing hypothesis and the heading hypothesis by manipulating the leg ratio. These two hypotheses are more likely to be distinguished with a larger leg ratio.

2.2.3.1 Experiment 1

Experiment 1 used distal landmarks and three different leg ratios (L2/L1 = 2, 1, or 0.5). The first purpose of this experiment was to dissociate the positioning hypothesis from the homing hypothesis by examining the cue combination in homing and heading estimations, especially when the leg ratio is large (i.e., L2/L1 = 2). The second purpose of this experiment was to test whether the homing estimations can be predicted by the mathematical model illustrated in Table 2.2.

As a preview, the results of this experiment showed that we could not disconfirm the Bayesian combination in heading estimations in any leg ratio groups. In contrast, we disconfirmed all cue combination models including a linear cue combination in homing estimations when the leg ratio was 2, although we could not disconfirm the Bayesian or the quasi-Bayesian combination in homing estimations when the leg ratio was 0.5 or 1. Therefore, in the following experiments, we further dissociated the positioning hypothesis from the homing hypothesis only using the leg ratio of 2.

2.2.3.2 Experiment 2

Experiment 2 differentiated the positioning hypothesis from the homing hypothesis in a typical homing paradigm with distal landmarks. Without learning any objects' locations, the participants walked the paths with the leg ratio of 2 (L2/L1=2) and then pointed to the origins of the paths in the four cue conditions. As people only pointed to the origin, we could not measure the heading estimations and position estimations in Experiment 2. However, we could still distinguished between these two hypotheses by examining cue combination in homing.

2.2.3.3 Experiment 3

Experiment 3 used proximal landmarks instead of distal landmarks. As distal landmarks were used in Experiment 1 and 2, one may argue that distal landmarks alone do not provide positional information, thus they cannot indicate home locations alone. As cue combination requires two separate estimations, cue combination in homing may not occur because distal landmarks fail to indicate homing estimations alone. The purpose of Experiment 3 was to test whether we could still distinguish between the homing hypothesis and the positioning hypothesis when homing estimations could be indicated by landmarks alone. Particularly, we replaced distal landmarks with proximal landmarks, as proximal ones could indicate home locations alone.

2.2.3.4 Experiment 4

Experiment 4 examined cue combination in position estimations as well as heading and homing estimations. In Experiment 4, instead of disorienting the participants in the LM condition at the end of the path, we disoriented the participants at the turning position (T in Figure 2.2) of the two-leg path. As the path integrations system cannot produce accurate position estimations

any further along the walking path after the participants have been disoriented (Mou & Zhang, 2014), the position estimations at the testing position in the LM condition of Experiment 4 would be solely determined by the piloting system. Therefore, we could examine cue combination in position, as well as heading and homing estimations.

2.3 Experiment 1

In Experiment 1, the participants learned the locations of five objects in the presence of the distal landmarks at the path origin (marked as O, Figure 2.5A & 2.5C) in an immersive virtual reality environment. The participants then walked two-leg paths (O-T-P) after the objects and the distal landmarks were removed. After walking each path, the participants (standing at P) replaced the five objects to their original locations in four different cue conditions. The participants' estimations of their heading, position, and the home location were calculated based on their response locations of the five objects on each path. Across the paths, the variabilities of the estimations of heading, position and home location were calculated.

Importantly, we used three different leg ratios of the second leg over the first leg (i.e., 0.5, 1, and 2). The homing hypothesis predicts that cue combination should occur during homing estimations regardless of the leg ratio in the traveled path. Unlike the homing hypothesis, the positioning hypothesis predicts the following: (1) the participants would combine the information from the path integration and piloting systems to determine their heading estimations, but not their homing estimations. This phenomenon is more likely to occur for the path with a larger leg ratio. (2) The participants would use the information in the path integration system to judge their positions in all four-cue conditions. (3) In the path integration system, the position estimations (PER_{PI}) would be a linear function of the heading estimations (HER_{PI}), and the slope of this function would increase with the leg ratio of the path (L2/L1). Therefore, the dependency

between HER_{PI} and PER_{PI} would also increase with the leg ratio. (4) The variability of homing estimations could be predicted by the mathematical model elaborating on the positioning hypothesis (see Table 2.2).

We shifted landmarks 45° in the CO condition. We speculated that a 45°shift was not too big to see cue combination. It is believed that cue combination occurs when landmarks are slightly or moderately shifted, whereas cue competition occurs when the predictions from the two cues differ significantly (Sjolund et al., in press; Zhao & Warren, 2015). Mou and Zhang's (2014) study suggests that people tend to dominantly use the distal landmarks to judge their headings when the landmarks rotated 100°. Meanwhile, in the present study, we speculated that 45° was not too small of a shift to statistically detect cue combination. If the shift angle was too small, then the experiment might not be able to statistically detect whether the response shift resulted from the landmark shift or random errors.

2.3.1 Method

2.3.1.1 Participants

Eighty-four university students (42 men) participated in the experiment to fulfill the partial requirement for an introductory psychology course. Before the experiment, all participants signed the consent form approved by the University of Alberta Research Ethics Board.

2.3.1.2 Material and Design

A virtual environment containing grassland and a distal circular wall was constructed in the software Sketchup (http://www.sketchup.com/, Sunnyvale, CA) and rendered in the software

Worldviz (http://www.worldviz.com/, Santa Barbara, CA). The virtual environment was displayed in stereo with an nVisor SX60 head-mounted display (HMD) (NVIS, Inc. Virginia). The participants' head motion was tracked with an InterSense IS-900 motion tracking system (InterSense, Inc., Massachusetts).

Three shapes (a circle, rectangle, and polygon) on a distal circular wall with a radius of 50m and a height of 10m served as distal landmarks (Figure 2.5A and 2.5B). The centre of the wall was overlapped with the centre of the room. A virtual blue stick was connected to an InterSense IS-900 wand for pointing (InterSense, Inc., Massachusetts). Similar to moving a cursor by controlling a mouse on the computer screen, the participants could move the wand to control the movement of the virtual stick to point to positions in the virtual environment.

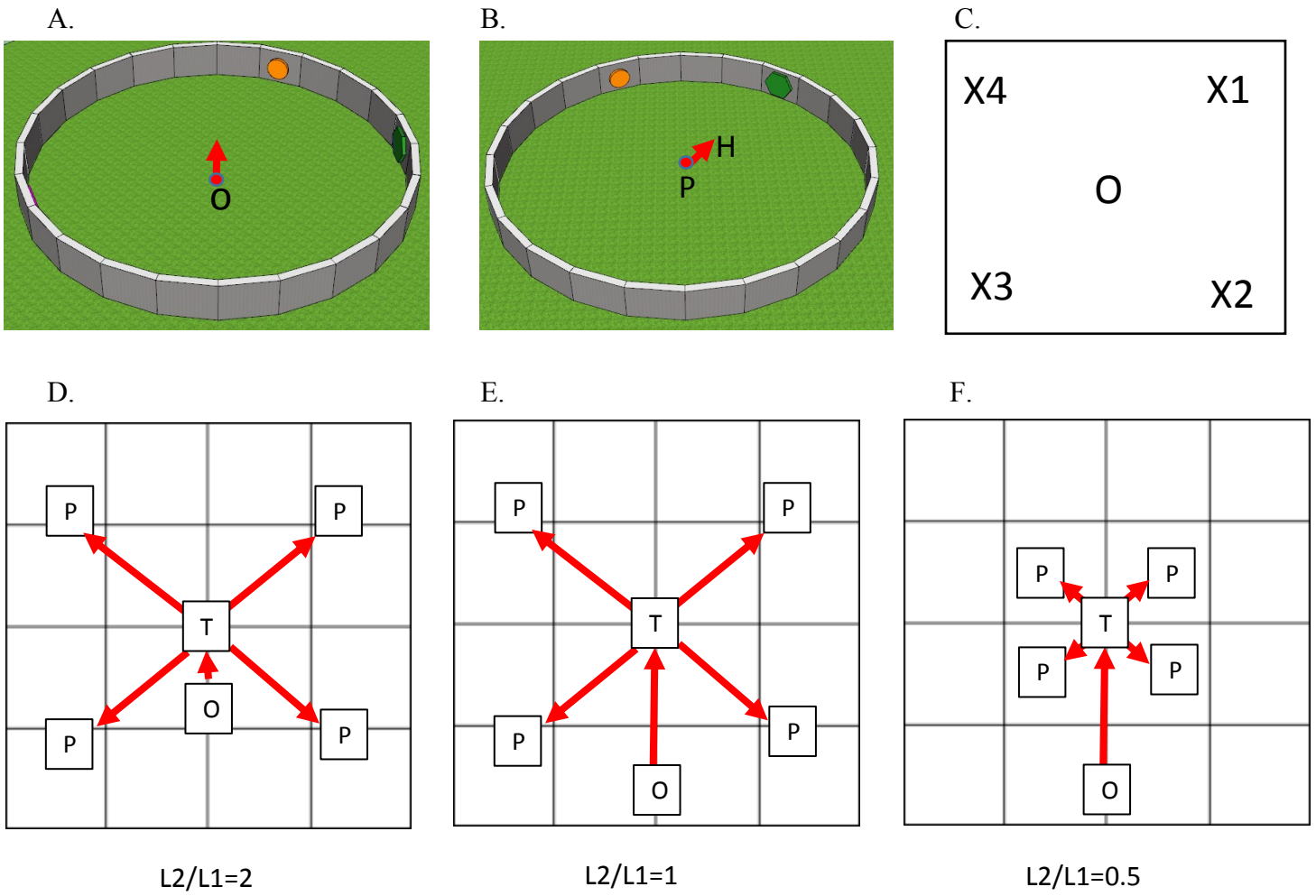

Figure 2.5 Layout and path configuration in Experiment 1 of Chapter 2.

(A) In a grassland, facing the direction indicated by the arrow, the participants learned five objects' locations in the presence of three distal landmarks (a circle, polygon, and rectangle attached to the wall with a radius of 50m) at the origin of the route (i.e., O). One of the objects was placed at the origin O. (B) Standing at P, facing H, the participants replaced the five objects under one of the following conditions: the landmarks were removed so only information in the path integration system was available (PI condition); the landmarks reappeared after the participants were disoriented in place (LM condition); the landmarks reappeared and information in the path integration system was available (BO condition); the landmarks reappeared after being rotated by 45° (an example of counter-clockwise rotation in the figure) and information in

the path integration system was also available (CO condition). (C) participants learned the five objects at O and replaced them at P. (D, E & F) The four paths were respectively used in three different leg ratio groups. Each P indicates one possible end of the second leg. L1 is the length for the first walking leg (OT) and L2 is the length for the second walking leg (TP). Grid squares represent $1m^2$.

Four cue conditions were created: the path integration only (PI), the landmark only (LM), both (BO), and conflict (CO). For all conditions, the distal landmarks (i.e., shapes on the walls) were displayed when the participants learned objects at the origin and walked the 1st leg (i.e., OT in Figure 2.5D & 2.5E & 2.5F). The shapes were removed when the participants reached the turning point (T), but the wall remained throughout the experiment. In the PI condition, the participants entered the testing phase eight seconds after they reached the testing position (P). In the LM condition, when the participants reached the testing location (P), they were rotated in a spinning chair (~90° per second) for eight seconds. After the spin, the shapes reappeared. In the BO condition, the shapes reappeared eight seconds after the participants reached the testing location. The CO condition was the same as the BO condition, except that the shapes reappeared at a 45° clockwise or counter-clockwise from the original direction (counter-clockwise rotation is shown in Figure 2.5B). The landmarks' rotation direction was the same within each participant, while it was clockwise for the half of the participants. Under all conditions, the participants undertook a counting task for eight seconds before entering the testing phase.

Twenty-eight participants (14 men) were randomly assigned to each of the three-leg ratio groups (L2/L1 = 0.5, 1, or 2). All participants completed four paths in each of the four cue

conditions (16 trials in total). The path configurations with different leg ratios are shown in Figure 2.5D, 2.5E, and 2.5F. For each participant, the 16 trials (four paths by four cue conditions) were randomly ordered. In each trial, the participants started from the location O to learn the locations of five objects (i.e., ball, brush, clock, mug, and phone). One object was located at the origin (O). The other four objects were located 1.41m from O in the directions of 45°, 135°, 225°, and 315° clockwise relative to the direction of OT (Figure 2.5C). The associations between objects and positions were random across participants but were consistent across 16 trials for each participant.

For the group of L2/L1 =2, the 1st leg was 0.9m and the 2nd leg was 1.8m. The lengths of the two legs were reversed for the group of L2/L1 = 0.5 (L1=1.8m, L2=0.9m). For the group of L2/L1 =1, both legs were 1.8m. The turning angle could be 50° or 130° clockwise or counter-clockwise, forming four paths. For each path, the origin (O) and the turning point (T) were indicated by two red poles and the test location (P) was indicated by a green pole. All poles were 2m in height, and 0.05m in radius. The poles were presented in sequence to guide the participants' walking (Zhao & Warren, 2015). The poles disappeared once the participants arrived at their positions.

2.3.1.3 Procedure

Before each experimental trial, the participants looked for a red pole that was placed in the origin (O) in the virtual environment and walked towards it. Once they reached the pole, it disappeared and the second red pole that was placed in the turning point (T) appeared. The participants were instructed to turn to face this pole to adopt their learning orientation. The red pole disappeared. The shapes appeared on the wall and five objects appeared on the ground. The

participants learned the directions of the shapes and the locations of the objects (for three minutes in the first trial and for 30 seconds in the remaining 15 trials, as the landmarks and objects remained at the same locations in all trials). Afterwards, the participants were asked to use the wand to replace five objects and indicate the directions of the three landmarks, probed by a small model of each at the left bottom corner of the HMD in a random order, by pointing the virtual stick to the remembered locations of the objects or directions of the shapes. Feedback was given by presenting the probed object or shape at the correct location for five seconds. The participants had two rounds of such replacing and feedback. When the objects disappeared, the participants started to walk the path. A red pole appeared at the turning position (T in Figure 2.5D, 2.5E, and 2.5F) and the participants walked towards it. Once they reached the pole, the shapes and the pole disappeared. A green pole at the test position appeared (illustrated as P in Figure 2.5D, 2.5E, and 2.5F) and guided the participants to walk towards it. Once they reached it, it disappeared. The procedure so far was the same for all cue conditions.

In the PI, BO, and CO conditions, the participants completed a counting task for 8s while they stood at P. They counted the number by repeatedly subtracting three from a given number provided by the experimenter. In the LM condition, the participants sat in a swivel chair and were rotated for 8s, while they were completing the counting task. After the 8s counting task, the shapes reappeared in the LM, BO, and CO conditions. The participants replaced all objects, probed in a random order, using the wand. No feedback was given.

After the participants replaced all objects, all visual items in the virtual environment except the grassland disappeared and the participants were led to a random location in the physical room. As a start of the next trial, a red pole was placed at the origin of the next path.

Before the experimental trials, the participants did a practice trial with different objects and a different path to be familiar with the procedure.

2.3.1.4 Data Analysis

We defined clockwise as the positive direction of angles. Therefore, a positive angular error indicated the clockwise angular distance from the correct direction to the response direction. In the CO condition, we flipped the sign of the individual angular error (i.e., PER, HER, and β) for the participants who experienced the clockwise rotation of the landmarks. Therefore, the HER_{CO} and the β_{CO}indicated by the rotated distal landmarks (all in the clockwise direction now) would be 45° and -45° (i.e., 315°) respectively.

To determine whether the heading or homing estimations were combined, we set the following comparisons: we used the homing estimations (β) as an example below.

To test whether the two cues were combined in the quasi-Bayesian manner, we compared the mean of observed SDs of β_{BO} (β_{CO}) with that in both single cue conditions. If the mean of observed SDs of β_{BO} (β_{CO}) was larger than that of any single cue, or was comparable to that in both single cue conditions, then we would reject the quasi-Bayesian combination model.

To test whether two cues were combined in the Bayesian manner, we compared the mean of observed SDs of β_{BO} (β_{CO}) with the mean of optimal SDs (Equation 2.5). If the former was larger than the latter, we would reject the Bayesian combination model.

In the CO condition, information in the piloting and path integration system would have two different predictions for β. $\beta_{PI-predict}$ would be 0°, whereas $\beta_{LM-predict}$ would be -45°, assuming that the landmarks rotated 45° counter-clockwise around the centre of the wall in the

CO condition. We used the following equation to calculate the observed weight assigned to each system in the CO condition for each participant[5]:

$$W_{\beta_{LM-observed}} = \frac{\beta_{\mathrm{CO-observed}} - \beta_{\mathrm{PI-predict}}}{\beta_{\mathrm{LM-predict}} - \beta_{\mathrm{PI-predict}}} \quad (2.8)$$

We compared the mean of observed weights assigned to the landmark with the mean of optimal weights assigned to the landmark (Equation 2.3 or 2.4) to further test the Bayesian combination. If the mean of observed landmark weights differed from the mean of optimal landmark weights, then we would reject the Bayesian combination model.

In addition, to determine whether the cues were combined in any linear combination way, we compared the mean of observed SDs in the CO condition to the mean of predicted SDs for the observed weights. To calculate the predicted SD for the observed weight for each participant (Equation 2.2), we used the mean of observed weights instead of the observed weight for that participant. If they differed, then we would reject the linear combination model (Nardini et al., 2008; Sjolund et al., in press).

The same testing procedures as described above were applied to test the cue combination for heading estimations. The only difference was that $\mathrm{HER}_{\mathrm{PI-predict}}$ was supposed to be 0°, whereas $\mathrm{HER}_{\mathrm{LM-predict}}$ would be 45° assuming that the landmarks rotated 45° counter-clockwise around the centre of the wall in the CO condition.

It is not theoretically meaningful to test any cue combination model for the position estimations, as the positioning hypothesis predicts that position estimations in all cue conditions

[5] Due to noise, the observed β of individual participants may lie outside the range of the predictions for β. For example, it may be larger than 0° or smaller than -45°. Accordingly, we allow that the observed weight for each participant to be larger than 1 or smaller than 0. However, the mean observed weights for all groups should be confirmed to be in the range of 0 and 1.

should be determined by the path integration system (see Table 2.2). However, the comparisons between the observed SDs and the optimal SDs in the BO/CO conditions were still presented for the readers who may be interested.

2.3.2 Results

2.3.2.1 Heading estimations

The means of the signed HERs in all conditions are listed in Table 2.3. The means of the HERs in the LM, PI and BO conditions for all groups of leg ratio were close to 0°. According to the 95% confidence interval test, none of them differed from 0°, indicating that there was no systematic bias in these conditions. In the CO conditions, the mean HER differed from both 0º (predicted by PI) and 45º (predicted by the rotated landmarks) for the groups of L2/L1 = 2 and L2/L1=1. For the group of L2/L1=0.5, the mean HER differed from 0º (predicted by PI) but not from 45º (predicted by the rotated landmarks).

Variabilities of HERs in the LM, PI, BO and CO conditions are shown in Figure 2.6. The means of optimal SDs are also plotted. The means of observed SDs were significantly smaller in the BO conditions than in the PI conditions for all three leg ratio groups, ts(27) $\geqslant$ 4.21, ps < .001, Cohen's ds $\geqslant$ 1.12 (Specifically, Cohen's d = 1.12, 1.44, and 1.61 when L2/L1 = 2, 1, and 0.5 respectively). The means of observed SDs in the BO conditions were comparable to the ones in the LM conditions in all leg ratio groups, ts(27) $\leqslant$ 1.64, ps $\geqslant$ .11, Cohen's ds $\leqslant$ 0.44 (Cohen's d =0.09, 0.44, and 0.17 when L2/L1 = 2, 1, and 0.5 respectively). The means of observed SDs in the BO conditions were comparable to the means of optimal SDs for all the leg ratio groups, ts(27) $\leqslant$ 1.23, ps $\geqslant$ .23, Cohen's ds$\leqslant$ 0.33 (Cohen's d =0.33, 0.06, and 0.09 when L2/L1 = 2, 1, and 0.5 respectively).

Table 2.3 The mean direction (the length of the mean vector) of HERs in Chapter 2.

The mean direction (the length of the mean vector) of heading errors (HER) and 95% confidence interval (CI) of the mean direction in the conditions of landmark (LM), path integration (PI), both cues (BO), and conflict (CO) in Experiment 1, 3 and 4.

	LM	PI	BO	CO
Exp 1: L2/L1 = 2	359° (.97)	5° (.90)	1° (.98)	30° (.95)
95% CI	[354°, 3°]	[355°, 15°]	[357°, 5°]	[22°, 36°]
Exp 1: L2/L1 = 1	358° (.90)	351° (.88)	359° (.93)	29° (.94)
95% CI	[348°, 8°]	[340°, 2°]	[350°, 7°]	[22°, 37°]
Exp 1: L2/L1 = 0.5	5° (.94)	1° (.87)	3° (.96)	39° (.93)
95% CI	[358°, 13°]	[350°, 12°]	[356°, 9°]	[31°, 47°]
Exp 3	358° (.90)	8° (.83)	350° (.92)	36° (.88)
95% CI	[348°, 8°]	[355°, 21°]	[342°, 359°]	[25°, 46°]
Exp 4	7° (.93)	359° (.90)	355° (.96)	33° (.87)
95% CI	[359°, 15°]	[350°, 9°]	[349°, 1°]	[21°, 44°]

The means of observed SDs in the CO conditions were significantly smaller than those in the PI conditions for all leg ratio groups, ts(27) $\geqslant$ 4.33, ps < .001, Cohen's ds $\geqslant$ 1.16 (Cohen's d =1.22, 1.16, and 1.35 when L2/L1 = 2, 1, and 0.5 respectively). The means of observed SDs in the CO conditions were comparable to those in the LM condition for all leg ratio groups, ts(27) $\leqslant$ 1.55, ps $\geqslant$ .13, Cohen's ds $\leqslant$ 0.41 (Cohen's d = 0.41, 0.35, and 0.15 when L2/L1 = 2, 1, and 0.5 respectively). The means of observed SDs were comparable to the means of optimal SDs for all leg ratio groups, ts(27) $\leqslant$ 1.64, ps $\geqslant$ .11, Cohen's ds $\leqslant$ 0.44 (Cohen's d = 0.02, 0.25, and 0.44 when L2/L1 = 2, 1, and 0.5 respectively).

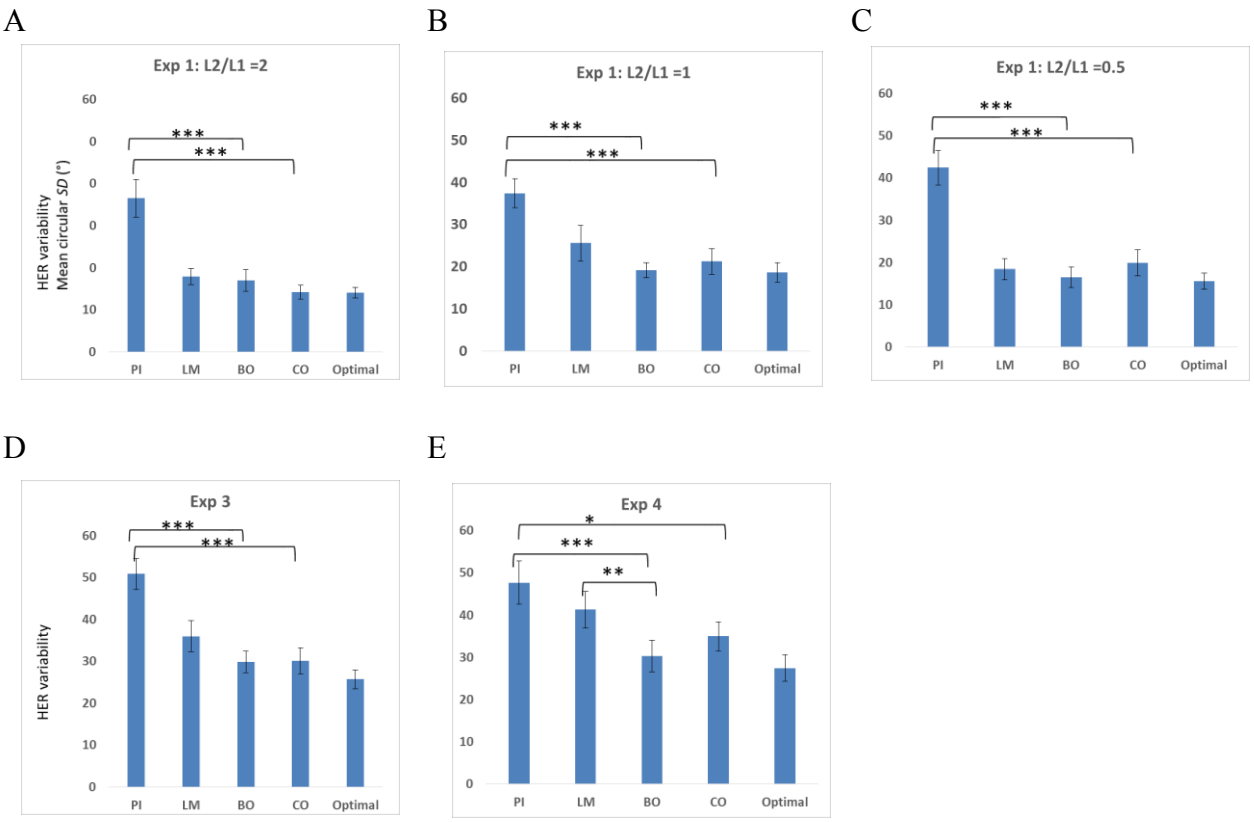

Figure 2.6 Mean observed SDs of HERs in Chapter 2

Mean observed standard deviations (SDs) of the heading errors (HER) in the path integration (PI), landmark (LM), both cues (BO), conflict (CO) conditions, and the optimal prediction by the Bayesian combination model (Optimal), when L2/L1 = 2 (A), L2/L1 = 1(B), and L2/L1 = 0.5 (C) in Experiment 1, Experiment 3(D), and Experiment 4 (E). Error bars represent ±1 SE. Asterisks indicate a significant difference between conditions (*$p \leq .05$; **$p \leq .01$; ***$p \leq .001$).

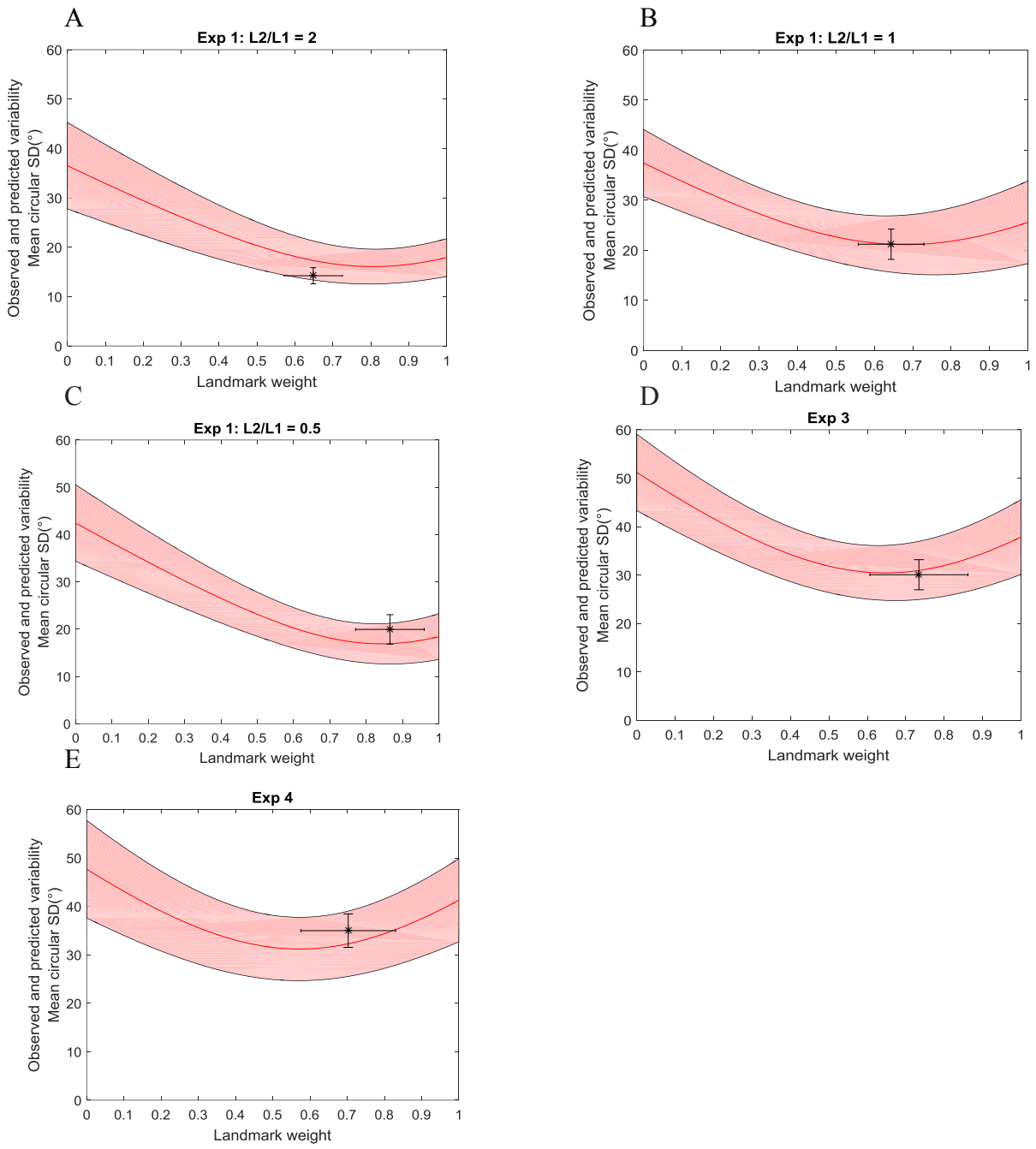

Figure 2.7 Mean observed SDs of HERs in the CO conditions in Chapter 2.

Mean observed standard deviations (SDs) of the heading errors (HER) in the conflict (CO) conditions, when L2/L1 = 2 (A), L2/L1 = 1(B), and L2/L1 = 0.5 (C) in Experiment 1, Experiment 3(D), and Experiment 4 (E). The black point indicates the mean observed SD of HER and the mean observed landmark weight in heading estimations in the conflict (CO)

conditions. The bar indicates the 95% confidence interval. The curves plot the mean predicted SDs using different landmark weights in heading estimations (the red line represents the mean and the red band indicates the 95% confidence interval).

The means of observed SDs and the means of observed landmark weights in the CO conditions are shown in Figure 2.7. For all leg ratio groups, the means of observed landmark weights were comparable to the means of optimal landmark weights, ts(27) $\leqslant$ 0.91, ps $\geqslant$ .37, Cohen's ds $\leqslant$ 0.24 (Cohen's d = 0.24, 0.08, and 0.22 when L2/L1 = 2, 1, and 0.5 respectively). For all leg ratio groups, the means of observed SDs in the CO conditions were comparable to the predicted SDs for the observed weights, ts(27) $\leqslant$ 1.80, ps $\geqslant$ .08, Cohen's ds $\leqslant$ 0.48 (Cohen's d = 0.48, 0.11, and 0.27 when L2/L1 = 2, 1, and 0.5 respectively).

The results of the comparisons that test the quasi-Bayesian, the Bayesian, and the linear combination models are listed in Table 2.4A and Table 2.4B. Illustrated by the tables, the observed SDs in the BO conditions for all leg ratio groups were consistent with the quasi-Bayesian combination and the Bayesian combination models. The observed SDs in the CO conditions for all leg ratios supported the quasi-Bayesian combination, the Bayesian combination, and the linear combination models for all the leg ratio groups.

Table 2.4 Summary of the Cohen's ds of the combination model testing for the heading estimations in Chapter 2.

(A) Summary of the Cohen's *d*s of the model testing for the heading estimations in the both cues (BO) condition against the quasi-Bayesian combination model and the Bayesian combination model in all experiments.

Heading Estimations (BO condition)						
	Quasi-Bayesian combination				Bayesian combination	
	SD in the PI condition		SD in the LM condition		optimal SD	
	>, =, or <	Cohen's d	>, =, or <	Cohen's d	>, =, or <	Cohen's d
Exp 1 L2/L1 =2	<	-1.12	=	-0.09	=	0.33
Exp 1 L2/L1 =1	<	-1.44	=	-0.44	=	0.06
Exp 1 L2/L1 =0.5	<	-1.61	=	-0.17	=	0.09
Exp 2	NA	NA	NA	NA	NA	NA
Exp 3	<	-1.20	=	-0.37	=	0.33
Exp 4	<	-0.97	<	-0.81	=	0.29

(B) Summary of the Cohen's *d*s of the model testing for the heading estimations in the conflict (CO) condition against the quasi-Bayesian combination model, the Bayesian combination model and the linear combination model in all experiments.

Heading Estimations (CO condition)										
	Quasi-Bayesian combination				Bayesian-combination				Linear combination	
	SD in the PI condition		SD in the LM condition		optimal SD		optimal weight		predicted SD for the observed weight	
	>, =, or <	Cohen's d	>, =, or <	Cohen's d	>, =, or <	Cohen's d	>, =, or <	Cohen's d	>, =, or <	Cohen's d
Exp 1 L2/L1 =2	<	-1.22	=	-0.41	=	0.02	=	-0.24	=	-0.48
Exp 1 L2/L1 =1	<	-1.16	=	-0.35	=	0.25	=	-0.08	=	-0.11
Exp 1 L2/L1 =0.5	<	-1.35	=	0.15	=	0.44	=	0.22	=	0.27
Exp 2	NA	NA	NA	NA	NA	NA	NA	NA	NA	NA
Exp 3	<	-1.19	=	-0.34	=	0.32	=	0.19	=	-0.05
Exp 4	<	-0.60	=	-0.31	=	0.47	=	0.30	=	0.10

Note: ">" indicates that the observed SD (or weight) in the BO/CO condition was significantly larger than the model prediction. "=" indicates that the observed SD (or weight) in the BO/CO condition was comparable to the model prediction. "<" indicates that the observed SD (or weight) in the BO/CO condition was significantly smaller than the model prediction.

2.3.2.2 Position estimations

The means of signed PERs in all conditions are listed in Table 2.5. The participants could estimate the positions without any systematic bias in all conditions across the different leg ratio groups. The means of the PERs in all these conditions and in all groups were close to 0°. None of

them differed from 0° according to the 95% confidence interval, except in the condition of BO for the group of L2/L1 = 0.5.

Variabilities of PERs in all conditions are shown in Figure 2.8. The means of optimal SDs are also plotted. The means of observed SDs in the PI condition were comparable to those in all other three conditions for all leg ratio groups, ts(27) $\leqslant$ 1.43, ps $\geqslant$ .16, Cohen's ds $\leqslant$ 0.38.

Table 2.5 The mean direction (the length of the mean vector) of PERs in Chapter 2.
The mean direction (the length of the mean vector) of position errors (PER) and 95% confidence interval (CI) of the mean direction in the conditions of landmark (LM), path integration (PI), both cues (BO), and conflict (CO) in Experiment 1, 3 and 4.

	LM	PI	BO	CO
L2/L1 = 2	359° (.95)	359° (.94)	5° (.94)	5° (.96)
95% CI	[352°, 6°]	[352°, 7°]	[357°, 12°]	[358°, 11°]
L2/L1 = 1	12° (.85)	3° (.90)	5° (.90)	5° (.94)
95% CI	[0°, 24°]	[353°, 13°]	[355°, 15°]	[357°, 13°]
L2/L1 = 0.5	6° (.93)	6° (.96)	8° (.98)	6° (.93)
95% CI	[358°, 14°]	[359°, 12°]	[3°, 13°]	[358°, 14°]
Exp 3	3° (.88)	12° (.90)	355° (.95)	7° (.95)
95% CI	[352°, 14°]	[3°, 22°]	[348°, 3°]	[0°, 14°]
Exp 4	16° (.89)	358° (.87)	5° (.90)	355° (.90)
95% CI	[6°, 29°]	[347°, 9°]	[356°, 15°]	[346°, 5°]

2.3.2.3 Homing estimations

The means of signed β in all conditions are listed in Table 2.6. The participants judged the homing directions without systematic biases in the LM, PI and BO conditions across different leg ratio groups. According to the 95% confidence interval test, the means of β in all these conditions and in all groups were comparable to 0°, except for the condition of LM and PI for the group of L2/L1 = 1. In the CO conditions, the means of β differed from both 0º (predicted by PI) and 315º (i.e., -45º, predicted by the rotated landmarks) in all groups.

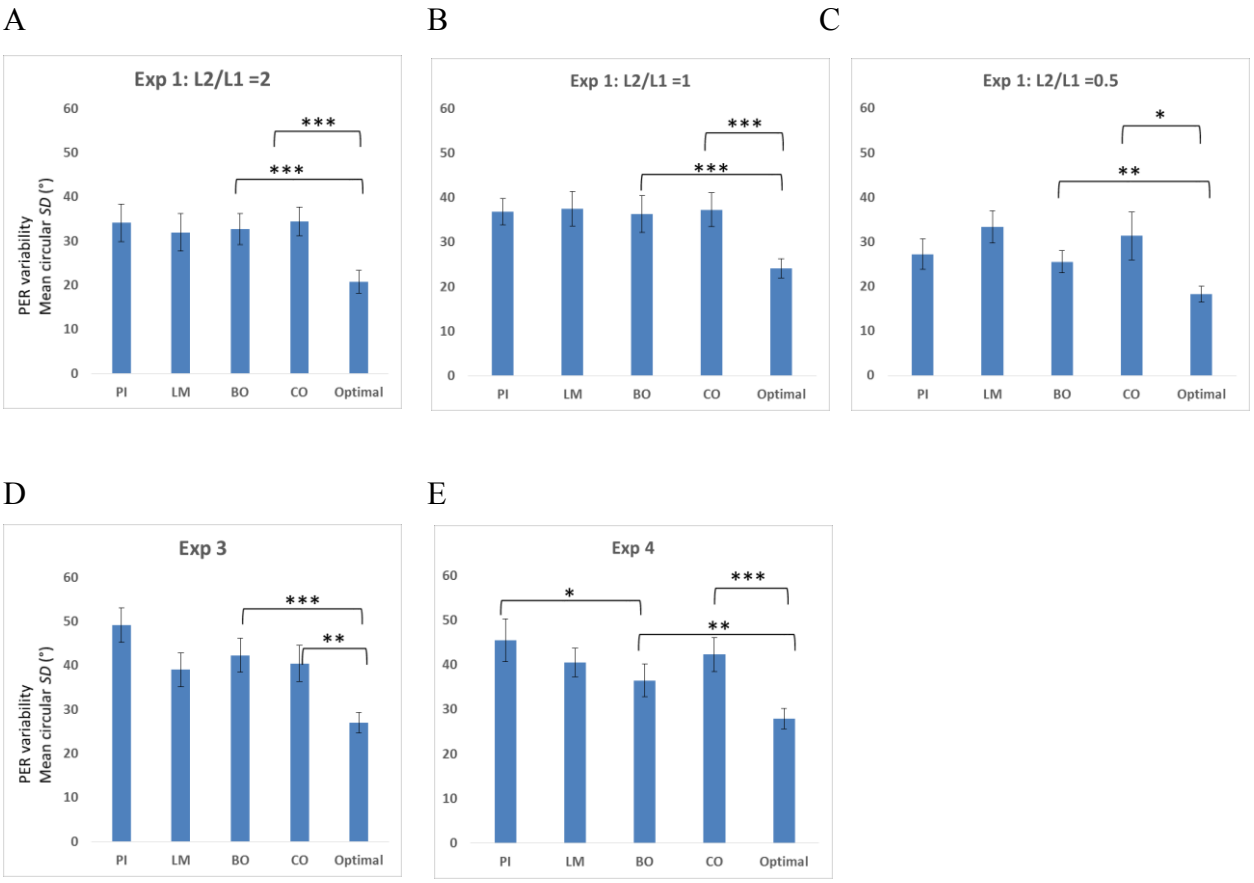

Figure 2.8 Mean observed SDs of PERs in Chapter 2.

Mean observed standard deviations (SDs) of the position errors (PER) in the path integration (PI), landmark (LM), both cues (BO), conflict (CO) conditions, and the optimal prediction by the

Bayesian combination model (Optimal), when L2/L1 = 2 (A), L2/L1 = 1(B), and L2/L1 = 0.5 (C) in Experiment 1, Experiment 3(D), and Experiment 4 (E). Error bars represent ±1 SE. Asterisks indicate a significant difference between conditions (*p ≤ .05; **p ≤ .01; ***p ≤ .001).

Variabilities of β in the conditions of PI, LM, BO, and CO for all leg ratio groups are plotted in Figure 2.9. The means of optimal SDs are also plotted. Compared to the mean of observed SDs in the PI condition, the mean of observed SDs in the BO condition was significantly larger in the group of L2/L1 = 2, $t(27) = 2.40$, $p = .02$, Cohen's $d = 0.64$, comparable in the group of L2/L1 = 1, $t(27) = 0.09$, $p = .93$, Cohen's $d = 0.02$, and significantly smaller in the group of L2/L1 = 0.5, $t(27) = 3.74$, $p < .001$, Cohen's $d = 1.00$. Compared to the mean of observed SDs in the LM condition, the mean of observed SDs in the BO condition was significantly smaller for the group of L2/L1= 1, $t(27) = 2.68$, $p = .01$, Cohen's $d = 0.72$ and for the group of L2/L1=0.5, $t(27) = 2.63$, $p = .01$, Cohen's $d = 0.70$, but comparable for the group of L2/L1 =2, $t(27) = 0.31$, $p = .76$, Cohen's $d = 0.08$. Compared to the mean optimal SDs, the mean of observed SDs in the BO condition was significantly larger for the group of L2/L1=2, $t(27) = 3.73$, $p < .001$, Cohen's $d = 1.00$ and for the group of L2/L1=1, $t(27) = 2.57$, $p = .02$, Cohen's $d = 0.69$, but was comparable for the group of L2/L1=0.5, $t(27) = 0.18$, $p = .86$, Cohen's $d = 0.05$.

Table 2.6 The mean direction (the length of the mean vector) of β in Chapter 2.

The mean direction (the length of the mean vector) of homing errors (β) and 95% confidence interval (CI) of the mean direction in the conditions of landmark (LM), path integration (PI), both cues (BO), and conflict (CO) for three leg ratio groups in Experiment 1, Experiment 2, Experiment 3 and Experiment 4.

	LM	PI	BO	CO
Exp 1: L2/L1 = 2	1° (.92)	355° (.96)	5° (.93)	335° (.95)
95% CI	[352°, 9°]	[349°, 1°]	[357°, 13°]	[328°, 341°]
Exp 1:L2/L1 = 1	21° (.80)	9° (.96)	5° (.91)	339° (.89)
95% CI	[7°, 35°]	[3°, 16°]	[356°, 14°]	[329°, 350°]
Exp 1: L2/L1 = 0.5	2° (.91)	3° (.94)	7° (.95)	332° (.90)
95% CI	[353°, 12°]	[355°, 10°]	[0°, 14°]	[322°, 341°]
Exp 2	8° (.83)	0° (.98)	2° (.94)	341° (.96)
95% CI	[351°, 25°]	[355°, 5°]	[352°, 12°]	[332°, 349°]
Exp 3	5° (.96)	1° (.92)	6° (.96)	335° (.96)
95% CI	[359°, 12°]	[352°, 10°]	[0°, 12°]	[323°, 347°]
Exp 4	10° (.97)	3° (.97)	11° (.98)	327° (.94)
95% CI	[5°, 15°]	[358°, 8°]	[7°, 16°]	[319°, 334°]

Compared to the mean of observed SDs in the PI condition, the mean of observed SDs in the CO condition was significantly larger for the group of L2/L1 = 2, $t(27) = 3.60$, $p = .001$, Cohen's $d = 0.96$, comparable for the group of L2/L1 = 1, $t(27) = 1.48$, $p = .15$, Cohen's $d = 0.40$, and significantly smaller for the group of L2/L1 = 0.5, $t(27) = 2.22$, $p = 0.04$, Cohen's $d = 0.59$. The means of observed SDs in the CO and LM conditions were comparable for all leg

ratios, $ts(27) \leqslant 1.42$, $ps \geqslant .17$, Cohen's $ds \leqslant 0.38$ (Cohen's $d = 0.07$, 0.31, and 0.38 when L2/L1 = 2, 1, and 0.5 respectively). Compared to the mean of optimal SDs, the mean of observed SDs in the CO condition was significantly larger for the group of L2/L1=2, $t(27) = 5.43$, $p < .001$, Cohen's $d = 1.45$, and for the group of L2/L1=1, $t(27) = 3.69$, $p < .001$, Cohen's $d = 0.99$, but was comparable for the group of L2/L1= 0.5, $t(27) = 0.66$, $p = .52$, Cohen's $d = 0.18$.

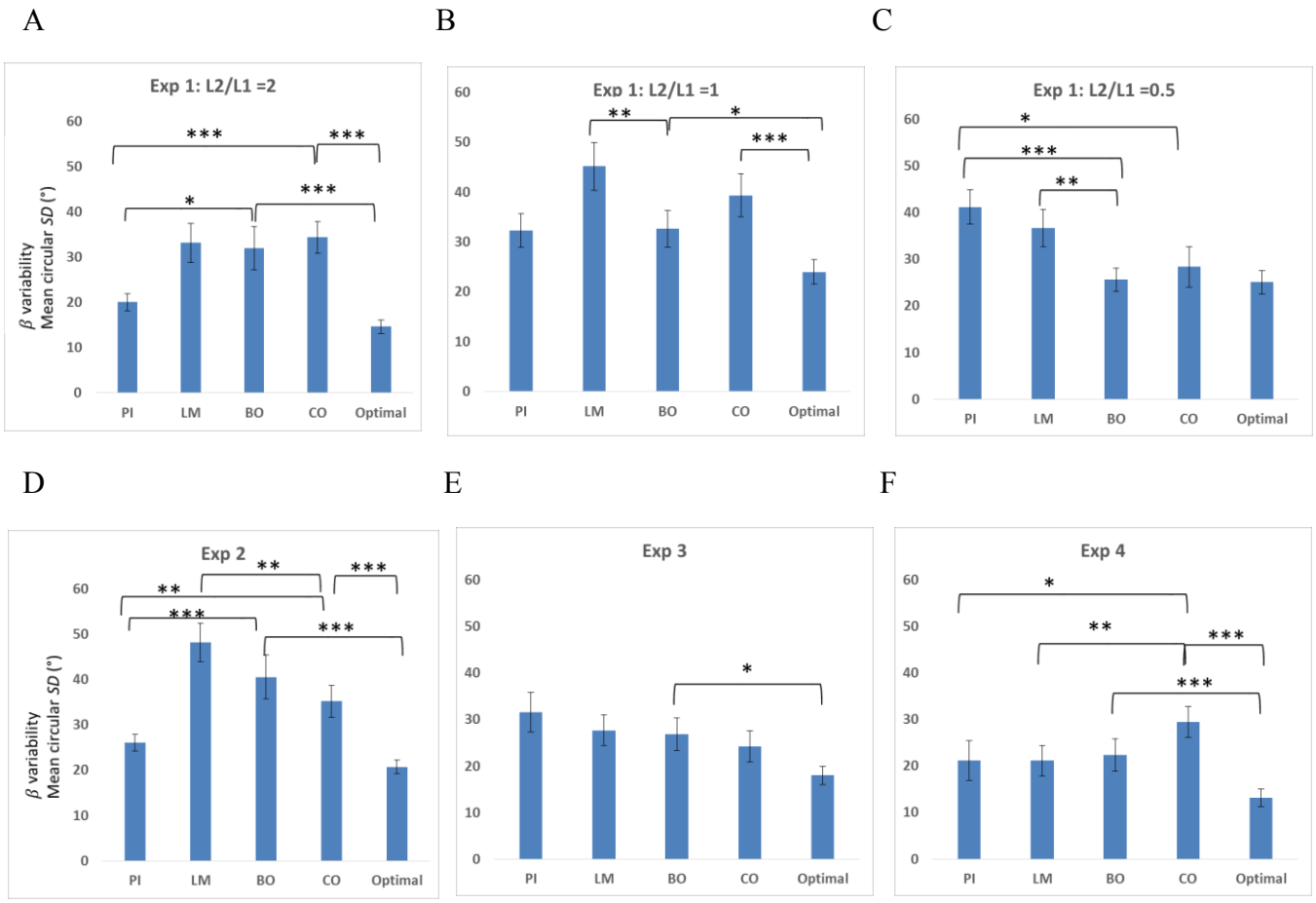

Figure 2.9 Mean observed SDs of β in Chapter 2.

Mean observed standard deviations (SDs) of the homing errors (β) in the path integration (PI), landmark (LM), both cues (BO), conflict (CO) conditions, and the optimal prediction by the Bayesian combination model (Optimal), when L2/L1 = 2 (A), L2/L1 = 1(B), and L2/L1 = 0.5 (C) in Experiment 1, Experiment 2(D), Experiment 3 (E), and Experiment 4 (F). Error bars represent

±1 SE. Asterisks indicate a significant difference between conditions (*p ≤ .05, **p ≤ .01, ***p ≤ .001).

The mean of observed SDs and the mean of observed landmark weights in the CO conditions are shown in Figure 2.10. Compared to the mean of optimal landmark weights, the mean of observed landmark weights was comparable for the group of L2/L1=1, $t(27) = 0.70$, $p = .49$, Cohen's $d = 0.19$, and for the group of L2/L1 = 0.5, $t(27) = 0.63$, $p = .54$, Cohen's $d = 0.17$, but was significantly larger for the group of L2/L1=2, $t(27) = 2.05$, $p = .05$, Cohen's $d = 0.55$. Compared to the mean of predicted SDs for the observed weights, the mean of observed SDs in the CO condition was significantly larger for the group of L2/L1=2, $t(27) = 3.71$, $p < .001$, Cohen's $d = 0.99$, and for the group of L2/L1 =1, $t(27) = 2.78$, $p = .01$, Cohen's $d = 0.74$, but was comparable for the group of L2/L1 = 0.5, $t(27) = .03$, $p = .98$, Cohen's $d = 0.01$.

The results of the comparisons that test the quasi-Bayesian, the Bayesian, and the linear combination models are listed in Table 2.7A and Table 2.7B. As illustrated in the table, in the group of L2/L1=2, none of the combination models could explain the observed SDs in the BO or CO conditions. In the group of L2/L1=1, only the quasi-Bayesian combination model could account for the observed SDs in the BO condition. In the group of L2/L1=0.5, all combination models could explain the observed SDs in the BO and CO conditions.

2.3.2.4 Dependence relation between PER and HER in the PI condition

To characterize the relationship between PER and HER in the PI condition, we conducted a linear regression between PER_{PI} and HER_{PI} for each leg ratio group (Figure 2.11A, 2.11B &

2.11C). All the three regression models were significant, *F*s (1, 113) ⩾ 33.27, *p*s < .001. As illustrated in Figure 2.11, both the slope *a* and R^2 increased with the leg ratio.

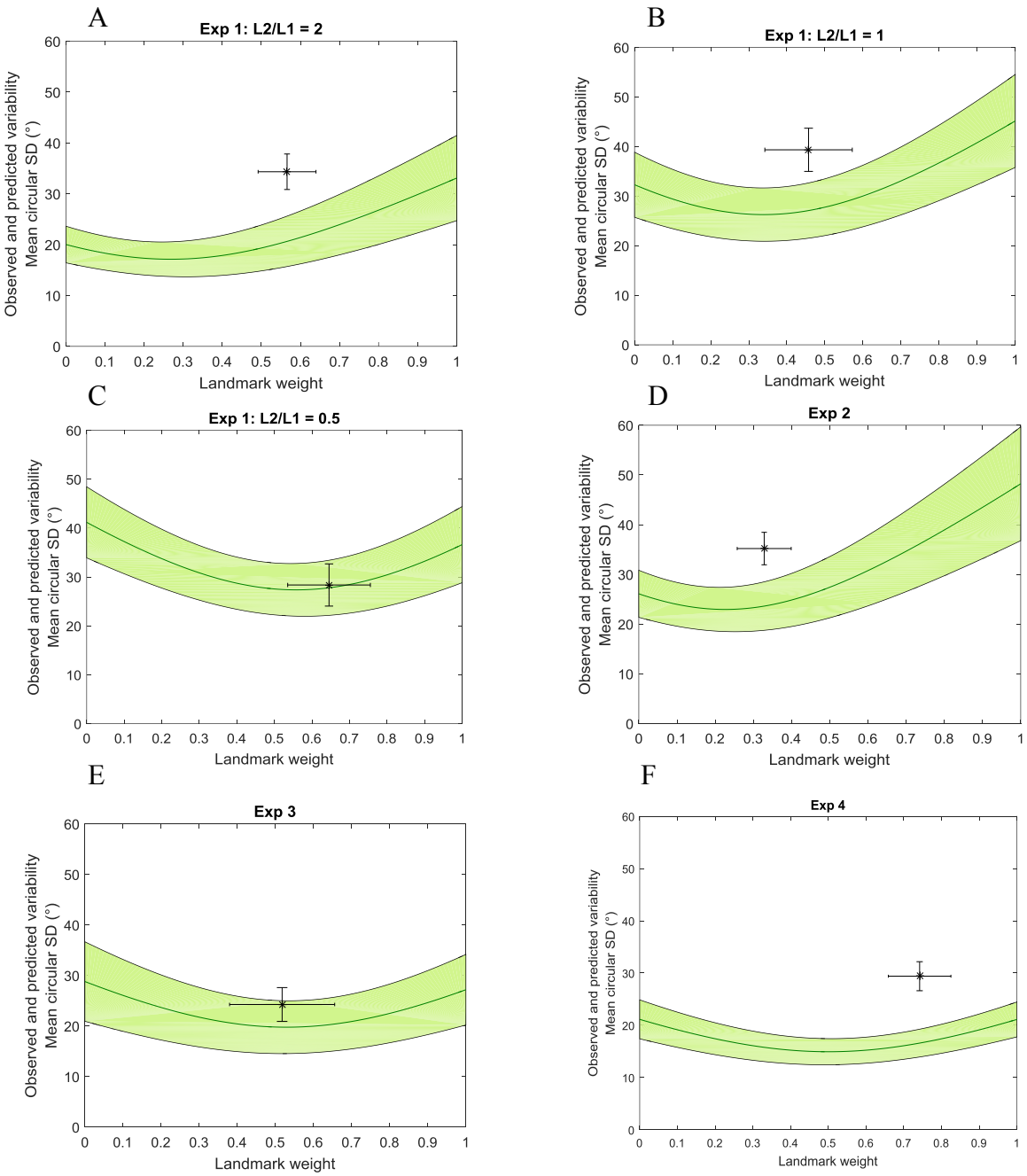

Figure 2.10 Mean observed SDs of β in the CO conditions of Chapter 2.

Mean observed standard deviations (SDs) of the homing errors (β) in the conflict (CO) conditions, when L2/L1 = 2 (A), L2/L1 = 1(B), and L2/L1 = 0.5 (C) in Experiment 1,

Experiment 2 (D), Experiment 3(E), and Experiment 4 (F). The black point indicates the mean observed SD of β and the mean observed landmark weight in homing estimations in the CO conditions. The bar indicates 95% confidence interval. The curves plot the mean observed SDs using different landmark weights in homing estimations according to the homing hypothesis (the green line represents the mean and the green band indicates the 95% confidence interval).

Table 2.7 Summary of the Cohen's ds of the combination model testing for the homing estimations in Chapter 2.

(A) Summary of the Cohen's *d*s of the model testing for the homing estimations in the both cue (BO) condition against the quasi-Bayesian combination model and the Bayesian-combination model in all experiments.

Homing Estimations (BO condition)						
	Quasi-Bayesian combination				Bayesian combination	
	SD in the PI condition		SD in the LM condition		optimal SD	
	>, =, or <	Cohen's d	>, =, or <	Cohen's d	>, =, or <	Cohen's d
Exp 1 L2/L1 =2	**>**	**0.64**	**=**	**-0.08**	**>**	**1.00**
Exp 1 L2/L1 =1	=	0.02	<	-0.72	**>**	**0.69**
Exp 1 L2/L1 =0.5	<	-1.00	<	-0.70	=	0.05
Exp 2	**>**	**1.21**	**=**	**-0.53**	**>**	**1.78**
Exp 3	**=**	**-0.25**	**=**	**-0.07**	**>**	**0.67**
Exp 4	**=**	**0.15**	**=**	**0.15**	**>**	**1.40**

(B) Summary of the Cohen's *d*s of the model testing for the homing estimations in the conflict (CO) condition against the quasi-Bayesian combination model, the Bayesian-combination model, and the linear-combination in all experiments.

Homing Estimations (CO condition)										
	Quasi-Bayesian combination				Bayesian-combination				Linear combination	
	SD in the PI condition		SD in the LM condition		optimal SD		optimal weight		predicted SD for the observed weight	
	>, =, or <	Cohen's d	>, =, or <	Cohen's d	>, =, or <	Cohen's d	>, =, or <	Cohen's d	>, =, or <	Cohen's d
Exp 1 L2/L1 =2	**>**	**0.96**	**=**	**0.07**	**>**	**1.45**	**>**	**0.55**	**>**	**0.99**
Exp 1 L2/L1 =1	**=**	**0.40**	**=**	**-0.31**	**>**	**0.99**	=	0.19	**>**	**0.74**
Exp 1 L2/L1 =0.5	<	-0.59	=	-0.38	=	0.18	=	0.17	=	-0.01
Exp 2	**>**	**0.89**	**<**	**-0.92**	**>**	**1.58**	=	0.05	>	**1.59**
Exp 3	**=**	**-0.38**	**=**	**-0.32**	=	0.52	=	-0.06	=	0.19
Exp 4	**>**	**0.62**	**>**	**0.73**	**>**	**1.48**	**>**	**0.73**	**>**	**1.15**

Note: ">" indicates that the observed SD (or weight) in the BO/CO condition was significantly larger than the model prediction. "=" indicates that the observed SD (or weight) in the BO/CO condition was comparable to the model prediction. "<" indicates that the observed SD (or weight) in the BO/CO condition was significantly smaller than the model prediction. The value in red and bold is the case when the observed data does not fit the model prediction.

A

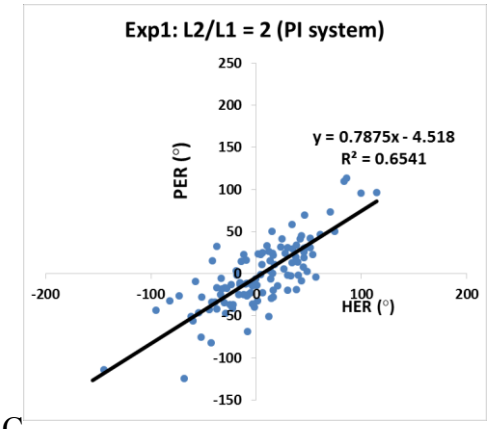

B

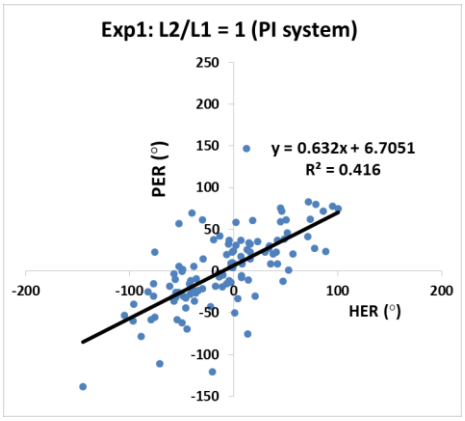

C

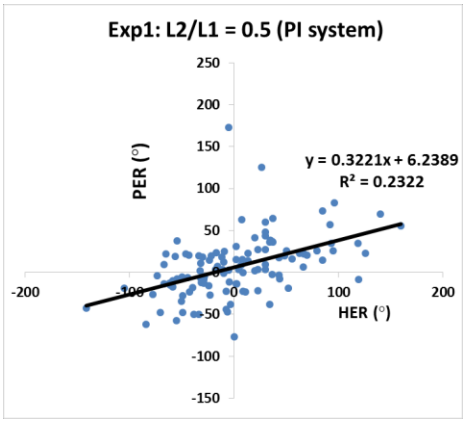

D

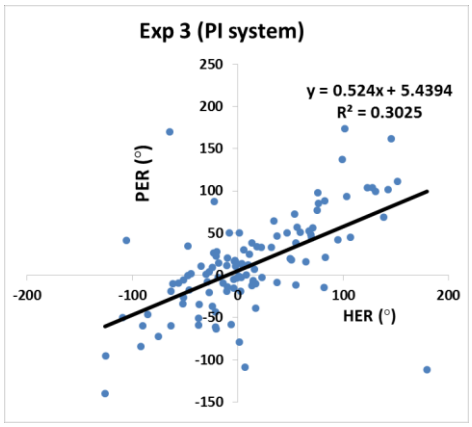

E

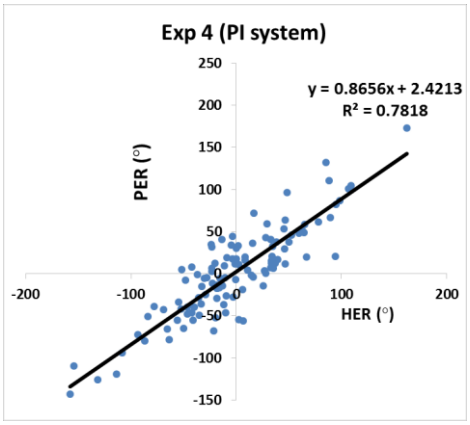

Figure 2.11 Scatter plots showing PER as a function of HER in the PI conditions in Chapter 2. Scatter plots (with best-fitting regression lines) showing the position errors (PER) as a function of the heading errors (HER) in the path integration (PI) condition, when L2/L1 = 2 (A), L2/L1 = 1(B), and L2/L1 = 0.5 (C) in Experiment 1, Experiment 3(D), and Experiment 4 (E). Each dot

represents a pair of HER and PER for one path and one participant. Asterisks indicate that the regression model explains a significant amount of variance (***p ≤ .001).

2.3.2.5 Variability of β can be predicted by the positioning hypothesis

For each group of L2/L1, using the linear regression of HER and PER (Figure 2.11), we obtained the estimations of slope *a* and σ_{ue}^2 (i.e., (mean observed SDs of PER_{PI}) ^{2} × (1- R^2)). Table 2.8 summarizes these estimations:

Table 2.8 Summary of the parameter values in modeling of Chapter 2.
Summary of the parameter values of a squared mean observed standard deviation of PER_{PI} ((mean observed SD of PER_{PI}) ^{2}), the slope of the regression line between PER_{PI} and HER_{PI} (a), the explained portion of the regression model (R^2), and variance of random error in the PER_{PI} that cannot be explained by HER_{PI} (σ_{ue}^2) for three leg ratio groups.

	(mean observed SD of PER_{PI}) ^{2}	a	R^2	σ_{ue}^2
Exp1 L2/L1 = 2	1162.83	0.79	0.65	406.99
Exp1 L2/L1 = 1	1357.19	0.63	0.42	787.17
Exp1 L2/L1 = 0.5	739.25	0.32	0.23	569.23

Following the equations in Table 2.2, we calculated the predicted $\sigma_{\beta_{PI}}^2$, $\sigma_{\beta_{LM}}^2$, $\sigma_{\beta_{BO}}^2$, and $\sigma_{\beta_{CO}}^2$ for each participants in each group of L2/L1. To calculate $\sigma_{\beta_{PI}}^2$, we used the estimations of *a* and σ_{ue}^2 in each leg ratio group, and the observed $\sigma_{HER_{PI}}^2$ from each participant. To calculate $\sigma_{\beta_{LM}}^2$, we used the *a* and σ_{ue}^2 in each group and observed $\sigma_{HER_{LM}}^2$ and $\sigma_{HER_{PI}}^2$ from each participant.

To calculate $\sigma^2_{\beta_{BO}}$, we used the slope a, σ^2_{ue} and the mean optimal weight for heading estimations in each group and observed $\sigma^2_{HER_{LM}}$ and $\sigma^2_{HER_{PI}}$ from each participant. The calculation of $\sigma^2_{\beta_{CO}}$ was the same as $\sigma^2_{\beta_{BO}}$ except that we used the mean observed weight instead of the mean optimal weight in each group[6]. The means of observed and predicted SDs of β for all cue conditions and all groups of L2/L1 are plotted in Figure 2.12. None of them differed significantly, *ts*(27) $\leqslant$ 1.48, *p*s $\geqslant$ .15, Cohen's *d*s $\leqslant$ 0.40, except in the LM condition for the group of L2/L1=2, $t(27) = 2.05$, $p = .05$, Cohen's $d = 0.55$.

2.3.3 Discussion

Cue combination models cannot explain homing estimations for all leg ratio groups. Although all combination models could explain the homing variability in the group of L2/L1= 0.5, cue combination models had difficulty explaining the homing variability for the groups of L2/L1 = 1 and 2. Particularly, for the group of L2/L1=2, we found no evidence that any combination model could account for the homing variability in either BO or CO conditions. In contrast, both Bayesian and quasi-Bayesian models can explain the heading variability in the BO and CO conditions for all leg ratio groups. Moreover, the observed variability and the prediction of homing estimations in all cue conditions based on the positioning hypothesis fit well (see Figure 2.12). Therefore, these findings favour the positioning hypothesis over the homing hypothesis.

[6] We also used the same predicted homing variability for the CO condition ($i.e. \sigma^2_{\beta_{CO}} = \sigma^2_{\beta_{BO}}$) and the conclusions of model fitting did not change.

A.

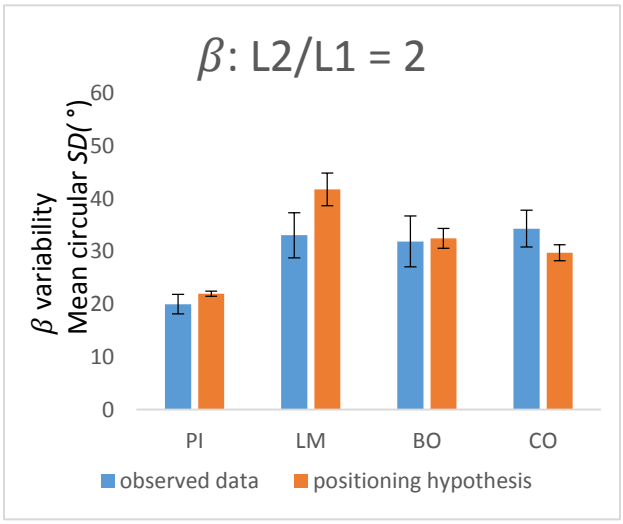

B.

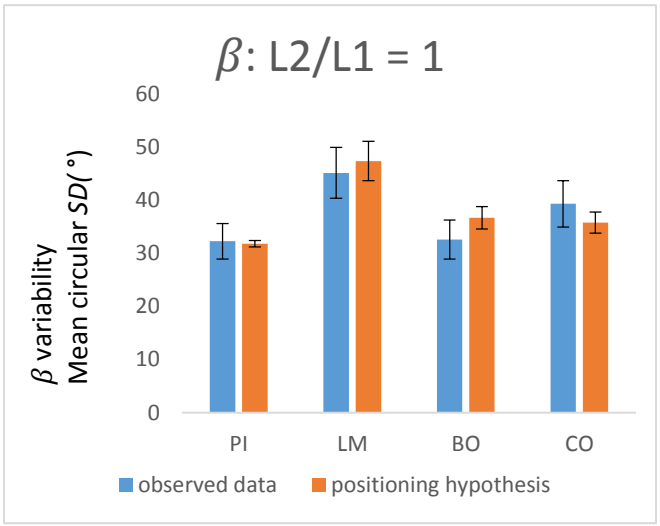

C.

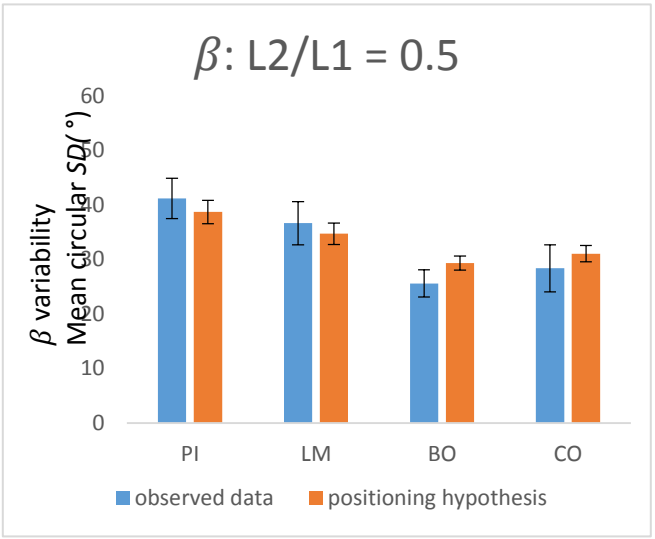

Figure 2.12 Comparison between the mean observed SDs of β and the mean SDs predicted by the positioning hypothesis in Chapter 2.

Comparison between the mean observed SDs of the homing errors (β) and the mean SDs predicted by the positioning hypothesis in the path integration (PI), landmark (LM), both cues

(BO), and conflict (CO) conditions, when the ratio is 2 (A), when the ratio is 1 (B), and when the ratio is 0.5 (C) in Experiment 1. Error bars represent ±1 SE.

There are other findings supporting the positioning hypothesis. The position estimations in the conditions of LM, BO, and CO were not different from those in the condition of PI for all leg ratio groups. This result suggests that the position estimations in all four cue conditions could be predicted by the estimations in the PI system as described by the mathematical model elaborating on the positioning hypothesis (see Table 2.2). Furthermore, the position estimations were a linear function of the heading estimations in the PI system and the dependency of PER on HER (both the slope a and R^2) increases with the leg ratio, as predicted by the model elaborating on the positioning hypothesis.

2.4. Experiment 2

In the paradigm used in Experiment 1, the participants learned objects before walking a path. Then they replaced the objects. The participants' responses were used to calculate position errors and heading errors. The paradigm in Experiment 1 differs from the typical homing paradigm, which may restrict generalization of the conclusion in Experiment 1 to the typical homing paradigm. The purpose of Experiment 2 was to differentiate the positioning hypothesis from the homing hypothesis in a typical homing paradigm. Without learning any objects' locations, the participants walked the paths with a leg ratio of 2 (L2/L1=2) and then pointed to the origins of the paths in the four cue conditions. Critically, the positioning hypothesis predicts neither the Bayesian nor the quasi-Bayesian cue combination for homing estimations, whereas the homing hypothesis predicts the Bayesian or quasi-Bayesian cue combination for homing

estimations. Note that, as in a typical homing paradigm, no positioning estimations were measured or analyzed.

2.4.1 Methods

2.4.1.1 Participants

Sixteen university students (eight men) participated in the experiment to fulfill the partial requirement for an introductory psychology course. Before the experiment, all participants signed the consent form approved by the University of Alberta Research Ethics Board.

2.4.1.2 Material, Design and Procedure

Experiment 2 was similar to Experiment 1 except for a few changes. First, this experiment only included one leg ratio group (L2/L1 = 2, Figure 2.13). Second, without learning any objects while standing at O, the participants walked the paths. Third, when the participants finished walking the path and reaching the location of P, they were asked to use the wand to point to the origin (O). Finally, each of the four testing conditions (PI, LM, BO and CO) had eight path configurations (Figure 2.13). The participants' homing errors (β) and standard deviation (SD) of the homing errors were calculated across the eight trials within each condition.

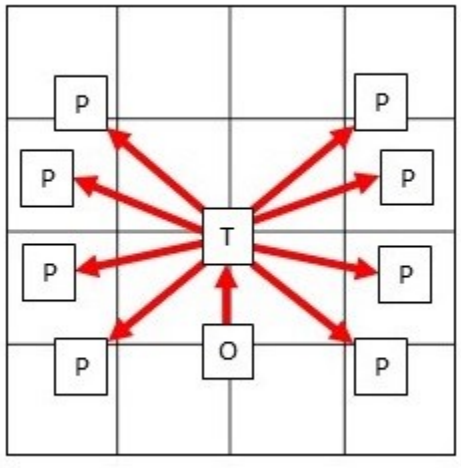

Figure 2.13 Layout in Experiment 2 of Chapter 2.

Participants walked from O to T, turned at T and walked from T to P. In each of the condition (i.e., PI, LM, BO and CO), the participants had to walk 8 different paths. Grid squares represent $1m^2$.

2.4.2 Results

The means of signed β in all conditions are listed in Table 2.6. The participants judged the homing directions without systematic biases in the LM, PI and BO conditions across different leg ratio groups. The means of β in all these conditions and in all groups were comparable to 0° according to the 95% confidence interval. In the CO condition, mean homing direction differed from both 0º (predicted by PI) and 315º (i.e., -45º, predicted by the rotated landmarks) from the confidence interval test.

The means of observed SDs in the conditions of PI, LM, BO, and CO for all groups are plotted in Figure 2.9. The mean of optimal SDs is also plotted. Similar to the findings of the leg ratio L2/L1=2 group in Experiment 1, the mean of observed SDs was larger in the BO condition

than in the PI condition, $t(27) = 4.54$, $p < .001$, Cohen's $d = 1.21$. The means of observed SDs were comparable in the BO condition and in the LM condition, $t(27) = 1.97$, $p = .06$, Cohen's $d = 0.53$. The mean of observed SDs in the BO condition was significantly larger than the mean of optimal SDs, $t(27) = 6.67$, $p < .001$, Cohen's $d = 1.78$.

The mean of observed SDs in the CO condition was significantly larger than that in the PI condition, $t(27) = 3.35$, $p = .002$, Cohen's $d = .89$, but significantly smaller than that in the LM condition, $t(27) = 3.44$, $p = .002$, Cohen's $d = .92$. The mean of observed SDs was also significantly larger than the mean of optimal SDs, $t(27) = 5.90$, $p < .001$, Cohen's $d = 1.58$.

The mean of observed landmark weights and the mean of observed SDs in the CO condition are plotted in Figure 2.10. The mean of observed weights was not significantly different from the mean of optimal weights, $t(27) = 0.18$, $p = .86$, Cohen's $d = .05$. However, the mean of observed SDs in the CO condition was significantly larger than the mean of predicted SDs for the observed weights, $t(27) = 5.94$, $p < .001$, Cohen's $d = 1.59$.

The comparison findings testing the quasi-Bayesian, the Bayesian, and the linear combination models, are listed in Table 2.7A and Table 2.7B. As illustrated in the tables, none of the combination models could explain the homing variability in the BO or CO conditions.

2.4.3 Discussion

None of the combination models could explain the homing variability in the BO or CO conditions, replicating the findings of the group of L2/L1=2 in Experiment 1. These findings support the positioning hypothesis but not the homing hypothesis regardless of whether there was an object array in the experimental paradigm.

2.5. Experiment 3

The purpose of Experiment 3 was to differentiate between the homing hypothesis and the positioning hypothesis when the piloting system could directly indicate the home locations. We replicated Experiment 1 using proximal landmarks, as the home locations could be specified by distance and direction with respect to proximal landmarks. In contrast to the 50m-radius circular wall to which the distal landmarks were attached, the circular wall was 5m in radius. The participants walked the path in which the second leg was twice as long as the first one (L2/L1 =2). Note that the rotation of the proximal landmarks around the origin (i.e., O) and around the testing position (i.e., P) differed. Following the previous studies (e.g., Chen et al., 2017; Nardini et al., 2008), we varied the origin of the path (i.e., O) for each path configuration, but kept the testing position (i.e., P) constant (Figure 2.14C) and the same as the centre of the wall across the trials so that the landmarks rotated around the testing position in the CO condition.

The homing hypothesis stipulates that people combine cues to determine their homing estimations. The positioning hypothesis has the following predictions: first, cue combination occurs during heading estimations but not in homing estimations. Second, for position estimations, as the participants in the LM condition were disoriented by spinning in place at the end of the path, the position estimations in both the path integration and the piloting systems would be available in the LM condition, as well as, in the BO and CO conditions. Consequently, although proximal landmarks could indicate position information, this experiment cannot inform whether the cues are combined for position estimations.

2.5.1 Method

2.5.1.1 Participants

Twenty-eight university students (14 men) participated in the experiment to fulfill the partial requirement for an introductory psychology course. Before the experiment, all participants signed the consent form approved by the University of Alberta Research Ethics Board.

2.5.1.2 Material, Design, and Procedure

The material, design and procedure were the same as those in the group of L2/L1=2 of Experiment 1 except that the circular wall had a radius of 5 m and a height of 1m (Figure 2.14A and 14B). The centre of the wall was the location of P.

A B

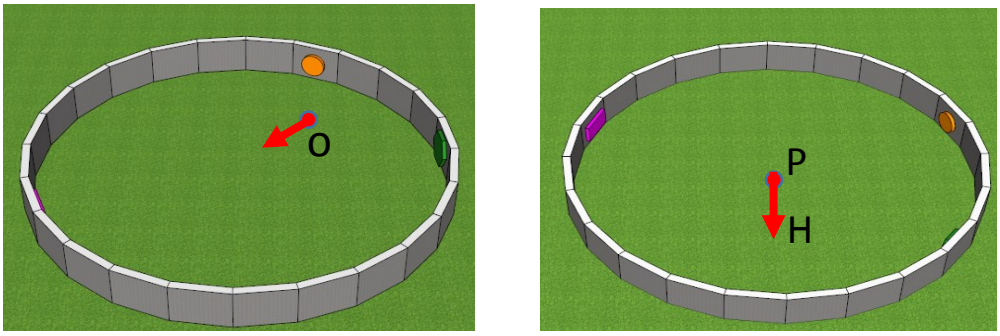

C

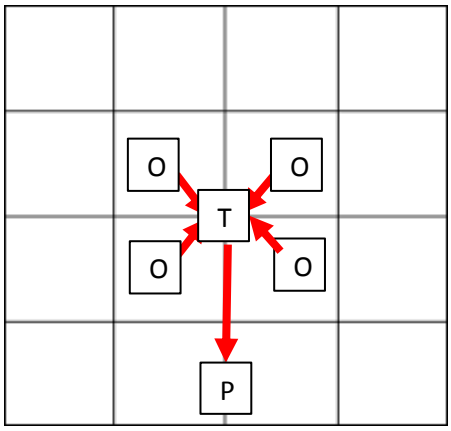

Figure 2.14 Experiment set-up and path configuration of Experiment 3 and 4 in Chapter 2. Experiment set-up and path configuration. (A) In a grassland, the participants faced the direction indicated by the arrow and learned five objects' locations in the presence of three proximal landmarks (a circle, polygon, and rectangle attached to a circular wall with the centre of P and a radius of 5 m) at the origin of the route (O). One of the objects was placed at this origin O. (B) Standing at P and facing H, the participants replaced the five objects under one of the four conditions: PI, LM, BO and CO. The figure shows an example of clockwise rotation of the landmarks in the CO condition. (C) The four paths were used in the three experiments. Each O indicates one possible origin location. Grid squares represents $1m^2$.

2.5.2 Results

2.5.2.1 Heading estimations

The means of signed HERs in all conditions are listed in Table 2.3. The participants could estimate the headings accurately in the LM, PI and BO conditions, as the means of the HERs in all these conditions were close to 0°. According to the 95% confidence interval test, none of them differed from 0°, except in the BO condition. People estimated their headings around 36° in the CO condition. Confidence interval test showed that the heading errors differed from 0º (predicted by PI) but not from 45º (predicted by the rotated landmark).

Variabilities of HERs in the LM, PI, BO and CO conditions are shown in Figure 2.6. The mean of optimal SDs is also plotted. The mean of observed SDs was significantly smaller in the BO condition than that in the PI condition, $t(27) = 4.49$, $p < .001$, Cohen's $d = 1.20$. The means of observed SDs were comparable in the BO condition and in the LM conditions, $t(27) = 1.39$, $p = .18$, Cohen's $d = 0.37$. Furthermore, the mean of observed SDs in the BO condition was not different from the mean of optimal SDs, $t(27) = 1.22$, $p = .23$, Cohen's $d = 0.33$.

The mean of observed SDs was significantly smaller in the CO condition than that in the PI condition, $t(27) = 4.46$, $p < .001$, Cohen's $d = 1.19$. The means of observed SDs were comparable in the CO condition and in the LM conditions, $t(27) = 1.27$, $p = .21$, Cohen's $d = 0.34$. The mean of observed SDs in the CO condition was not significantly different from the mean optimal SDs, $t(27) = 1.20$, $p = .24$, Cohen's $d = 0.32$.

The mean of observed landmark weights and the mean of observed SD in the CO condition are shown in Figure 2.8. The mean of observed weights was comparable to the mean of

optimal weights, $t(27) = 0.70$, $p = .49$, Cohen's $d = 0.19$. The mean of observed SDs in the CO condition was also comparable to the mean of predicted SDs for the observed weights, $t(27) = 0.17$, $p = .86$, Cohen's $d = 0.05$.

The findings of the comparisons that test the quasi-Bayesian, the Bayesian, and the linear combination models are listed in Table 2.4A and Table 2.4B. Illustrated by the tables, all the combination models could explain the observed SDs of the heading estimations in the BO and CO condition.

2.5.2.2 Position estimations

The means of signed PERs in all conditions are listed in Table 2.5. The participants could estimate the positions accurately without any systematic bias in all conditions, as the means of the PERs in all these conditions were close to 0° and none of them differed from 0° except in the PI condition.

Variabilities of PERs in all conditions, together with the mean of optimal SDs are plotted in Figure 2.7. The mean SDs in the BO and CO conditions were both comparable to the mean SDs in the PI and the LM conditions, $ts(27) \leqslant 1.74$, $ps \geqslant .09$, Cohen's $ds \leqslant 0.47$.

2.5.2.3 Homing estimations

The means of signed β in all conditions are listed in Table 2.6. The participants could judge the homing directions accurately in the LM, PI and BO conditions, as the means of β in all these conditions were close to 0° and none of them were significantly different from 0°, according to the 95% confidence interval test. In the CO condition, the mean of the homing

directions was 335°, significantly different from the prediction by the piloting system (315°, i.e., -45°) and the prediction by the path integration system (0°).

Variabilities of β in the conditions of PI, LM, BO, and CO for all groups are plotted in Figure 2.9. The mean of optimal SDs is also plotted. The mean of observed SDs in the BO condition was comparable to that in the PI condition, $t(27) = 0.95$, $p = .35$, Cohen's $d = 0.25$ and that in the LM condition, $t(27) = 0.27$, $p = .79$, Cohen's $d = 0.07$. The mean of observed SDs in the BO condition was larger than the mean of optimal SDs, $t(27) = 2.52$, $p = .02$, Cohen's $d = 0.67$.

The mean of observed SDs in the CO condition was comparable to that in the PI condition, $t(27) = 1.44$, $p = .16$, Cohen's $d = 0.38$ and that in the LM condition, $t(27) = 1.21$, $p = .24$, Cohen's $d = 0.32$. The mean of observed SDs in the CO condition was also comparable to the mean of optimal SDs, $t(27) = 1.96$, $p = .06$, Cohen's $d = 0.52$.

The mean of observed landmark weights and the mean of observed SDs in the CO condition are plotted in Figure 2.10. The mean of observed weights was comparable to the mean of optimal weights, $t(27) = 0.22$, $p = .83$, Cohen's $d = 0.06$. The mean of observed SDs in the CO condition was comparable to the mean of predicted SDs for the observed weights, $t(27) = 0.73$, $p = .47$, Cohen's $d = 0.19$.

The findings of the comparisons testing the quasi-Bayesian, the Bayesian, and the linear combination models are listed in Table 2.7A and Table 2.7B. As illustrated in the tables, the homing variability in the BO condition could not be explained by any combination model. In addition, the homing variability in the CO condition could not be explained by the quasi-Bayesian model.

2.5.2.4 Dependence relation between PER and HER in the PI condition

To characterize the relationship between PER and HER in the PI condition, we conducted a linear regression between PER_{PI} and HER_{PI} (Figure 2.11D). The regression model was significant, $F(1, 111) = 47.72$, $p < .001$.

2.5.3 Discussion

Consistent with the positioning hypothesis, we found that people combine two cues for their heading estimations. All the combination models could explain the heading estimations in the BO and CO conditions. In contrast, the homing hypothesis was not supported. There was partial evidence of cue combination of the homing estimations only in the CO condition. These results suggest that even when the proximal landmarks could indicate the home locations, people still combined heading estimations rather than homing estimations.

2.6. Experiment 4

The purpose of Experiment 4 was to demonstrate cue combination for position estimations, in addition to further examining cue combination for heading and homing estimations. According to the positioning hypothesis, cue combination occurs in estimating people's current headings and positions that are then joined to produce homing estimations. In Experiment 1 and 3, we found that people combine their heading estimations from the two cues, regardless of the leg ratio of the travelled path and landmark types (proximal vs distal landmarks). However, we could not test cue combination of position estimations. In Experiment 1, cue combination of position estimations was prevented because distal landmarks could not provide any positional information, and, thus, it could not indicate the participants' positions. In Experiment 3, although we used proximal landmarks, the position estimations in the path

integration system was not disrupted completely in the LM condition, as the participants were disoriented by spinning in place in the end of the path. Therefore, Experiment 3 cannot examine the cue combination of position estimations either.

Experiment 4 was designed to address this issue. Instead of disorienting the participants in the LM condition at the end of the path, we disoriented them at the turning position of the two-leg path. As the past studies have shown, the path integration system cannot produce accurate position estimations any further along the walking path after the participants have been disoriented (Mou & Zhang, 2014). Therefore, the position estimations at the testing position in the LM condition of Experiment 4 would be solely determined by the piloting system. As a result, using the new disorientation procedure in Experiment 4 allowed us to obtain pure position estimations from the piloting system in the LM condition. Then by comparing the position estimations in the BO and CO conditions with the predictions from the combination models, we could determine whether the position estimations in the BO and CO conditions could be combined.

In addition, we still tested cue combination for heading and homing estimations to dissociate the positioning hypothesis from the homing hypothesis.

2.6.1 Method

2.6.1.1 Participants

Twenty-eight university students (14 men) participated in the experiment to fulfill the partial requirement for an introductory psychology course. Before the experiment, all participants signed the consent form approved by the University of Alberta Research Ethics Board.

2.6.1.2 Material, Design & Procedure

Experiment 4 was very similar to Experiment 3 except for a few changes in the LM condition. When the participants reached the turning point (T, Figure 2.14C), they sat in a swivel chair and were span for eight seconds in place while the landmarks were removed but the wall remained. They had to count during the spinning. After the spinning, they were asked to search for a green pole and walk the 2nd leg of the path (TP in Figure 2.14C). After reaching the green pole, the landmarks reappeared.

2.6.2 Results

2.6.2.1 Heading estimations

The means of the signed HERs in all conditions are listed in Table 2.3. The participants could estimate the headings accurately in the LM, PI and BO conditions, as the means of the HERs in all these conditions were close to 0° according to the 95% confidence interval test. In the CO condition, people estimated their headings around 33°. The mean heading errors significantly differed from 0º (predicted by PI) and from 45º (predicted by the rotated landmark), suggesting that people could combine their heading estimations from the path integration and the piloting systems.

Variabilities of HERs in the LM, PI, BO and CO conditions are shown in Figure 2.6. The mean of optimal SDs is also plotted. The mean of observed SDs in the BO condition was significantly smaller than that in the PI condition, $t(27) = 3.64$, $p = .001$, Cohen's $d = 0.97$, and that in the LM conditions, $t(27) = 3.02$, $p = .005$, Cohen's $d = 0.81$. Furthermore, the mean of

observed SDs in the BO condition was comparable to the mean of optimal SDs, $t(27) = 1.07$, $p = .29$, Cohen's $d = 0.29$.

The mean of observed SDs in the CO condition was significantly smaller than that in the PI condition, $t(27) = 2.25$, $p = .03$, Cohen's $d = 0.60$ but was comparable to that in the LM condition, $t(27) = 1.15$, $p = .26$, Cohen's $d = 0.31$. The mean of observed SDs in the CO condition was not different from the mean of optimal SDs, $t(27) = 1.77$, $p = .09$, Cohen's $d = 0.47$.

The mean of observed landmark weights and the mean of observed SDs in the CO condition are shown in Figure 2.7. The mean of observed weights was comparable to the mean of optimal weights, $t(27) = 1.12$, $p = .27$, Cohen's $d = 0.30$. The mean of observed SDs in the CO condition was also comparable to the mean of predicted SDs for the observed weights, $t(27) = 0.38$, $p = .71$, Cohen's $d = 0.10$.

The findings of the comparisons testing the quasi-Bayesian, the Bayesian, and the linear combination models are listed in Table 2.4A and Table 2.4B. As illustrated in the tables, all the combination models could explain the observed SDs of the heading estimations in the BO and CO conditions.

2.6.2.2 Position estimations

The means of signed PERs in all conditions are listed in Table 2.5. The participants could estimate the positions accurately in all conditions, as the means of the PERs in all these conditions were close to 0°, except in the LM condition from the 95% confidence interval test.

Variability of the PERs in all conditions, together with the optimal variability are plotted in Figure 2.8. The mean of observed SDs in the BO condition was significantly smaller than that in the PI condition, $t(27) = 2.02$, $p = .05$, Cohen's $d = 0.54$, but was comparable to that in the LM condition, $t(27) = 1.05$, $p = .30$, Cohen's $d = 0.28$. The mean of observed SDs in the BO condition was significantly larger than the mean of optimal SDs, $t(27) = 2.65$, $p = .01$, Cohen's $d = 0.71$.

The mean of observed SDs in the CO condition was comparable to those in the PI and the LM conditions, $ts(27) \leqslant 0.65$, $ps \geqslant .52$, Cohen's $ds \leqslant 0.17$. The mean of observed SDs in the CO condition was significantly larger than the mean of optimal SDs, $t(27) = 3.85$, $p < .001$, Cohen's $d = 1.03$.

These results suggest that the quasi-Bayesian model could explain the position variability in the BO condition. However, such combination was not optimal.

2.6.2.3 Homing estimations

The means of β in all conditions are listed in Table 2.6. The mean of β in the PI condition was close to 0°, whereas the means of β in the LM and BO conditions were biased to be more than 0° from the 95% confidence interval test. In the CO condition, the mean of the homing directions was 327°, significantly different from the prediction by the piloting system (315°, i.e., -45°) and the prediction by the path integration system (0°).

Variability of β in the conditions of PI, LM, BO, and CO for all groups is plotted in Figure 2.9. The predicted β variability corresponding to the Bayesian combination is also plotted. The mean of observed SDs in the BO condition was comparable to that in the PI condition, $t(27)$

= 0.55, p =.59 , Cohen's d = 0.15, and that in the LM condition, $t(27) = 0.56$, p =.58, Cohen's d = 0.15. The mean of observed SDs was significantly larger than the mean of optimal SDs, $t(27) = 5.26$, p <.001 , Cohen's d = 1.40.

The mean of observed SDs in the CO condition was significantly larger than that in the PI condition, $t(27) = 2.32$, p = .03, Cohen's d = 0.62, but significantly smaller than that in the LM condition, $t(27) = 2.72$, p = .01, Cohen's d = 0.73. The mean of observed SDs in the CO condition was significantly larger than the mean of optimal SDs, $t(27) = 5.55$, $p < .001$, Cohen's d = 1.48.

The mean of observed landmark weights and the mean of observed SDs in the CO condition are plotted in Figure 2.10. The mean pf observed weights was significantly different from the mean of optimal weights, $t(27) = 2.75$, p = .01, Cohen's d = 0.73. The mean of observed SDs in the CO condition was significantly larger than the mean of predicted SDs for the observed weights, $t(27) = 4.31$, $p < .001$, Cohen's d = 1.15.

The findings of the comparisons testing the quasi-Bayesian, the Bayesian, and the linear combination models are listed in Table 2.7A and Table 2.7B. As illustrated in the tables, none of the combination models could account for the observed SD in the either BO or CO conditions.

2.6.2.4 Dependence relation between PER and HER in the PI condition

To characterize the relationship between PER and HER in the PI condition, we conducted a linear regression between PER_{PI} and HER_{PI} (Figure 2.11E). The regression model was significant, $F(1, 111) = 394.24$, $p < .001$.

2.6.3 Discussion

Inconsistent with the homing hypothesis, none of the combination models could account for the observed SDs in the BO or CO conditions. Consistent with the positioning hypothesis, all the combination models could explain the heading variability in the BO and CO conditions.

For the position estimations, we found that the variability of the position estimations in the BO condition was reduced compared to that in the PI condition, but it was different from the prediction by the Bayesian combination. These results suggest that the position estimations were not combined in an optimal manner, but could form the quasi-Bayesian combination. Note that the ending position of the path (P) is also the centre of the circular wall. The landmarks rotated with respect to the testing position (P) in the CO condition. As a result, there were no conflicting predictions for the position estimations. Therefore, we were unable to calculate the relative proximity and the observed PER weight assigned to each system in the CO condition.

2.7. General Discussion

The purpose of the current study was to investigate when the cues from the piloting and path integration systems combine in human homing behaviors, specifically whether cue combination occurs during positioning (heading and position) or homing estimations. There are three important findings. First, there was evidence disconfirming cue combination in the homing estimations especially when the leg ratio was large (L2/L1=2), no matter whether the landmarks were distal or proximal. Second, for any leg ratio and either landmark type, there was no evidence rejecting the Bayesian combination in heading estimations. Third, when we removed the position estimations from the path integration system in the landmark condition (proximal landmarks), there was evidence of the quasi-Bayesian cue combination in position estimations. Last, evidence supporting a cue combination model in homing estimations was modulated by the

leg ratio of the travelled path (L2/L1). There was evidence of cue combination in homing estimations for a small leg ratio (L2/L1=0.5), but not for a large leg ratio (L2/L1=2).

As summarized in Tables 4A and 4B, the Bayesian cue combination model could explain the heading estimations in the conditions of BO and CO for all experiments (100% success rate for all 12 tests across all experiments). In contrast, as shown in Table 2.7A and 2.7B, the Bayesian cue combination could only explain homing variability in the BO condition for the group of L2/L1=0.5 in Experiment 1, and the CO condition for the group of L2/L1=0.5 in Experiment 1 and in Experiment 3 (only 3 out of 12 success rate). The quasi-Bayesian combination model could only predict the homing variability in the BO condition of the group of L2/L1=1, and L2/L1=0.5 in Experiment 1, and the CO condition for the group of L2/L1=0.5 in Experiment 1 (only 3 out of 12 success rate). Moreover, the linear combination model could only explain the homing variability in the CO condition for the group of L2/L1= 0.5 in Experiment 1 and Experiment 3 (2 out of 6 success rate). If we only consider the success rate for four situations using the leg ratio of 2 (the group of L2/L1=2 in Experiment 1 and in Experiments 2-4), the success rate of using the quasi-Bayesian combination models to explain the homing variability in the CO and BO conditions is 0. Even the linear combination model could only explain the homing variability for Experiment 3 (1 out of 4 success rate). Therefore, overall evidence across all experiments clearly favours the positioning hypothesis over the homing hypothesis.

We found evidence for the heading combination, but not for the homing combination in distal landmarks experiment (Experiment 1, especially when L2/L1=2). One may argue that the finding of the heading combination, but not the homing combination, occurred just because the participants in the distal landmarks had two heading estimations but only one homing estimation,

as distal landmarks alone could not indicate home locations directly. Hence, it is not surprising that there was no combination in homing estimations in Experiments 1 and 2. However, in Experiments 3 and 4, proximal landmarks could directly indicate home locations. We still found evidence of heading combination, but not homing combination, indicating that evidence that favoured the positioning hypothesis over the homing hypothesis did not only result from the use of the distal landmarks in Experiments 1 and 2.

The finding of the position combination in Experiment 4 provides further support to the positioning hypothesis. Experiment 1 did not examine the position combination, as distal landmarks provided no distance or positional information. Furthermore, the participants were disoriented in place at the end of the path in the LM condition. Therefore, the position estimations were supposed to be the same in all cue conditions and were solely determined by the path integration system. Although Experiment 3 used proximal landmarks that could indicate position information, the participants were still disoriented in the testing position in the LM condition. As a result, the position estimation in the LM condition was jointly determined by both systems in the BO/CO conditions. Therefore, we could not test cue combination for position estimations. In Experiment 4, using proximal landmarks, we disoriented the participants at the turning point before walking the second leg of the path in the LM condition. This procedure made the participants only rely on the piloting cues to determine their positions in the LM condition. The result showed that people could combine their position estimations from the two cues in the quasi-Bayesian manner. As the positioning hypothesis predicts the position combination as well as the heading combination, the finding of the sub-optimal position combination in Experiment 4 supports the positioning hypothesis.

One may argue that evidence that favoured the positioning hypothesis over the homing hypothesis in Experiments 1, 3, and 4 was specific to the experiment paradigm where the participants learned objects at the origin of the path and replaced them at the end of the path. This experimental paradigm was very different from the typical homing paradigm used in the previous studies (Chen et al., 2017; Nardini et al., 2008). This concern was addressed by the finding in Experiment 2 where the typical homing paradigm was used. The participants walked the path with L2/L1=2 and pointed to the origin without learning any object array in Experiment 2. The results still showed the absence of cue combination for the homing estimations in the BO and CO conditions, disconfirming the homing hypothesis.

Although there was evidence of the cue combination in the homing estimations for the group of the leg ratio of 0.5 in Experiment 1, we should not conclude that the participants in that group combined homing estimations from the path integration system and from the piloting system, therefore, partially supporting the homing hypothesis. It is very hard for the homing hypothesis to explain why people combine cues in homing estimations for a small leg ratio but not for a large leg ratio. Furthermore, as illustrated by Figure 2.12, the mathematical model elaborating on the positioning hypothesis also well explained the observed homing variability in the group of the leg ratio of 0.5 as well as other groups of the leg ratio (1 and 2) in Experiment 1. Following the principle of parsimony, we would conclude that the participants in the group of the leg ratio of 0.5 in Experiment 1 also combined positioning estimations but not homing estimations just as in other groups of leg ratios.

The findings of the current study that favour the positioning hypothesis over the homing hypothesis are theoretically important. The positioning and homing hypotheses have very different theoretical assumptions and computational implications. The positioning hypothesis

assumes that both the path integration and piloting systems form and rely on spatial representations of locations in the same cognitive maps (Gallistel, 1990; Gallistel & Matzel, 2013; Müller & Wehner, 1998; Zhang et al., 2011). Referring to the same cognitive map, people estimate their heading and position by combining the estimations from the path integration and piloting systems and then use the estimated heading and position to determine their home location. In contrast, the homing hypothesis assumes that the path integration system and the piloting system have separate spatial maps of goals including home (Vickerstaff & Cheung, 2011). Referring to the spatial map within the system, the path integration system and the piloting system produce separate home location estimations. These two estimations are then combined to determine the home location.

Combining estimations of one's positions and headings relative to the same cognitive map seems computationally much simpler than combining estimations of home locations from separate spatial maps. In real-life navigation, people have multiple goal locations simultaneously, such as home, office, and grocery stores (Wang, 2016). According to the positioning hypothesis, the path integration and piloting systems produce separate estimations of people's position and heading but only maintain single representation for all goal locations in the same cognitive map. By contrast, according to the homing hypothesis, the path integration and piloting systems may need to produce separate estimations for each goal using the spatial map within the system. Producing and combining dual representations of multiple goals is much more complicated than producing and combining dual representations of people's position and heading estimations.

The positioning hypothesis was partially supported by the findings in non-human studies. For example, head direction cells and place cells can be activated by both landmarks and inertial cues (Taube, 2007; Wang, 2016; Fetsch et al., 2010; 2012; 2013). The positioning hypothesis

was also consistent with the previous human studies showing that visual landmarks reset positioning estimations in the path integration system (Mou & Zhang, 2014; Zhang & Mou, 2017). However, no prior studies examined cue interaction in both positioning estimations and homing estimations. For the first time, the current study demonstrates that for human adults, cue interaction occurs in positioning estimations rather than in homing estimations, supporting the hypothesis that the path integrations and piloting systems estimate individuals' positions/headings in the same cognitive map of locations rather than determine the goals' location in two separate spatial maps of locations (one self-to-object and one object-to-object maps) and then combine them.

Previous studies showed that homing estimations of human adults could be explained by the Bayesian or quasi-Bayesian combination model (e.g., Chen et al., 2017; Nardini et al., 2008; Sjolund et al., in press). We speculate that these findings might have occurred because these studies used various leg ratios and analyzed the data by collapsing all leg ratios. As we found in Experiment 1, evidence disconfirming the Bayesian or quasi-Bayesian combination model for homing estimations is the clearest when the leg ratio is 2, whereas there is no evidence disconfirming the Bayesian or quasi-Bayesian combination when the leg ratio is 0.5. Evidence in the group of the leg ratio of 1 is in between. Thus, it might have been hard to find evidence to disconfirm the Bayesian or quasi-Bayesian combination model if collapsed data across all leg ratios were analyzed in the previous studies.

Examining cue combination in homing estimations is one standard paradigm that is used to understand how the path integration system and the piloting system interact in human navigation (Chen et al., 2017). The findings of the current study suggest that researchers should be cautious in using this standard paradigm. The conclusion based on the analyses of homing

estimation could sometimes be misleading. For example, although cue combination occurs in positioning estimations, we may conclude that no cue combination occurs if we only analyze the homing estimations in the group of L2/L1=2. Consequently, we suggest that we should examine positioning estimations in addition to homing estimations when we study cue interaction in human navigation.

Some findings in the previous studies examining homing estimations are at odd with the cue combination models. For example, Zhao and Warren (2015) reported that the mean of the combined estimation was determined by one system (the piloting or the path integration system), consistent with the competition model, whereas variance of the combined estimation was reduced, supporting the Bayesian combination. A linear combination model cannot explain how reduced variability and cue competition occur together. If an observed weight is 1, a linear combination (i.e., broadly-defined cue combination model) predicts that the observed variance in the CO condition should be the same as that in the condition of the single cue that was assigned the weight of 1. The current study also showed that homing estimations in the leg ratio 2 could not be explained by a linear combination model, consistent with the findings of Zhao and Warren. Future studies need to examine positioning estimations as well as homing estimations by using the leg ratios and conflicting angles in the study of Zhao and Warren (2015) and investigate whether cue combination and cue competition simultaneously occur in positioning as well as in homing estimations.

Elaborating on the positioning hypothesis, we developed a mathematical model that quantitatively describes how people use the path integration system and the piloting system to guide homing behavior when distal landmarks are used (see Table 2.2). This model is based on the conjecture that the position estimation error (PER) and the heading estimation error (HER)

jointly determine the homing direction error (see Equation 2.6) (Mou & Zhang, 2014; Zhang & Mou, 2017). In addition, this model is based on the findings that rotated distal landmarks changed the participants' heading estimations and the disorientation at the end of the outbound path disrupted participants' heading estimations; however, neither the rotated landmarks nor the disorientation changed the participants' position estimation from the path integration system (Mou & Zhang, 2014). This model is also based on the fact that in the path integration system, the position estimation error is determined by the heading estimation error during walking (i.e., the error of estimating the turning angle, see Equation 2.7; also see Müller & Wehner, 1988). In addition, this dependency (explaining PER_{PI} with HER_{PI}) increases with the leg ratio. For example, PER_{PI} is independent of HER_{PI} when L2/L1=0, whereas PER_{PI} equals HER_{PI} when L2/L1 is an infinite number. As far as we know, this is the first time that a mathematical model quantitatively describing the relations between position, heading, and homing estimations in terms of variability is proposed and empirically confirmed. This model accurately predicted the homing variability in the conditions of LM, BO, and CO using the PER_{PI}, HER_{PI} and HER_{LM} (Figure 2.12). The dependency of PER_{PI} on HER_{PI} in the path integration system is clearly supported by the regression analyses shown in Figure 2.11. Furthermore, the simulation based on this model in Figure 2.4 predicts that when L2/L1 increases, the homing variability in the BO condition more likely departs from the prediction based on the model of combining homing estimations and may be larger than that in the PI condition. This prediction was confirmed by the current finding (Figure 2.9).

It is important to note that the mathematical model described above assumes that distal landmarks are used. A mathematical model that allows for proximal landmarks will be much more complicated, as both position and heading estimations are combined to determine homing

estimations, and yet be developed in the future. However, one key characteristic of the current model seems also applicable to the situations when proximal landmarks are used. In the current model, when the leg ratio is large (i.e., L2/L1=2), the strong dependency of PER_{PI} on HER_{PI} can yield a very small homing variability in the path integration system (see Figure 2.4). It occurs because in homing estimations, PER_{PI} and HER_{PI} cancel out (see Equation 2.6). Due to the small homing variability in the PI condition, it is hard to observe an even smaller homing variability in the both cue (BO/CO) conditions to produce evidence of the Bayesian or quasi-Bayesian combination. As a result, the Bayesian or quasi-Bayesian combination model is more likely to be rejected when the leg ratio is large. This analysis is also applied to Experiments 3 and 4 where the leg ratio of 2 and the proximal landmarks were used. Consistently, the findings in Experiments 3 and 4 also rejected the Bayesian or quasi-Bayesian combination model, although the current mathematical model cannot calculate the predicted homing variability in Experiments 3 and 4 as in Experiment 1.

Can we develop a mathematical model elaborating on the homing hypothesis so that it can also accommodate the findings in Experiment 1 just as the mathematical model elaborating on the positioning hypothesis? We doubt it, unless we use a nonlinear combination model. The homing hypothesis proposed in the current paper stipulates that a linear cue combination of the path integration system and the piloting system occurs in homing estimations. A mathematical model elaborating on a linear cue combination was well-developed (for the broadly defined cue combination model, see Equations 2.1 and 2.2 in the current paper) and used in the previous studies (e.g., Nardini et al., 2008). We also adopted this mathematical model elaborating on a linear cue combination model to analyze the homing variability in the CO conditions for all four

experiments in the current study. This model only succeeded in Experiment 3 (one out of the four situations using L2/L1=2 across all experiments).

In the current study, consistent with the procedures used in the previous studies, we rotated landmarks with respect to the participants' standing location in the testing phase in the CO condition (Chen et al., 2017; Nardini et al., 2008; Zhao & Warren, 2015). It is important to note that this manipulation objectively makes the heading estimations from the two systems in the CO condition discrepant in a predicted degree (i.e., 45º), but not for the position estimations. Therefore, in Experiment 4, although we concluded that the position estimations in the BO condition were predicted by the quasi-Bayesian combination, we could not calculate the weight assigned to each cue system using the position estimations in the CO condition, as we did not have a predicted angular difference of position estimations between these two systems. Future studies should systematically manipulate the discrepancy of the positions indicated by the two cues and examine cue combination of the position estimations. For example, we may use a single proximal landmark and displace this landmark to make the position estimations predicted from the two cues discrepant. By having two different position estimations from the two cues, we could determine the observed weight assigned to each single cue system in the CO condition.

Last but not least, in all experiments, the observed variability of heading estimations in the BO and CO conditions did not differ from the optimal variability in Experiments 1, 3, and 4 (not applied to Experiment 2). However, in most of these cases (except Experiment 4), the observed variabilities of the heading estimations in the BO and CO conditions were not significantly smaller than that in the LM conditions, which was also often observed in the previous studies (see Table 2.1A and 2.1B). These findings could result from two possibilities. First, as landmarks are more reliable (with a smaller variance) than the path integration cues, the

participants might have only used landmarks in the BO and CO conditions (weight for landmarks is 1). Second, as landmarks are more reliable (with a smaller variance) than the path integration cues, the participants might have weighed the landmarks heavier than the path integration cues in the Bayesian manner. Although the variability of the Bayesian combination should be numerically smaller than that in the LM condition, they may not differ significantly due to the statistic power especially when the variability in the LM condition is much smaller than that of the PI condition. To distinguish between these two possibilities, we compared the observed weight assigned to landmarks for heading estimations to 1 in the CO conditions for Experiments 1, 3, and 4. As illustrated in Table 2.9, all comparisons but one (Experiment 1 L2/L1 = 0.5) indicated that the observed weight assigned to LM was significantly smaller than 1. These findings favoured the second possibility that the participants might have weighed cues in the Bayesian manner.

Table 2.9 Summary of the comparison testing between the observed landmark weights and the value of 1 assuming the landmark dominance in the heading estimations in Chapter 2.

Experiment	*t*	*p*	Cohen's *d*
Exp 1 L2/L1 = 2	4.48	< .001	1.20
Exp 1 L2/L1 = 1	4.10	< .001	1.09
Exp 1 L2/L1 = 0.5	1.40	0.17	0.37
Exp 3	2.04	0.05	0.55
Exp 4	2.30	0.03	0.61

In conclusion, the current findings support the positioning hypothesis that explains how people determine the origin of a traveled path. People estimate their positioning (positions and headings) using the cues from the piloting and path integration systems. Then people use the combined positioning estimations to determine the home location. Cue combination occurs during positioning estimations, rather than during homing estimations.

2.8. References

Benhamou, S., Sauvé, J. P., & Bovet, P. (1990). Spatial memory in large scale movements: efficiency and limitation of the egocentric coding process. *Journal of Theoretical Biology, 145*(9), 1-12.

Chen, X., McNamara, T. P., Kelly, J.W., & Wolbers, T. (2017). Cue combination in human spatial navigation. *Cognitive Psychology, 95*, 105-144.

Cheng, K., Shettleworth, S. J., Huttenlocher, J., & Rieser, J. J. (2007). Bayesian integration of spatial information. *Psychological Bulletin, 133,* 625–637.

Collett, M., & Collett, T. S. (2000). How do insects use path integration for their navigation? *Biological Cybernetics, 83*(3), 245-259.

Ernst, M. O., & Banks, M. S. (2002). Humans integrate visual and haptic information in a statistically optimal fashion. *Nature, 415,* 429–433.

Etienne, A. S., Maurer, R., Boulens, V., Levy, A., & Rowe, T. (2004). Resetting the path integrator: A basic condition for route-based navigation. *The Journal of Experimental Biology, 207*, 1491–1508.

Fetsch, C. R., DeAngelis, G. C., & Angelaki, D. E. (2010). Visual–vestibular cue integration for heading perception: applications of optimal cue integration theory. *European Journal of Neuroscience, 31*(10), 1721-1729.

Fetsch, C. R., DeAngelis, G. C., & Angelaki, D. E. (2013). Bridging the gap between theories of sensory cue integration and the physiology of multisensory neurons. *Nature Review Neuroscience, 14*, 429-442.

Fetsch, C. R., Pouget, A., DeAngelis, G. C., & Angelaki, D. E. (2012). Neural correlates of reliability-based cue weighting during multisensory integration. *Nature Neuroscience*, *15,* 146-154.

Fujita, N., Loomis, J. M., Klatzky, R. L., & Golledge, R. G. (1990). A Minimal Representation for Dead-Reckoning Navigation: Updating the Homing Vector. *Geographical Analysis, 22*(4), 324-335.

Gallistel, C. R. (1990). *The organization of learning*. Cambridge, MA: MIT Press

Gallistel, C. R., & Matzel, L. D. (2013). The neuroscience of learning: beyond the Hebbian synapse. *Annual Review of Psychology*, *64*, 169-200.

Loomis, J. M., Klatzky, R. L., Golledge, R. G., Cicinelli, J. G., Pellegrino, J. W., & Fry, P. A. (1993). Nonvisual navigation by blind and sighted: Assessment of path integration ability. *Journal of Experimental Psychology: General, 122*(1), 73-91.

Mou, W., & Zhang, L. (2014). Dissociating position and heading estimation: rotated visual orientation cues perceived after walking reset headings but not positions. *Cognition*, *133,* 553-571.

Müller, M., & Wehner, R. (1988). Path integration in desert ants, Cataglyphis fortis. *Proceedings of the National Academy of Sciences*, *85*(14), 5287-5290.

Muller, R. (1996). A quarter of a century of place cells. *Neuron*, *17*(5), 813-822.

Nardini, M., Jones, P., Bedford, R., & Braddick, O. (2008). Development of cue integration in human navigation. *Current Biology, 18*(9), 689-693.

Petrini, K., Caradonna, A., Foster, C., Burgess, N. & Nardini, M. (2016). How vision and self-motion combine or compete during path reproduction changes with age. *Scientific Reports, 6*, 29163.

Sjolund, L. A., Kelly, J. W., & McNamara, T. P. (in press). Optimal combination of environmental cues and path integration during navigation. *Memory & Cognition.*

Taube, J. S. (2007). The head direction signal: origins and sensory-motor integration. *Annual Review of Neuroscience*, *30*, 181-207.

Tcheang, L., Bülthoff, H. H., & Burgess, N. (2011). Visual influence on path integration in darkness indicates a multimodal representation of large-scale space. *Proceedings of the National Academy of Sciences*, *108*(3), 1152-1157.

Vickerstaff, R. J., & Cheung, A. (2010). Which coordinate system for modelling path integration? *Journal of Theoretical Biology, 263*(2), 242-261.

Wang, R. F., & Spelke, E. S. (2002). Human spatial representation: Insights from animals. *Trends in Cognitive. Sciences*, *6*(9), 376-382.

Wang, R. F. (2016). Building a cognitive map by assembling multiple path integration systems. *Psychonomic Bulletin & Review, 23*(3), 692-702.

Zhang, H., Mou, W., & McNamara, T. P. (2011). Spatial updating according to a fixed reference direction of a briefly viewed layout. *Cognition, 119*(3), 419-429.

Zhang, L., & Mou, W. (2017) Piloting systems reset path integration systems during position estimation. *Journal of Experimental Psychology: Learning, Memory and Cognition, 43*(3), 472-491.

Zhao, M., & Warren, W. H. (2015). How you get there from here: Interaction of visual landmarks and path integration in human navigation. *Psychological Science, 26*(6), 915-924.

Chapter 3

Selective resetting position and heading estimations during driving in a large-scale environment

3.1 Abstract

Two experiments investigated how self-motion cues and landmarks interact in determining a human's position and heading estimations during driving in a large-scale environment. In an immersive virtual city, participants learned five buildings' locations in the presence of two proximal towers and four distal scenes. Then participants drove two streets without viewing these buildings, towers or scenes. When they finished driving, either one tower with displacement to the testing position or the scenes with rotation reappeared. Participants pointed to the five buildings' directions. The least squares fitting method was used to calculate participants' estimated positions and headings. The results showed that when the displaced proximal tower reappeared, participants used this tower to determine their positions, but used self-motion cues to determine their headings. When the rotated distal scenes reappeared, participants used these scenes to determine their headings. However, if they were instructed to continuously keep track of the origin of the path while driving, their position estimations followed self-motion cues, and if they were not given instructions, their position estimations were random. These findings suggest that when people drive in a large-scale environment, relying on self-motion cues, the path integration system calculates headings continuously (online) but calculates positions only when they are required (offline); relying on the displaced proximal landmark or the rotated distal scenes, the piloting system selectively resets the position or heading representations produced by the path integration system.

Keywords: self-motion cues, landmarks, driving, heading estimations, position estimations

3.2. Introduction

Knowing our positions and headings in an environment is important for successful navigation. In everyday life, we use two navigation systems to estimate our positions and headings. One is the *path integration system* using self-motion cues to obtain moving directions and distances by which we then calculate our positions and headings relative to items experienced on the path. Self-motion cues (idiothetic cues) comprise *optic flow* and *inertial cue*s. The latter includes vestibular cues, proprioceptive cues, and motor efference copies (e.g., Klatzky, Loomis, Beall, Chance, & Golledge, 1998; Muller & Wehner, 1988; Warren, Kay, Zosh, Duchon, & Sahuc, 2001). The other system is the *piloting system* using previously encoded visual landmarks to determine our positions and headings (e.g., Cheng & Spetch, 1998; Gallistel, 1990). Several studies have examined the roles of these two systems in position and heading estimations when people walk in a small space (e.g., Mou & Zhang, 2014; Zhang & Mou, 2017). The current study, however, examined the roles of these two systems in position and heading estimations when people drive in a large-scale environment.

In everyday life, people usually see visual landmarks while walking around. Therefore, the piloting system and the path integration system work together in determining people's positions and headings. One popular theory about the roles of these two systems in people's estimations of positions and headings is that the path integration system dynamically calculates people's positions and headings, whereas the piloting system intermittently corrects the errors accumulated in the path integration system (Etienne & Jeffery, 2004; Gallistel, 1990). This error-correcting process is called resetting. Most studies use a homing paradigm to test this resetting theory (e.g., Chen & McNamara, 2017; Nardini, Jones, Bedford, & Braddick, 2008; Zhao & Warren, 2015). In the homing paradigm, participants walk an outbound path and then judge the

origin of the path. Before judgments are made, the visual landmark is displaced, indicating a home location different from that indicated by the piloting system. If participants estimate their home location based primarily on the displaced landmark, the conclusion drawn is that the piloting system has reset the path integration system.

Mou and Zhang (2014) argued that we could not separate position and heading estimations using home estimation because people's homing estimation is jointly determined by their position and heading estimations. Thus, the findings about the piloting and path integration systems' roles in determining people's homing behavior cannot precisely illustrate how these systems affect the way people estimate their position and heading. Extending the homing paradigm, Mou and Zhang developed a new paradigm that assesses people's position and heading estimations. In the new paradigm, participants learn several locations in an environment before walking the outbound path. During testing, participants indicate the previously learned locations in addition to the origin of the outbound path. Participants' heading and position estimations are calculated from their response locations of the origin and the previously learned locations. Using this new paradigm, Mou and Zhang demonstrated that rotated distal visual landmarks reset participants' heading estimations but not their position estimations from the path integration system. Furthermore, Zhang and Mou (2017) reported that a proximal visual landmark that had been displaced to the participants' testing position reset the participants' position estimations but not their heading estimations from the path integration system.

These two studies suggest that people separately maintain their position and heading representations; both representations are dynamically updated by the path integration system; and the heading or position representations in the path integration system can be reset selectively by rotated distal cues or by a proximal landmark displaced to the testing position. We refer to

this elaborated resetting model as the selective resetting hypothesis to differentiate it from the original resetting theory (Etienne & Jeffery, 2004; Gallistel, 1990).

In the current study, we tested the selective resetting hypothesis when participants drove in a large-scale environment. There are two important theoretical motivations. The first motivation is to investigate whether the selective resetting hypothesis can be generalized to a different environment scale and a different locomotion mode. In previous studies (Mou & Zhang, 2014; Zhang & Mou, 2017), participants walked in a small space (approximately four-by-four meters). The environment scale and the locomotion mode may impact the interaction between the piloting system and the path integration system, as human spatial cognition in general depends on the environment scale (Montello, 1993) and the locomotion mode (Klatzky et al., 1998).

The interaction between the piloting system and the path integration system in a large-scale environment may differ from that in a small space. In a small space, people usually see all items while standing at a single position. Therefore, the role of the piloting system might be critical, whereas the role of the path integration system is trivial in people's position and heading estimation in a small space. In contrast, in a large-scale environment, people cannot view all items while standing at a single position and need to locomote to view them. Estimating positions and headings is challenging in the piloting system and thus requires more contributions from the path integration system (e.g., Ishikawa & Montello, 2006; Waller, Loomis, & Steck, 2003). Furthermore, the interaction between the piloting system and the path integration system during driving may also differ from that in walking. More inertial cues (especially proprioceptive cues) are available in walking than in driving. Studies have indicated that proprioceptive

information is critical to efficient spatial updating (Chrastil & Warren, 2013). As a consequence, the path integration system may be less efficient in driving than in walking.

Therefore, it is theoretically important to investigate whether the selective resetting hypothesis, inferred from the findings when participants walked in a small space, can be generalized to a situation when participants drive in a large-scale environment. The selective resetting hypothesis would be much strengthened if it could be empirically supported regardless of the scale of the environment (small or large) and the locomotion mode (driving or walking).

The second important motivation is to test the selective resetting hypothesis when people drive in a large-scale environment is to examine the claims of dynamic updating of positions and headings in the path integration system. The resetting hypotheses, both the original resetting hypothesis and the selective resetting hypothesis, claim that the path integration system dynamically calculates one's positions and headings. However, Wiener, Berthoz, and Wolbers (2011, see also He & McNamara, 2017) reported that participants could be instructed to update the home estimation while walking the path (online) or only when they were asked to judge the home location (offline). The online home estimation occurred when participants were asked to keep track of the origin of the outbound path while walking, whereas the offline home estimation occurred when participants were asked to pay attention to the shape of the outbound path while walking. Inspired by their findings, we speculate that people's position estimations are updated online in walking but updated offline in driving; people's heading estimations are updated online regardless of the locomotion methods (walking or driving). We elaborated on the reasons for this speculation in the following paragraphs.

During locomotion, people's position estimations in the path integration system rely on their heading estimations, which are the same as the travelling direction in general. However, people's heading estimations do not rely on their position estimations. Because of this asymmetrical dependency between position and heading estimations, estimating one's position is harder than estimating one's heading. The difficulty in estimating positions might not be significant or noticeable when participants walk but becomes significant and noticeable when participants drive. There are a number of reasons for this, starting with the fact that walking has a much longer history than driving in human evolution. Individuals have richer inertial cues, especially proprioceptive, during walking than during driving. Furthermore, driving is usually much faster than walking. Driving requires the path integration system to process motion information and calculate the positions much faster than walking does. As a result, when people walk, the path integration system can update both representations of headings and positions online. In contrast, when people drive, the path integration system updates the heading representation dynamically (online), but calculates the positions only when they are required (offline).

Given that the mechanism of position updating (i.e., online versus offline) in the path integration system might depend on the locomotion mode, we modify the selective resetting hypothesis. In the modified version, the selective resetting hypothesis is still valid when people walk. However, when people drive, the path integration system produces the heading estimations online, but produces the position estimations offline. Despite this modification, the heading or position representations in the path integration system can still be reset selectively by rotated distal cues or by a displaced proximal landmark when people drive. We refer to this hypothesis as the locomotion-dependent selective resetting hypothesis. Two experiments were conducted to

test the selective resetting hypothesis and the locomotion-dependent selective resetting hypothesis.

3.3. Experiment 1

In an immersive virtual city, participants learned five buildings' locations in the presence of four distal scenes and two proximal towers (illustrated in Figure 3.1A and Figure 3.2A). Without viewing the buildings, scenes, and towers, they then drove on a street, turned at one intersection, and drove on a second street. After driving, participants, while standing at P and facing H, pointed to the five buildings' directions in the presence of a no-piloting cue (the *no-piloting cue condition*, Figure 3.1C and Figure 3.2B), a displaced single tower (the *displaced proximal landmark* condition, Table 3.1D and Table 3.2C), or the rotated distal scenes (the *rotated distal scene* condition, Table 3.1E and Table 3.2D). We calculated their estimated positions (P') and headings (H') using the least squares method to fit their response directions of the buildings.[7] The direction of the estimated heading (H') and the direction of the position vector (i.e., OP') from the origin of the path (O, Table 3.2) to the estimated testing position (P') were then used to diagnose whether position and heading estimations followed self-motion cues or piloting cues. We summarize the cues available in the three conditions in Table 3.1.

[7] Note that we did not use the method developed in Mou and Zhang (2014), because this method requires people to indicate targets' locations. In a large-scale environment, however, it is more realistic to point to the targets' directions.

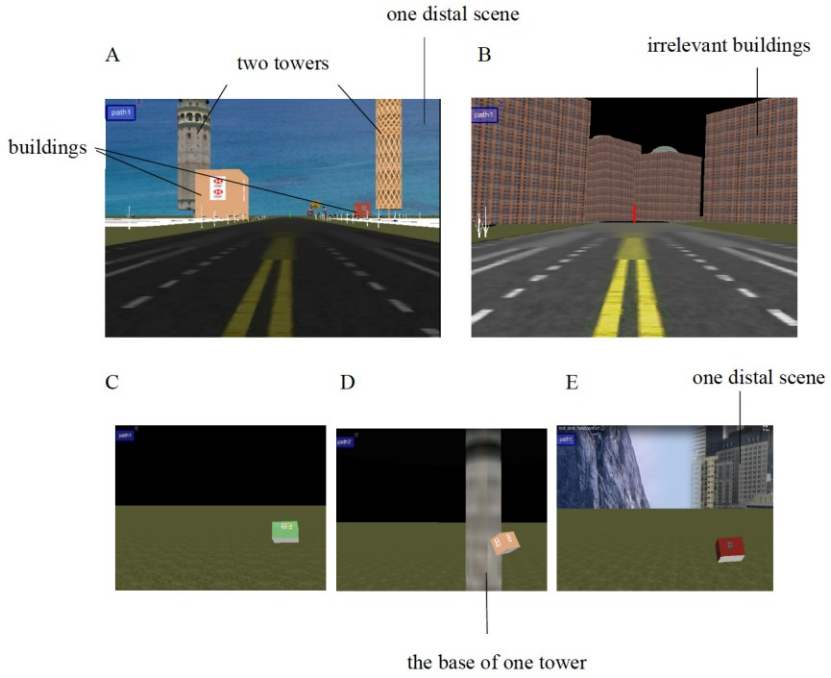

Figure 3.1 The snapshots of experiment setup in Chapter 3.

The snapshots of the first-person view in each experimental phase in Experiment 1 across conditions: the study phase (A), the driving phase (B), the testing phase in the no-piloting cue condition (C), the testing phase in the displaced proximal landmark condition (D), and the testing phase in the rotated distal scene condition (E). The floating object in (B), (C), and (D) is the one probed for testing.

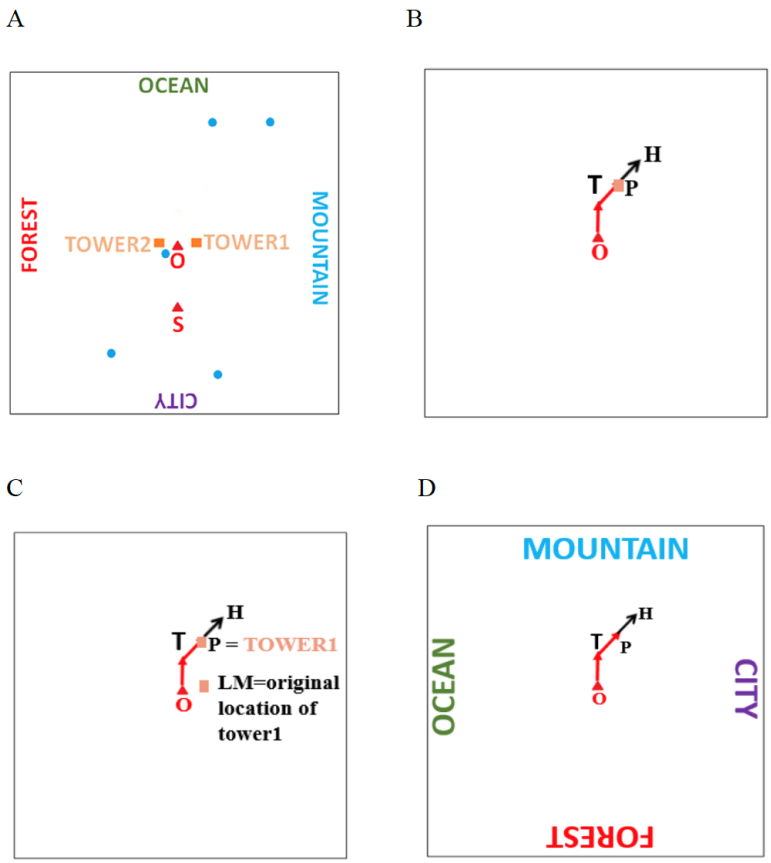

Figure 3.2 Schematic diagrams of the experimental set-up in Experiment 1 of Chapter 3.

(A) The study phase across all conditions. The red triangles represent the two study perspectives (S and O). The orange squares represent the two proximal landmarks (two towers). The words ocean, forest, city and mountain are used in place of visual representations of the distal scenes. Blue dots are the five target buildings. (B) The driving path and testing phase in the no-piloting cue condition, (C) in the displaced proximal landmark condition, and (D) in the rotated distal scene condition. O is also the origin of the path. T is the turning point. P is the testing position. H is the heading in the testing. LM is the original location of one tower (Panel C). Lengths of vectors: OT = TP = T-LM =100m. Directions of vectors with respect to OT: TP = 50°, O-LM = 75°, OP = 25°.

Table 3.1 Cues that are available to determine OP' and H' in Chapter 3.

Cues that were available to determine the estimated testing position vector (OP') and the estimated heading (H'), and cues that were used to determine the directions of OP' and H' in different experimental conditions. The first three conditions were used in Experiment 1 and the last one was used in Experiment 2.

Conditions	OP'	H'	Observed OP'	Observed H'
No-piloting cue	self-motion cues	self-motion cues	self-motion cues	self-motion cues
Displaced proximal landmark	self-motion cues and landmarks	self-motion cues	landmark	self-motion cues
Rotated distal scene	self-motion cues	self-motion cues and landmarks	undetermined	landmarks
Rotated distal scene & instruction	self-motion cues	self-motion cues and landmarks	self-motion cues	landmarks

The first purpose of this experiment was to investigate whether resetting also occurred when participants drove in a large-scale environment. The *rotated distal scene* condition was used to investigate whether the rotated distal scenes reset participants' heading estimations. In this condition, as the distal scenes were rotated 100° in the testing phase (Table 3.2D), the headings determined by self-motion cues available in driving and by the rotated distal scenes were in conflict. If participants' heading followed the rotated distal scenes, then we would conclude that distal piloting cues had reset participants' heading estimations in the path integration system. The *displaced proximal landmark* condition was used to investigate whether the displaced proximal landmark reset participants' estimated positions. In this condition, as the proximal landmark was displaced to the testing position (Table 3.2C), the positions determined by self-motion cues available in driving were in conflict with those available by the proximal landmark. If participants' positions followed the displaced landmark, then we would conclude

that the proximal piloting cue had reset the participants' position estimations in the path integration system.

The second purpose of this experiment was to investigate whether the representations that were not reset by the visual piloting cues followed self-motion cues. The selective resetting hypothesis and the locomotion-dependent selective resetting hypothesis have different predictions in the *rotated distal scene* condition. The selective resetting hypothesis claims that the path integration system dynamically produces people's position estimations in driving as in walking. According to this hypothesis, participants' position estimations have been produced in the path integration system when the rotated distal scenes reappear. Consequently, participants' position estimations would follow self-motion cues available in driving. In contrast, the locomotion-dependent selective resetting hypothesis claims that the path integration system produces people's position estimations offline. According to this hypothesis, when participants stop driving, the path integration system has not yet produced a position representation using self-motion cues. Furthermore, when they see the distal scenes, the position calculation in the path integration system will be disrupted by the rotated scenes. The rotated distal scenes indicate a turning angle that conflicts with that indicated by self-motion cues. The path integration system cannot make a decision about which turning angle should be used for the position calculation. As there was no position representation yet in the path integration system when participants stopped driving and no further position representation were calculated when they saw the rotated distal scenes, the position estimations would not follow self-motion cues and might be random. The key differences between these two hypotheses are listed in Table 3.2.

Table 3.2 Differences between the selective resetting hypothesis and the locomotion-dependent selective resetting hypothesis.

	Selective resetting hypothesis	Locomotion-dependent selective resetting hypothesis
Mechanism of updating position representations	Online	Offline
Prediction on the position estimations in the *rotated distal scene* condition	following self-motion cues	random

Nevertheless, the selective resetting hypothesis and the locomotion-dependent selective resetting hypothesis have the same prediction for the *displaced proximal landmark* condition. Both hypotheses claim that the path integration system dynamically produces people's heading estimations. Therefore, both hypotheses predict that participants' heading estimations will follow self-motion cues.

We also used the *no-piloting cue* condition, as a baseline, to measure how accurately participants could primarily use self-motion cues to update their positions and headings in our experimental setup. Participants in our experimental setup primarily used optic flow as self-motion cues. Waller et al. (2003) showed that participants were able to use optic flow to estimate objects' locations (see also Kearns, Warren, Duchon, & Tarr, 2002; Riecke, Cunningham, & Bulthoff, 2007). Other studies, however, showed that optic flow was insufficient for the spatial updating (Ruddle & Lessels, 2009). Hence, although we know the theoretical values of the position and heading estimations that follow self-motion cues, it is also important to empirically measure these values and show if the empirical values are consistent with the theoretical values.

In addition, the consistency between the empirical measurements and the theoretical values can also ensure that our method to calculate participants' position and heading estimations is valid.

3.3.1 Method

3.3.1.1 Participants

Thirty-six university students (18 men) participated in the experiment to fulfill the partial requirement for an introductory psychology course. Before the experiment, all participants signed the consent form approved by University of Alberta Research Ethics Board.

3.3.1.2 Apparatus and Stimuli

The virtual city was displayed in stereo with an nVisor SX60 head-mounted display (HMD) (NVIS, Inc. Virginia). Participants used a gaming wheel and paddles from Logitech driving Force GT (Logitech International S.A., California) for driving and held an InterSense IS-900 Wand for pointing. Their head motions were tracked with an InterSense IS-900 motion tracking system (InterSense, Inc., Massachusetts).

In the virtual city (Table 3.1), five buildings (7-11, DQ, Subway, HSBC and NQ) were used as the targets that participants pointed to in the testing phase. Four different scenes (ocean, forest, mountain and city) were used as distal landmarks and two different towers (a grey tower and a golden tower) were used as proximal landmarks. To encourage participants to perceive the locations of the buildings and landmarks more accurately, we had participants perceive them at two viewing locations: the starting position (S) and the origin of the driving path (O). The distance between these two positions was 200m.

The four different scenes were set at infinity as distal orientation cues. The two towers were located 51.76m from O in the direction of 75° clockwise and counter-clockwise with respect to the first street (i.e., OT in Table 3.2). The five buildings were located 44.72m, 364.01m, 443.27m, 379.47m, and 360.56m away from the origin O. The driving path started from O and consisted of two streets (100m each) and one turn with 50° either left or right. The first street extended the road from S to O. Only the first street was presented to participants in the study phase. Each participant completed two trials in the experiment (driving two paths with either a left or right turn). The order of the trials was randomized.

The primary independent variable was the cues available to participants after driving the path. In the *no-piloting cue* condition, neither the distal scenes nor the towers were presented. In the *rotated distal scene* condition, the distal scenes reappeared with a rotation of 100°. The direction of the rotation was opposite to the turning direction on the path. Thus, if participants used the rotated distal scenes to estimate the turning angle, they would feel that they had turned 150°. In the *displaced proximal landmark* condition, only the tower that was in the same direction of the turning path with respect to the first street was presented. The tower was displaced to the testing position (i.e., P). Thus, participants saw that they were standing at the base of the tower after driving. Participants were randomly assigned to one of the above three conditions, with an equal number of males and females in each condition. The dependent variables were their estimated testing positions (i.e., OP') and headings (H').

3.3.1.3 Procedure

Before the experiment, participants were given three minutes to read and memorize a map that contained the five target buildings and two study locations (S and O). Then, while

wearing a blindfold, participants entered the testing room under the guidance of the experimenter. They then removed the blindfold and donned the HMD.

In the virtual reality environment, participants were teleported to the first study location (S). They studied the distal scenes, two towers, and five buildings for three minutes (Table 3.1A & 4.2A). Then the buildings disappeared. Participants used the wand to point to the directions of buildings in two blocks. In each block, all five buildings were probed in a random order. The feedback of the correct location was provided after each pointing. After studying at S, participants drove from S to O and studied the five target buildings for another 30 seconds followed by the two rounds of pointing and feedback. After studying at O, participants drove a path (O-T-P, Table 3.2B, 3.2C & 3.2D) without seeing the landmarks, distal scenes, or target buildings. However, some irrelevant buildings were presented on the street to provide rich optic flow and to block the complete view of the driving path. At the end of the second street (the testing position P), participants pointed to the five target buildings' directions in one of the three conditions: the *no-piloting cue* condition, the *rotated distal scene* condition, or the *displaced proximal landmark* condition. After that, participants were teleported to S and started the second experimental trial, which was the same as the first one except for the turning direction (left or right) on the path. Before these two experimental trials, participants had one practice trial to familiarize themselves with the procedure. In the practice trial, they learned two target buildings that were different from those in the experimental trials. In addition, the turning angle of the path was 90°.

3.3.1.4 Data analysis

We used the least squares fitting method to calculate the estimations of the testing position and heading for each participant on each experimental path. The least squares fitting method is widely used (e.g., in a regression analysis) and has also been used in estimating people's headings (e.g., Yerramsetti, Marchette, & Shelton, 2013). For each participant and each path, we searched for a position (P') and a heading (H') that led to the least sum of squares of the errors in pointing buildings. The error in pointing to each building is measured with the angular difference between the original direction of this building, relative to this hypothetical position and heading, and the participant's response direction to this building, relative to the participant's testing position and heading after driving.[8] For example, given a hypothetical position and heading, the direction from the hypothetic position to building A relative to the hypothetical heading is 90º; a participant points to the direction of 80º when they points to building A. Then the error will be 10º. As in our previous studies, we used the estimated position vector, OP', as the position measurement (Mou & Zhang, 2014; Zhang & Mou, 2017). As we were not interested in the turning direction, we flipped the signs of OP' and H' for the left turning path and combined them with the right turning one.

In the interest of exposition, in the experiment below we used the driving direction on the first street as the reference direction. If participants used self-motion cues to determine their positions and headings, OP' should be 25°, half of the turning angle, given the equal length of the two legs; H' should be 50°, the turning angle. If participants used the displaced tower to determine their positions, OP' should be 75°, the original direction of the tower relative to O (Table 3.2C). If participants used the rotated distal scenes to determine their headings, H' should

[8] We used the fminsearch function in Matlab as the searching algorithm.

be 150°, as the scenes were rotated 100° in the direction opposite to the turning angle of the path. We used the 95% confidence interval of the mean to diagnose the cues that determined OP' and H' (Batschelet, 1981). We summarize all the predictions in the three conditions in Table 3.3.

Table 3.3 Predicted and observed directions of OP' and H' in Chapter 4.
Predicted directions of the estimated testing position (OP') and the estimated testing heading (H') based on self-motion cues or landmarks, and the observed OP' and H' in different experimental conditions. The predicted OP's and H's consistent with the observed OP's and H's are underlined.

Conditions	Prediction from self-motion cues		Prediction from landmarks		Observed circular mean (length of mean vector, r)	
	OP'	H'	OP'	H'	OP'	H'
No-piloting cue	**25º**	**50º**	undetermined	undetermined	20º (.48)	57º (.67)
Displaced proximal landmark	25º	**50º**	**75º**	undetermined	95º (.48)	72º (.79)
Rotated distal scene	25º	50º	**undetermined**	**150º**	undetermined	140º (.71)
Rotated distal scene & instruction	**25º**	50º	undetermined	**150º**	30º (.48)	138º (.75)

3.3.2 Results and Discussion

In the *no-piloting cue* condition, participants used self-motion cues to estimate their positions (Table 3.3A) and headings (Table 3.4A) (OP'_{mean} = 20°, 95% CI [348° - 52°]; H'_{mean} = 57°, 95% CI [36° - 78°]). The confidence intervals included the predictions from self-motion cues for both OP' and H', 25° and 50° respectively. The observed means of OP' and the predicted means of OP' based on self-motion cues were consistent. This finding indicates that

participants were able to update the representations of their positions and headings using self-motion cues. It also confirms the validity of the least squares fitting method that calculated the observed position and heading estimations.

In the *displaced proximal landmark* condition, the estimated positions (Table 3.3B) followed the displaced tower (OP'_{mean} = 95°, 95% CI [63° - 126°]). The confidence interval included the prediction from the landmark (75°) but excluded the prediction from self-motion cues (25°). The estimated headings (Table 3.4B) were close to what was predicted by self-motion cues (H'_{mean} = 72°, 95% CI [57° - 87°]). The confidence interval excluded the prediction from self-motion cues (50°), although the lower boundary was close to the prediction.

In the *rotated distal scene* condition, the estimated headings (Table 3.4C) followed the rotated distal scenes (H'_{mean} = 140°, 95% CI [121° - 159°]). The confidence interval included the prediction from the landmark (150°) but excluded the prediction from self-motion cues (50°). Critically, participants' position estimations (Table 3.3C) were random, as there was no reliable confidence interval for OP'.

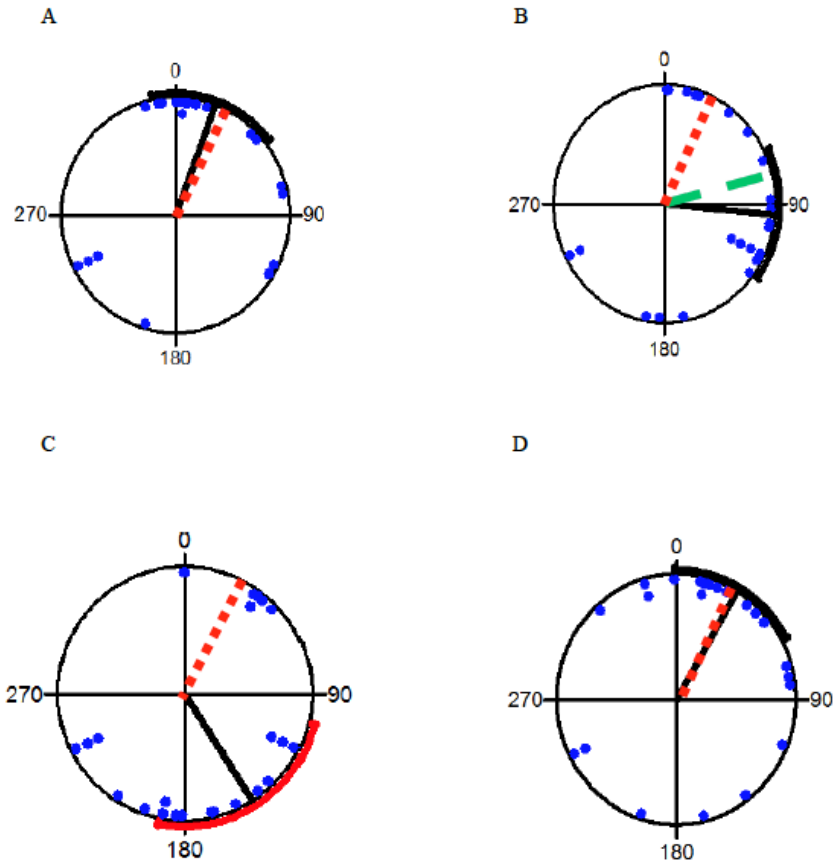

Figure 3.3 Observed and predicted directions of OP' in Chapter 3.

Observed and predicted angular directions of the estimated testing position (OP') in the no-piloting cue condition in Experiment 1 (A), in the displaced proximal landmark condition in Experiment 1 (B), in the rotated distal scene condition in Experiment 1 (C), and in the rotated distal scene & instruction condition in Experiment 2 (D). Each blue dot indicates one observed OP' of one path of one participant (the signs of OP' for the left turning path are converted by flipping the sign). The solid black line indicates the circular mean of the observed OP's. The black arc above the mean direction indicates the 95% confidence interval of the mean direction of the observed OP's. The red arc indicates no reliable confidence interval. The dotted red line indicates the predicted direction of OP' following self-motion cues (25°). The dashed green line

indicates the predicted direction of OP' following the proximal landmark (75°) in the displaced proximal landmark condition.

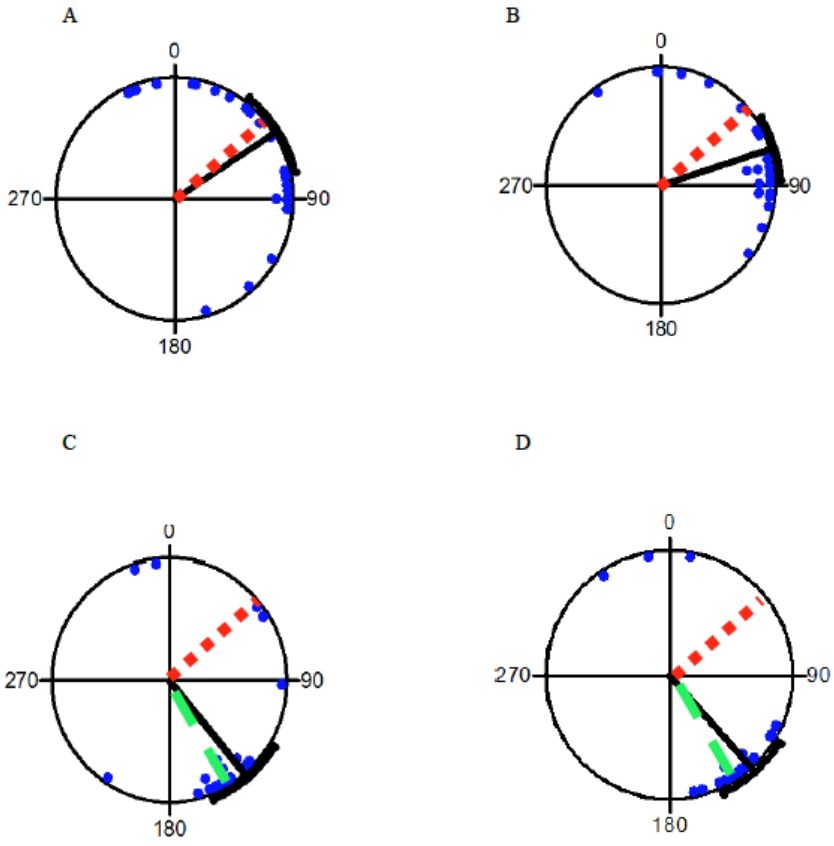

Figure 3.4 Observed and predicted directions of H' in Chapter 3.

Observed and predicted angular directions of the estimated testing heading (H') in the no-piloting cue condition in Experiment 1 (A), in the displaced proximal landmark condition in Experiment 1 (B), in the rotated distal scene condition in Experiment 1 (C), and in the rotated distal scene & instruction condition in Experiment 2 (D). Each blue dot indicates one observed H' for one path of one participant (the signs of H' for the left turning path are converted by flipping the sign). The solid black line indicates the circular mean of the observed H's. The arc above the mean direction indicates the 95% confidence interval of the mean direction of the observed H's.

The dotted red line indicates the predicted direction of H' following self-motion cues (50°). The dashed green line indicates the predicted direction of H' following the distal scenes in the rotated distal scene condition in Experiment 1 and in the rotated distal scene & instruction condition in Experiment 2 (150°).

Most of these findings were consistent with the selective resetting hypothesis, which was based on the findings when participants walked in a small space. One exception was that when participants saw rotated distal scenes, their position estimations were random in the current experiment, which is inconsistent with the prediction that participants' position estimations followed self-motion cues when they saw rotated distal landmarks (Mou & Zhang, 2014). However, this finding can be explained by the locomotion-dependent selective resetting hypothesis. According to this hypothesis, when people drive in a large-scale environment, the path integration system updates heading estimations dynamically, but updates position estimations offline. One possible explanation for the offline updating is that calculating the positions during driving is a challenge. In the current experiment, position representations in the path integration system had not been produced when participants saw the rotated distal scenes. Thus participants' position estimations did not follow self-motion cues and were random.

To further test this conjecture, Experiment 2 modified the *rotated distal scene* condition. Participants were instructed to keep track of the origin of the path (O) while driving. In addition, after driving, they were asked to point to the origin of the path before the rotated distal scenes were presented. We assume that people use both position and heading representations to estimate the origin of the path (Mou & Zhang, 2014). Thus, participants had to update their position

estimations before pointing to the origin. As a result, this instruction forced them to produce their position representation using self-motion cues before they saw the rotated distal scenes. Therefore, their position estimations would follow self-motion cues.

3.4. Experiment 2

3.4.1 Method

3.4.1.1 Participants

Twelve university students (six men) participated in the experiment to fulfill the partial requirement for an introductory psychology course. Before the experiment, all participants signed the consent form approved by University of Alberta Research Ethics Board.

3.4.1.2 Design and Procedure

This experiment used the *rotated distal scene* condition in Experiment 1, with two modifications. First, participants were instructed to keep track of the origin of the path while driving. Second, when participants finished driving in the testing position, they were asked to point to the origin before viewing the rotated distal scenes. We termed this condition the *rotated distal scene & instruction* condition.

3.4.2 Results and Discussion

As in Experiment 1, participants' heading estimations (Table 3.4D) followed the rotated distal scenes (H'_{mean} = 138°, 95% CI [121° - 156°]). The confidence interval included the prediction from the landmark (150°) but excluded the prediction from self-motion cues (50°). Consistent with our conjectures, the participants' position estimations (Table 3.3D) followed

self-motion cues (OP'_{mean} = 30°, 95% CI [359° - 62°]). The confidence interval included the prediction from self-motion cues (25°).

3.5 General Discussion

There are two important findings in the current study. First, when the proximal landmark reappeared at the testing position, participants' position estimations followed the displaced proximal landmark. When the distal scene reappeared with a 100º rotation, participants' heading estimations followed the rotated distal scene. Second, when the displaced proximal landmark reappeared, participants' heading estimations followed self-motion cues. When the rotated distal scene reappeared, the participants' position estimations depended on whether participants were instructed to keep track of the origin of the path during locomotion. In particular, their position estimations followed self-motion cues with such instruction but were random without such instruction.

The current findings significantly strengthen the selective resetting hypothesis. The results, together with the previous studies (Mou & Zhang, 2014; Zhang & Mou, 2016), indicate that regardless of the travelling modes (walking or driving) and the scale (small or large) of the environment, a displaced proximal landmark determines people's position estimations, whereas rotated distal scenes determine their heading estimations. These findings suggest that different piloting cues (i.e., heading cues or position cues) selectively reset the headings or positions estimated by the path integration system.

However, one finding in the current study strikingly differed from those in Mou and Zhang's (2014) study and questioned the selective resetting hypothesis. In Mou and Zhang's study, when rotated distal cues reappeared, participants' position estimations followed self-

motion cues (2014). By contrast, in Experiment 1 of the current study, when rotated distal scenes reappeared, participants' position estimations appeared to be random. This novel finding undermined one important claim of the selective resetting model. According to the selective resetting model, the path integration system dynamically updated participants' position representations as well as their heading representations. Therefore, both position and heading representations should have been updated in the path integration system before the rotated distal landmarks reappeared. As a consequence, participants' position estimations should have followed self-motion cues regardless of the locomotion mode. These predictions are inconsistent with the findings in Experiment 1.

The locomotion-dependent resetting hypothesis, however, could explain the discrepancy in Mou and Zhang's findings (2014) and in Experiment 1 of the current study. According to this hypothesis, when people walk, the path integration system updates their position and heading representations online. In contrast, when people drive, the path integration system updates their heading representations online, but updates their position representations offline (i.e., when participants are required to do so). Offline updating of positions but online updating of headings occurs because updating position representations is more complex than updating heading representations. One possible reason is that calculating position representations requires the input of heading representations, but not vice versa. The complexity in updating position representations, relative to updating heading representations, might be unnoticeable when people walk but might be significant when people drive. Historically, humans have much more experience walking than driving. Furthermore, walking provides people with richer self-motion cues than driving does. In addition, walking is much slower than driving. Therefore, for that reason, it makes sense that positions would be updated online for walking but offline for driving.

In particular, when the rotated distal landmark reappeared, participants in Mou and Zhang's study had obtained the position representation in the path integration system, whereas participants in Experiment 1 of the current study had not produced the position representations in the path integration system. We assumed that seeing the rotated distal landmark interrupted the process of calculating the position. That is why participants' position estimations followed self-motion cues in Mou and Zhang's study but were random in Experiment 1 of the current study.

The speculation that the random position estimations in the *rotated distal scene* condition of Experiment 1 resulted from the offline updating of position representations was further supported in Experiment 2 of the current study. In Experiment 2, participants were instructed to keep track of the origin of the path (He & McNamara, 2017; Wiener et al., 2011). The result showed that participants' position estimations followed self-motion cues when the rotated distal scenes reappeared, replicating the findings in Mou and Zhang's (2014) study. As discussed in the introduction, people need to know their positions and headings before they estimate their home location. That explains why, in Experiment 2, participants updated their position estimations when they kept track of the origin of the path while driving. The path integration system had produced the position estimation before the rotated distal scene reappeared, and the participants' position estimations followed self-motion cues.

Although the rotated distal landmark led to random position estimates, the displaced proximal landmark did not lead to a random heading estimation in driving. The locomotion-dependent resetting hypothesis provides an explanation. According to this hypothesis, the path integration system updates the heading representations online whether people drive or walk. In the current study, the heading representations in the path integration system had been produced

before the displaced proximal landmark reappeared. Consequently, participants' heading estimations followed self-motion cues.

We acknowledge that the online and offline updating mechanisms distinguished in the locomotion-dependent resetting hypothesis were inspired by the idea that individuals can have two spatial updating mechanisms while walking (e.g., Fujita et al., 1993; Muller & Wehner, 1988; Wiener et al., 2011). According to the original idea, the online updating mechanism is individuals continuously update the homing vector during locomotion (*continuous updating*). The offline updating mechanism is individuals maintaining the path configuration (i.e., shape) during locomotion. They calculate the homing vector at the end of the path (*configural updating*). Extending this original idea, the current study's findings suggest three new insights.

First, the two spatial updating mechanisms in the previous studies focus on whether the homing vector is calculated online or offline (He & McNamara, 2017; Wiener et al., 2011). By contrast, in the locomotion-dependent resetting hypothesis, the two spatial updating mechanisms focus on whether participants' positions are calculated online or offline. In the current study, during the test, participants pointed to buildings. Their position estimations were calculated with their response directions of the buildings. Participants' responses to the home location were not collected or used to calculate their position estimations. As a consequence, participants should have updated their positions with respect to many locations in the environment rather than the home only. This suggests that offline or online updating is about vectors between people' position and several important locations in the environment. The homing vector might just be one of these vectors.

Second, the previous studies found that the two spatial updating mechanisms were selected by instruction. The current study further shows that two spatial updating mechanisms could be selected by the locomotion mode, as the locomotion-dependent resetting hypothesis suggests. In Wiener et al.'s study (2011, see also He & McNamara, 2017 and Experiment 2 of the current study), participants could be instructed to use the offline (e.g., pay attention to the shape of the path) or online (e.g., keep track of the origin of the path) updating mechanism. Nevertheless, without such instruction, participants who walked used the online mechanism (Mou & Zhang, 2014), whereas participants who drove used the offline mechanism (Experiment 1 of the current study). There might be other ways to activate the two spatial updating mechanisms. Future studies may test whether the complexity of the outbound path can also activate the offline or online mechanism. For example, if participants walk in a more complicated path with more legs (e.g., Kelly, McNamara, Bodenheimer, Carr, & Rieser, 2008), position estimations might also be updated offline.

Third, the previous theories hypothesized that people might represent the configuration (i.e., shape) of the path in the configural updating mechanism (e.g., Fujita et al., 1993; Wiener et al., 2011). However, the random position estimations in the *rotated distal scenes* condition in Experiment 1 indicated that at least during driving, the length of travel legs and the turning angle are still separately represented as a cognitive graph (Warren, Rothman, Schnapp, & Ericson, 2017) and have not been integrated into an enduring representation of the path shape, a cognitive map. If an enduring representation of the path shape has been formed, the rotated distal scene should not impair it. Thus, participants should be able to use the enduring representation of the path shape to calculate the position, producing a position estimation that is consistent with self-motion cues rather than a random position estimation as indicated by the result.

In future studies, we may test whether participants who are instructed to form an enduring representation of a path shape will show random position estimations when they see a rotated distal scene like in the *rotated distal scenes* condition in Experiment 1. It is possible that being instructed to pay attention to the shape of the path (Wiener et al., 2011) in driving can lead to an enduring representation of the outbound path, which participants can use to calculate their position offline even when they see the rotated distal landmark.

In conclusion, when people drive in a large-scale environment, the rotated distal scenes and the displaced proximal landmark selectively reset the heading and position estimations. The path integration system uses self-motion cues to update position and heading estimations. The heading updating is online and automatic, but the position updating may require more cognitive effort to switch from offline to online. These results, together with the findings in previous studies (Mou & Zhang, 2014; Zhang & Mou, 2017), support the locomotion-dependent selective resetting hypothesis.

3.6 References

Batschelet, E. (1981). *Cirular statistics in biology*. London: Academic Press.

Chen, X., McNamara, T. P., Kelly, J.W., & Wolbers, T. (2017). Cue combination in human spatial navigation. *Cognitive Psychology, 95*, 105-144.

Cheng, K., & Spetch, M. L. (1998). Mechanisms of landmark use in mammals and birds. In S. Healy (Ed.), *Spatial representation in animals* (pp. 1-17). Oxford: Oxford University Press.

Chrastil, E.R., & Warren, W.H. (2013). Active and passive spatial learning in human navigation: Acquisition of survey knowledge. *Journal of Experimental Psychology: Learning, Memory, and Cognition, 39*(5), 1520-1537.

Etienne, A. S., & Jeffery, K. J. (2004). Path integration in mammals. *Hippocampus, 14*(2), 180-192.

Fujita, N., Klatzky, R. L., Loomis, J. M., & Golledge, R. G. (1993). The encoding-error model of pathway completion without vision. *Geographical Analysis*, *25*(4), 295-314.

Gallistel, C. R. (1990). *The organization of learning*. Cambridge, MA: MIT Press

He, Q., & McNamara, T. P. (2017). Spatial Updating Strategy Affects the Reference Frame in Path Integration. *Psychonomic Bulletin & Review*, 1-7.

Ishikawa, T., & Montello, D. R. (2006). Spatial knowledge acquisition from direct experience in the environment: Individual differences in the development of metric knowledge and the integration of separately learned places. *Cognitive psychology*, *52*(2), 93-129.

Kearns, M. J., Warren, W. H., Duchon, A. P., & Tarr, M. J. (2002). Path integration from optic flow and body senses in a homing task. *Perception*, *31*(3), 349-374.

Kelly, J. W., McNamara, T. P., Bodenheimer, B., Carr, T. H., & Rieser, J. J. (2008). The shape of human navigation: How environmental geometry is used in maintenance of spatial orientation. *Cognition, 109*(2), 281-286.

Klatzky, R. L., Loomis, J. M., Beall, A. C., Chance, S. S., & Golledge, R. G. (1998). Spatial updating of self-position and orientation during real, imagined, and virtual locomotion. *Psychological Science, 9*(4), 293-298.

Mou, W., & Zhang, L. (2014). Dissociating position and heading estimation: rotated visual orientation cues perceived after walking reset headings but not positions. *Cognition*, *133,* 553-571.

Montello, D. R. (1993). Scale and multiple psychologies of space. *In Spatial information theory a theoretical basis for GIS* (pp. 312-321). Springer Berlin Heidelberg.

Müller, M., & Wehner, R. (1988). Path integration in desert ants, Cataglyphis fortis. *Proceedings of the National Academy of Sciences*, *85*(14), 5287-5290.

Nardini, M., Jones, P., Bedford, R., & Braddick, O. (2008). Development of cue integration in human navigation. *Current Biology, 18*(9), 689-693.

Riecke, B. E., Cunningham, D. W., & Bülthoff, H. H. (2007). Spatial updating in virtual reality: the sufficiency of visual information. *Psychological Research*, *71*(3), 298-313.

Ruddle, R. A., & Lessels, S. (2009). The benefits of using a walking interface to navigate virtual environments. *ACM Transactions on Computer-Human Interaction (TOCHI)*, *16*(1), 1-18.

Yerramsetti, A., Marchette, S. A., & Shelton, A. L. (2013). Accessibility versus accuracy in retrieving spatial memory: Evidence for suboptimal assumed headings. *Journal of Experimental Psychology: Learning, Memory, and Cognition*, *39*(4), 1106.

Waller, D., Loomis, J. M., & Steck, S. D. (2003). Inertial cues do not enhance knowledge of environmental layout. *Psychonomic Bulletin & Review, 10,* 987-993.

Warren, W. H., Kay, B. A., Zosh, W. D., Duchon, A. P., & Sahuc, S. (2001). Optic flow is used to control human walking. *Nature Neuroscience*, *4*(2), 213-216.

Warren, W. H., Rothman, D. B., Schnapp, B. H., & Ericson, J. D. (2017). Wormholes in virtual space: From cognitive maps to cognitive graphs. *Cognition*, *166*, 152-163.

Wiener, J. M., Berthoz, A., & Wolbers, T. (2011). Dissociable cognitive mechanisms underlying human path integration. *Experimental Brain Research*, *208*(1), 61-71.

Zhang, L., & Mou, W. (2017). Piloting systems reset path integration systems during position estimation. *Journal of Experimental Psychology: Learning, Memory and Cognition, 43*(3), 472-491.

Zhao, M., & Warren, W. H. (2015). How you get there from here: Interaction of visual landmarks and path integration in human navigation. *Psychological Science, 26*(6), 915-924.

Chapter 4

Summary and General Discussion

4.1 Summary

The primary goal of my thesis is to differentiate between the homing hypothesis and the positioning hypothesis. The homing hypothesis claims that the path integration system and the piloting system directly interact in homing estimations. This hypothesis speculates that each of the systems produces an independent homing estimation (Chen, McNamara, Kelly, & Wolbers, 2017; Cheng, Shettleworth, Huttenlocher, & Riser, 2007; Nardini, Jones, Bedford, & Braddick, 2008; Zhao & Warren, 2015a). Then when both systems are available, the homing representations could be combined or competed. Contrary to the homing hypothesis, the positioning hypothesis states that each system produces an independent positioning (heading/position) estimation. These positioning estimations from the two systems then interact for combination or competition. Finally, after interaction, the positioning estimations can be used to determine goal locations including home locations.

Two studies contrasted the homing hypothesis and the positioning hypothesis. The studies in Chapter 2 examined cue combination of positioning estimations when people walked in a small-scale environment. The study in Chapter 3 examined cue competition of positioning estimations when people drove in a large-scale environment. The results of the two studies support the positioning hypothesis.

In Chapter 2, Experiment 1 used distal landmarks to simplify the contrast between the two hypotheses. As distal landmarks only affected participants' heading estimations but not their position estimations, participants just used the path integration system to judge their positions in the conditions of landmarks only (LM), both cue (BO) and conflict (CO). Therefore, this study tested whether the path integration and piloting systems interact during heading estimations or homing estimations by manipulating the path configuration. The results do not support the

homing hypothesis, as the homing estimations were not combined for all path configurations. However, the results support the positioning hypothesis, as the heading estimations were combined in an optimal manner for all path configurations. Importantly, people used their heading and position estimations after interaction to determine home locations. Experiment 2 used the typical homing paradigm without measuring the heading and position estimations and found similar results that the homing estimations from the two cue systems were not combined. Experiment 3 and 4 were similar to Experiment 1 except proximal landmarks were used. We found that cue combination occurred during position as well as heading estimations but not during homing estimations.

In Chapter 3, cue interaction of positioning estimations is further studied in a large-scale environment. The participants studied in an immersive virtual city with two proximal towers and four distal scenes. Then the participants drove two streets without viewing towers or scenes. When they finished driving, either one tower with displacement to the testing position or the scenes with rotation reappeared. Their heading and position estimations were calculated. The results showed that when the displaced proximal tower reappeared, the participants used the tower to determine their positions; and when the rotated distal scenes reappeared, the participants used the scenes to determine their headings. These findings support the positioning hypothesis and suggest that when people drive in a large-scale environment, two cues compete for positioning estimations.

4.2 Discussion

4.2.1 Cue combination in positioning estimations

The finding of the heading combination supports the positioning hypothesis. Experiment 1 in Chapter 2 found that people combined the path integration cues and distal landmarks to

determine their headings but not homing locations. One may argue that the failure of the homing combination could be a consequence of an absent homing representation by distal landmarks, as cue combination requires two separate estimations, and distal landmarks alone do not provide positional information to indicate home locations. This concern has been justified in Experiment 3 and 4 where proximal landmarks are used to directly indicate the home locations. The results, however, showed that people still did not combine their homing estimations, but combined heading estimations. Taken together, people combine their heading estimations but not homing estimations, regardless of whether or not landmarks could indicate home locations directly.

The finding of the position combination further supports the positioning hypothesis. Experiment 4 in Chapter 2 used proximal landmarks and disoriented participants at the turning point in the LM condition, and the results showed the position combination. However, we did not find the position combination in Experiment 1 in Chapter 2 by using distal landmarks. This is because distal landmarks provided no distance or positional information. Furthermore, although proximal landmarks were used in Experiment 3 in Chapter 2, the participants did not combine their position estimations, as they were disoriented in place at the end of the path in the LM condition. This procedure might not completely disrupt the position estimations in the path integration system, and thus the participants might have the positions estimated by both systems in the LM condition.

The combination of positioning estimations are consistent with previous neuroscientific findings that directly measure the heading and position codings from single cells or neural networks. Recent studies have shown that monkeys could combine visual and vestibular cues to discriminate their headings. Such a cue combination manner can also be reflected by the neural responses in the dorsal medial superior temporal area (Fetsch, DeAngelis, & Angelaki, 2010;

2013; Fetsch, Pouget, DeAngelis, & Angelaki; 2012). In another study, Knight et al. (2014) found that the head direction cell system tends to combine information from the path integration and piloting systems for firing activities when there is a moderate landmark shift.

4.2.2 Cue competition in positioning estimations

The finding that people dominantly use landmarks to determine their headings or positions is also consistent with the positioning hypothesis. The positioning hypothesis explicitly stipulates that cue interaction occurs in positioning estimations. However, it does not exclusively claim cue interaction should only be cue combination. The study in Chapter 3 showed the cue competition for positioning estimations. This study suggests that people could make use of spatial information by the nature of landmarks to determine their headings or positions or both. If landmarks could provide orientation (or position or both) information, participants would use them to determine their headings (or positions or both).

The landmark dominance in positioning estimations is consistent with previous studies. For instance, Mou and Zhang (2014) found that people use rotated distal landmarks to determine their headings after walking a two-leg path. In another study, Zhang and Mou (2017) also found that people's position estimations follow the displaced landmark after walking a two-leg path.

Across the studies in my thesis, I also found that people dominantly use the path integration cues in the following situations. (1) After walking in an environment with distal landmarks, people used the path integration system to determine their positions. (2) After people drove in a large-scale environment and viewed a single tower that was displaced to the standing position during the test, they used the path integration system to determine their headings. (3) If people were instructed to keep track of the origin of the path during driving, they used the path

integration system to determine their positions after they finished driving and viewed rotated distal landmarks.

These results are consistent with the previous findings. Mou and Zhang (2014) showed that people follow the path integration system to estimate their positions after walking a path, when distal landmarks were rotated. Zhang and Mou (2017) also found that people use the headings determined by the path integration system after walking, when they view a single proximal landmark displaced to their standing location during the test.

These results also reveal the different mechanisms of the path integration system between walking and driving. During walking, the path integration system could calculate both headings and positions continuously. This system functions as a back-up in case the piloting system is not available or not reliable (Chen et al., 2017; Cheng et al., 2007; Zhao & Warren, 2015a; 2015b). During driving, the heading could be calculated continuously (online) in the path integration system, whereas the position could be calculated only when they are required (offline).

4.2.3 Cue combination vs cue competition in positioning estimations

In the literature, some studies found that the positioning representations from the path integration system and the piloting system compete with each other, whereas other studies found these representations could be combined (Etienne, Maurer, Boulens, Levy, & Rowe, 2004; Foo, Warren, Duchon, & Tarr, 2005; Knierim, Kudrimoti, & McNaughton, 1998; Knight et al., 2014; Mou & Zhang, 2004; Taube, 2007; Taube & Burton, 1995; Tcheang, Bülthoff, & Burgess, 2011; Zhang & Mou, 2017; Zhao & Warren, 2015a). Consistent with previous studies, I also found cue combination for heading estimations in Chapter 2, while cue competition for heading or position estimations in Chapter 3.

Previous studies have suggested that such factors as cue accuracy, cue reliance, and cue stability could determine whether the two cues combine or compete. In addition to these factors, I speculate that the temporal onset of familiar visual cues could be critical to how the two cues interact. In Chapter 2, when familiar visual cues were presented during the path of walking, two cues combined for heading or position estimations. In Chapter 3, when familiar visual cues were not presented during the path of driving, two cues competed for heading or position estimations. As suggested by Chen et al.'s study (2017), people's subjective confidence in the use of the cue system could affect their cue preference. I speculate that when people were not allowed to view familiar visual cues during walking but could view the reappeared landmarks with small or moderate shift in the conflict condition after walking (similar to the procedure in the study of Chapter 2), people could assume that an error in the path integration system, rather than the landmark rotation, leads to the discrepant estimations between the path integration cues and landmarks. Therefore, once people could view landmarks during testing, they could have more confidence in the piloting system, and thus switch to landmarks. On the other hand, when the familiar visual cues were presented during locomotion (similar to the procedure in the study of Chapter 2), people could have confidence in using both cues. They could not even notice the landmarks were turned off when the landmarks would have been out of people's field of view if they were presented. They might hold perceptual information of landmarks throughout walking. This perceptual sense would facilitate the confidence of using both cues in spatial navigation and thus motivate people to combine their estimations from the two cue systems.

4.2.4 No cue interaction in homing estimations

Chapter 2 examines cue interaction for homing estimations. In all experiments, the Bayesian cue combination could only explain the homing variability in the BO condition for the

group of L2/L1=0.5 in Experiment 1, and the CO condition for the group of L2/L1=0.5 in Experiment 1 and in Experiment 3 (only 3 out of 12 success). The quasi-Bayesian combination model could only predict the homing variability in the BO condition of the group of L2/L1=1, and L2/L1=0.5 in Experiment 1, and the CO condition for the group of L2/L1=0.5 in Experiment 1 (only 3 out of 12 success). Moreover, the linear combination model could only explain the homing variability in the CO condition for the group of L2/L1= 0.5 in Experiment 1 and Experiment 3 (2 out of 6 success).

None of the experiments showed evidence of cue competition of homing estimations. Although the homing variabilities in the BO and CO conditions in most experiments were not different from that in the PI or LM conditions, none of the mean of observed homing weights assigned to the piloting system was close to 0 or 1. It suggests that people do not assign a full weight to either the path integration cues or landmarks. Therefore, the results in Chapter 2 cannot be interpreted as cue competition of homing estimations.

The absence of cue interaction of homing estimations is not consistent with previous studies (e.g., Zhao & Warren, 2015a; Nardini et al., 2008). For instance, Zhao and Warren used distal landmarks and asked participants to complete the homing task in the conditions of PI, LM, BO and CO after walking the path. They had CO conditions in which the landmarks were shifted 15°, 30°, 45°, 90°, 115°, and 135°. By calculating the observed homing weight in the CO condition, they found that five out of twelve people followed distal landmarks up to 90°, whereas the other seven people used the path integration system to determine home locations. Zhao and Warren also used proximal landmarks and asked people to complete the same homing task in the PI, LM, BO and CO conditions. They found that all people consistently followed proximal landmarks up to 90°. Therefore, these results essentially reflect that the observed homing weight

indicates cue competition of homing estimations. However, in both the distal and proximal landmarks conditions, the homing variability in the BO and CO conditions could be predicted by the Beysian combination. Hence, the observed homing weight and the homing variability support different cue interaction models.

In the studies of my thesis, I never had results that the mean of observed homing weight was close to 0 or 1, while the homing variability in the BO or CO condition was comparable to the optimal combination prediction. Instead, except for the group of L2/L1=2 in Experiment 1 and Experiment 4, in all experiments presented in Chapter 2, the observed homing weight indicates homing combination, while the homing variability indicates homing competition (e.g., Figure 2.10). The discrepant conclusion drawn from the observed homing weight and the observed homing variability could essentially reflect the discrepancy between the observed standard deviation (SD) and the predicted SD of homing estimations as a function of the observed homing weight by the cue combination model (Equation 2.2). For instance, in Figure 2.10A, the black point with error bars (i.e., the observed SD with 95% confidence interval) does not lie within the green band (i.e., the predicted SD with 95% confidence interval). This also suggests that the homing estimations cannot be predicted by the Bayesian cue combination or the linear cue combination model or the cue competition model.

Similar to our findings, Chen et al. (2017) also found discrepant results between the observed SD and the predicted SD of the homing estimations as a function of the observed weight of homing estimations. In an experiment with three proximal landmarks, Chen et al. found the variability of the homing estimations in the BO and CO conditions could be predicted by the Bayesian combination model, but the observed weight calculated from the CO condition was significantly different from the optimal weight. In another experiment in which the

landmarks' positions changed across trials but remained constant within one trial, the observed weight calculated from the CO condition was comparable to the optimal one, but the observed homing variability in the BO and CO conditions was significantly larger than the one predicted by the Bayesian combination model.

The dominant reliance on the single cues indicated by the result of the observed homing weight in Zhao and Warren's study (2015a) might be attributed to their blocked design in the CO condition in which the participants progressively experienced larger and larger landmarks' shift. However, in Chen et al.'s study (2017) and my experiments, we only have one CO condition in which landmarks were shifted to a fixed angle and the CO condition was randomly intermixed with the other three conditions.

The discrepant results suggested by the observed homing weight and the homing variability in previous studies could be reconciled if we look at the results of heading, position, and homing estimations altogether. In the simulations of distal landmarks experiments (Figure 2.4) in Chapter 2, despite the leg ratio that was manipulated, the largest reduction of heading estimations in the BO condition (HER_{BO}) occurs when the landmark weight is 0.8 (i.e., the red dot on the axis of the landmark weight), regardless of the leg ratio (L2/L1). Importantly, the landmark weight in the heading estimations that produces the largest reduction in the variance of homing estimations (β_{BO}) depends on the leg ratio. Note that with an increase in the leg ratio, the distance between the landmark weight that produces the largest reduction of homing estimation variability (i.e., smallest SD of β_{BO}) and the landmark weight that produces the largest reduction of the HER_{BO} variability (i.e., smallest SD of HER_{BO}) increases. Therefore, in current studies and Chen et al.'s experiments, the observed SD of β_{BO} as a function of the observed β landmark weight would lie outside of the predicted SD of β_{BO} using the cue combination model (e.g.,

Figure 2.10 in current study). The simulation and the results suggest that people do not use the observed β landmark weight but rather use the observed HER landmark weight, together with the PER, to calculate the homing estimations.

4.3 Future research

Although we can use a mathematical model to quantitatively predict the variability of β in the BO and CO condition in distal landmarks experiments (Experiment 1 and 2 in Chapter 2), we cannot do this in proximal landmarks experiments (Experiment 3 and 4 in Chapter 2). In the current study, the proximal landmarks were rotated with respect to the participants' standing location in the testing phase. This procedure just caused the discrepancy between the heading estimations from the path integration and piloting systems in the CO condition, but not between their position estimations from the two cue systems. Therefore, in Experiment 4 of Chapter 2, once we found that people did not use an optimal weight to combine two cues for their position estimations, we were unable to calculate the observed PER weight and the predicted position estimations in the BO condition, and thus we were unable to quantitatively use the mathematical model to predict the homing estimation variabilities in the BO and CO conditions. Future studies could use a single proximal landmark and displace this landmark to make the two position estimation predictions in the CO condition discrepant (Zhang & Mou, 2017). By having two different position estimations from the two cue systems, we could determine the observed PER weight, and thus use the mathematical model to quantify the homing estimation variability in the BO and CO conditions.

In Chapter 3, we used the CO condition to examine cue interaction of positioning estimations when people drive in a large-scale environment. However, we did not have one participant complete the single cue and both cue conditions in one experiment. Additionally, we

did not include enough trials to measure the variability of positioning estimations and homing estimations in different cue conditions. Therefore, future studies could follow the design in Chapter 2 and measure the observed weight and the variability of heading, position and homing estimations in the four cue conditions to further contrast between the homing hypothesis and the positioning hypothesis when people drive in a large-scale environment.

Future studies could explore the dynamic relationship among HER weight, PER weight, and β weight by manipulating various factors. In Chapter 2, we provided evidence that the nature of landmarks (distal vs proximal) could influence PER weight and thus affect β weight. In Experiment 1 of Chapter 2, we further showed that changing the leg ratio of the path could impact β weight but not HER weight and PER weight. In Experiment 3 and 4 of Chapter 2, we also found whether disorientating people in the turning point or at the end of the path could influence PER weight. In past studies, Chen et al. (2017) have also explored how such factors as the cue reliability, cue stability, prior experience, and subjective evaluation on the cues could affect β weight. Future studies could further examine how these factors dynamically influence HER weight, PER weight, β weight and their relationships.

4.4 References

Chen, X., McNamara, T. P., Kelly, J.W., & Wolbers, T. (2017). Cue combination in human spatial navigation. *Cognitive Psychology, 95*, 105-144.

Cheng, K., Shettleworth, S.J., Huttenlocher, J., & Rieser, J.J. (2007). Bayesian integration of spatial information. *Psychological Bulletin*, *133*(4), 625-637.

Etienne, A. S., Maurer, R., Boulens, V., Levy, A., & Rowe, T. (2004). Resetting the path integrator: a basic condition for route-based navigation. *Journal of Experimental Biology, 207*(9), 1491-1508.

Fetsch, C. R., DeAngelis, G. C., & Angelaki, D. E. (2010). Visual–vestibular cue integration for heading perception: applications of optimal cue integration theory. *European Journal of Neuroscience, 31*(10), 1721-1729.

Fetsch, C. R., DeAngelis, G. C., & Angelaki, D. E. (2013). Bridging the gap between theories of sensory cue integration and the physiology of multisensory neurons. *Nature Review Neuroscience, 14*, 429-442.

Fetsch, C. R., Pouget, A., DeAngelis, G. C., & Angelaki, D. E. (2012). Neural correlates of reliability-based cue weighting during multisensory integration. *Nature Neuroscience*, *15,* 146-154.

Foo, P., Warren, W. H., Duchon, A., & Tarr, M. J. (2005). Do humans integrate routes into a cognitive map? Map- versus landmark-based navigation of novel shortcuts. *Journal of Experiment Psychology: Learning, Memory and Cognition, 31*(2), 195-215.

Knierim, J. J., Kudrimoti, H. S., & McNaughton, B. L. (1998). Interactions between idiothetic cues and external landmarks in the control of place cells and head direction cells.

Knight, R., Piette, C. E., Page, H., Walters, D., Marozzi, E., Nardini, M., ... & Jeffery, K. J. (2014). Weighted cue integration in the rodent head direction system. *Philosophical Transactions of the Royal Society of London B: Biological Sciences*, *369*(1635), 20120512.

Mou, W., & Zhang, L. (2014). Dissociating position and heading estimation: rotated visual orientation cues perceived after walking reset headings but not positions. *Cognition*, *133,* 553-571.

Nardini, M., Jones, P., Bedford, R., & Braddick, O. (2008). Development of cue integration in human navigation. *Current Biology, 18*(9), 689-693.

Taube, J. S. (2007). The head direction signal: origins and sensory-motor integration. *Annual Review of Neuroscience*, *30*, 181-207.

Taube, J. S., & Burton, H. L. (1995). Head direction cell activity monitored in a novel environment and during a cue conflict situation. *Journal of Neurophysiology*, *74*(5), 1953-1971.

Tcheang, L., Bülthoff, H. H., & Burgess, N. (2011). Visual influence on path integration in darkness indicates a multimodal representation of large-scale space. *Proceedings of the National Academy of Sciences*, *108*(3), 1152-1157.

Zhang, L., & Mou, W. (2017). Piloting systems reset path integration systems during position estimation. *Journal of Experimental Psychology: Learning, Memory and Cognition, 43*(3), 472-491.

Zhao, M., & Warren, W. H. (2015a). How you get there from here: Interaction of visual landmarks and path integration in human navigation. *Psychological Science, 26*(6), 915-924.

Zhao, M., & Warren, W. H. (2015b). Environmental stability modulates the roles of path integration in human navigation. *Cognition, 142,* 96-109.

Bibliography

Benhamou, S., Sauvé, J. P., & Bovet, P. (1990). Spatial memory in large scale movements: efficiency and limitation of the egocentric coding process. *Journal of Theoretical Biology, 145*(9), 1-12.

Batschelet, E. (1981). *Cirular statistics in biology*. London: Academic Press.

Calton, J. L., Stackman, R. W., Goodridge, J. P., Archey, W. B., Dudchenko, P. A., & Taube, J. S. (2003). Hippocampal place cell instability after lesions of the head direction cell network. *The Journal of Neuroscience*, *23*(30), 9719-9731.

Chen, X., McNamara, T. P., Kelly, J.W., & Wolbers, T. (2017). Cue combination in human spatial navigation. *Cognitive Psychology, 95*, 105-144.

Cheng, K., Shettleworth, S.J., Huttenlocher, J., & Rieser, J.J. (2007). Bayesian integration of spatial information. *Psychological Bulletin*, *133*(4), 625-637.

Cheng, K., & Spetch, M. L. (1998). Mechanisms of landmark use in mammals and birds. In S. Healy (Ed.), *Spatial representation in animals* (pp. 1-17). Oxford: Oxford University Press.

Chrastil, E.R., & Warren, W.H. (2013). Active and passive spatial learning in human navigation: Acquisition of survey knowledge. *Journal of Experimental Psychology: Learning, Memory, and Cognition, 39*(5), 1520-1537.

Collett, M., & Collett, T. S. (2000). How do insects use path integration for their navigation? *Biological Cybernetics, 83*(3), 245-259.

Doeller, C. F., & Burgess, N. (2008). Distinct error-correcting and incidental learning of location relative to landmarks and boundaries. *Proceedings of the National Academy of Sciences of the United States of America, 105*(15), 5909-5914.

Dyer, F. C. (1991). Bees acquire route-based memories but not cognitive maps in a familiar landscape. *Animal Behaviour, 41*, 239-246.

Ernst, M. O., & Banks, M. S. (2002). Humans integrate visual and haptic information in a statistically optimal fashion. *Nature, 415*, 429–433.

Etienne, A. S., & Jeffery, K. J. (2004). Path integration in mammals. *Hippocampus, 14*(2), 180-192.

Etienne, A. S., Maurer, R., Boulens, V., Levy, A., & Rowe, T. (2004). Resetting the path integrator: A basic condition for route-based navigation. *The Journal of Experimental Biology, 207*, 1491–1508.

Fetsch, C. R., DeAngelis, G. C., & Angelaki, D. E. (2010). Visual–vestibular cue integration for heading perception: applications of optimal cue integration theory. *European Journal of Neuroscience, 31*(10), 1721-1729.

Fetsch, C. R., DeAngelis, G. C., & Angelaki, D. E. (2013). Bridging the gap between theories of sensory cue integration and the physiology of multisensory neurons. *Nature Review Neuroscience, 14*, 429-442.

Fetsch, C. R., Pouget, A., DeAngelis, G. C., & Angelaki, D. E. (2012). Neural correlates of reliability-based cue weighting during multisensory integration. *Nature Neuroscience*, *15,* 146-154.

Foo, P., Warren, W. H., Duchon, A., & Tarr, M. J. (2005). Do humans integrate routes into a cognitive map? Map- versus landmark-based navigation of novel shortcuts. *Journal of Experiment Psychology: Learning, Memory and Cognition, 31*(2), 195-215.

Fujita, N., Klatzky, R. L., Loomis, J. M., & Golledge, R. G. (1993). The encoding-error model of pathway completion without vision. *Geographical Analysis*, *25*(4), 295-314.

Fujita, N., Loomis, J. M., Klatzky, R. L., & Golledge, R. G. (1990). A Minimal Representation for Dead-Reckoning Navigation: Updating the Homing Vector. *Geographical Analysis, 22*(4), 324-335.

Gallistel, C. R. (1990). *The organization of learning*. Cambridge, MA: MIT Press.

Gallistel, C. R., & Matzel, L. D. (2013). The neuroscience of learning: beyond the Hebbian synapse. *Annual Review of Psychology*, *64*, 169-200.

He, Q., & McNamara, T. P. (2017). Spatial Updating Strategy Affects the Reference Frame in Path Integration. *Psychonomic Bulletin & Review*, 1-7.

Ishikawa, T., & Montello, D. R. (2006). Spatial knowledge acquisition from direct experience in the environment: Individual differences in the development of metric knowledge and the integration of separately learned places. *Cognitive psychology*, *52*(2), 93-129.

Kearns, M. J., Warren, W. H., Duchon, A. P., & Tarr, M. J. (2002). Path integration from optic flow and body senses in a homing task. *Perception*, *31*(3), 349-374.

Kelly, J. W., McNamara, T. P., Bodenheimer, B., Carr, T. H., & Rieser, J. J. (2008). The shape of human navigation: How environmental geometry is used in maintenance of spatial orientation. *Cognition, 109*(2), 281-286.

Klatzky, R. L., Loomis, J. M., Beall, A. C., Chance, S. S., & Golledge, R. G. (1998). Spatial updating of self-position and orientation during real, imagined, and virtual locomotion. *Psychological Science, 9*(4), 293-298.

Knierim, J. J., Kudrimoti, H. S., & McNaughton, B. L. (1998). Interactions between idiothetic cues and external landmarks in the control of place cells and head direction cells. *Journal of Neurophysiology, 80*(1), 425-446.

Knight, R., Piette, C. E., Page, H., Walters, D., Marozzi, E., Nardini, M., ... & Jeffery, K. J. (2014). Weighted cue integration in the rodent head direction system. *Philosophical Transactions of the Royal Society of London B: Biological Sciences*, *369*(1635), 20120512.

Loomis, J. M., Klatzky, R. L., Golledge, R. G., Cicinelli, J. G., Pellegrino, J. W., & Fry, P. A. (1993). Nonvisual navigation by blind and sighted: Assessment of path integration ability. *Journal of Experimental Psychology: General, 122*(1), 73-91.

Loomis, J. M., Klatzky, R. L., Golledge, R. G., & Philbeck, J. W. (1999). Human navigation by path integration. In R. G. Golledge (Ed.), *Wayfinding: Cognitive mapping and other spatial processes* (pp. 125-151). Baltimore: Johns Hopkins.

Mou, W., & Zhang, L. (2014). Dissociating position and heading estimation: rotated visual orientation cues perceived after walking reset headings but not positions. *Cognition*, *133,* 553-571.

Montello, D. R. (1993). Scale and multiple psychologies of space. *In Spatial information theory a theoretical basis for GIS* (pp. 312-321). Springer Berlin Heidelberg.

Müller, M., & Wehner, R. (1988). Path integration in desert ants, Cataglyphis fortis. *Proceedings of the National Academy of Sciences*, *85*(14), 5287-5290.

Muller, R. (1996). A quarter of a century of place cells. *Neuron*, *17*(5), 813-822.

Nardini, M., Jones, P., Bedford, R., & Braddick, O. (2008). Development of cue integration in human navigation. *Current Biology, 18*(9), 689-693.

Riecke, B. E., Cunningham, D. W., & Bülthoff, H. H. (2007). Spatial updating in virtual reality: the sufficiency of visual information. *Psychological Research*, *71*(3), 298-313.

Ruddle, R. A., & Lessels, S. (2009). The benefits of using a walking interface to navigate virtual environments. *ACM Transactions on Computer-Human Interaction (TOCHI)*, *16*(1), 1-18.

Shettleworth, S. J., & Sutton, J. E. (2005). Multiple systems for spatial learning: dead reckoning and beacon homing in rats. *Journal of Experimental Psychology: Animal Behavior Processes, 31*, 125-141.

Petrini, K., Caradonna, A., Foster, C., Burgess, N. & Nardini, M. (2016). How vision and self-motion combine or compete during path reproduction changes with age. *Scientific Reports, 6*, 29163.

Sjolund, L. A., Kelly, J. W., & McNamara, T. P. (in press). Optimal combination of environmental cues and path integration during navigation. *Memory & Cognition.*

Taube, J. S. (2007). The head direction signal: origins and sensory-motor integration. *Annual Review of Neuroscience*, *30*, 181-207. doi: 10.1146/annurev.neuro.29.051605.112854

Taube, J. S., & Burton, H. L. (1995). Head direction cell activity monitored in a novel environment and during a cue conflict situation. *Journal of Neurophysiology, 74,* 1953–1971.

Tcheang, L., Bülthoff, H. H., & Burgess, N. (2011). Visual influence on path integration in darkness indicates a multimodal representation of large-scale space. *Proceedings of the National Academy of Sciences*, *108*(3), 1152-1157.

Vickerstaff, R. J., & Cheung, A. (2010). Which coordinate system for modelling path integration? *Journal of Theoretical Biology, 263*(2), 242-261.

Wang, R. F., & Spelke, E. S. (2002). Human spatial representation: Insights from animals. *Trends in Cognitive. Sciences*, *6*(9), 376-382.

Wang, R. F. (2016) Building a cognitive map by assembling multiple path integration systems. *Psychonomic Bulletin & Review, 23*(3), 692-702.

Warren, W. H., Kay, B. A., Zosh, W. D., Duchon, A. P., & Sahuc, S. (2001). Optic flow is used to control human walking. *Nature Neuroscience*, *4*(2), 213-216.

Wehner, R. (2003). Desert ant navigation: how miniature brains solve complex tasks. *Journal of Comparative Physiology A*, *189*(8), 579-588.

Wiener, J. M., Berthoz, A., & Wolbers, T. (2011). Dissociable cognitive mechanisms underlying human path integration. *Experimental Brain Research, 208*(1), 61-71.

Whishaw, I. Q., & Brooks, B. L. (1999). Calibrating space: exploration is important for allothetic and idiothetic navigation. *Hippocampus, 9*(6), 659–667.

Yerramsetti, A., Marchette, S. A., & Shelton, A. L. (2013). Accessibility versus accuracy in retrieving spatial memory: Evidence for suboptimal assumed headings. *Journal of Experimental Psychology: Learning, Memory, and Cognition*, *39*(4), 1106.

Yoder, R. M., Clark, B. J., & Taube, J. S. (2011). Origins of landmark encoding in the brain. *Trends in Neurosciences, 34*(11), 561-571.

Waller, D., Loomis, J. M., & Steck, S. D. (2003). Inertial cues do not enhance knowledge of environmental layout. *Psychonomic Bulletin & Review, 10,* 987-993.

Warren, W. H., Kay, B. A., Zosh, W. D., Duchon, A. P., & Sahuc, S. (2001). Optic flow is used to control human walking. *Nature Neuroscience*, *4*(2), 213-216.

Warren, W. H., Rothman, D. B., Schnapp, B. H., & Ericson, J. D. (2017). Wormholes in virtual space: From cognitive maps to cognitive graphs. *Cognition*, *166*, 152-163.

Wiener, J. M., Berthoz, A., & Wolbers, T. (2011). Dissociable cognitive mechanisms underlying human path integration. *Experimental Brain Research*, *208*(1), 61-71.

Zhang, H., Mou, W., & McNamara, T. P. (2011). Spatial updating according to a fixed reference direction of a briefly viewed layout. *Cognition, 119*(3), 419-429.

Zhang, L., & Mou, W. (2017). Piloting systems reset path integration systems during position estimation. *Journal of Experimental Psychology: Learning, Memory, and Cognition, 43*(3), 472-491.

Zhao, M., & Warren, W. H. (2015a). How you get there from here: Interaction of visual landmarks and path integration in human navigation. *Psychological Science, 26*(6), 915-924.

Zhao, M., & Warren, W. H. (2015b). Environmental stability modulates the roles of path integration in human navigation. *Cognition, 142,* 96-109.